Can the Hock Process Be Used to Produce Phenol from Polystyrene?

Doohyun Baek,[a,b] Abdullah J. Al Abdulghani,[c] Dylan J. Walsh,[a,b] Dillon T. Hofsommer,[a,b] James B. Gerken,[a] Changxia Shi,[d] Eugene Y.-X. Chen,[d] Ive Hermans,[a,b,c*] and Shannon S. Stahl[a,b*]

[a]Department of Chemistry, University of Wisconsin−Madison, Madison, Wisconsin 53706, United States

[b]The Wisconsin Energy Institute, University of Wisconsin−Madison, Madison, Wisconsin 53726, United States

[c]Department of Chemical and Biological Engineering, University of Wisconsin−Madison, Madison, Wisconsin 53706, United States

[d]Department of Chemistry, Colorado State University, Fort Collins, Colorado 80523, United States

KEYWORDS: Chemical recycling, polystyrene, autoxidation, Hock process, Phenol

ABSTRACT: Polystyrene (PS) is a widely used thermoplastic polymer, but its very low recycling rate has motivated consideration of chemical conversion strategies to convert waste PS in into value-added products. Oxidation methods have been widely studied, but they typically generate benzoic acid, a product with relatively low market demand. Phenol is a higher volume chemical that would be an appealing target, but no methods currently exist for conversion of PS into phenol. The repeat unit in PS closely resembles cumene, the primary feedstock used to produce phenol through the Hock process. Here, we investigate prospects for adapting the Hock process to PS, generating hydroperoxides through autooxidation of benzylic C–H bonds followed by acid-promoted rearrangement of the hydroperoxides to afford phenol and a partially oxygenated polymer. Experimental and computational studies of dimeric and trimeric PS model compounds show that neighboring phenyl rings impose conformational constraints that raise the barrier to hydrogen-atom transfer (HAT) from the tertiary benzylic C–H bond. These effects are also evident with PS and contribute to lower yields of phenol when PS is subjected to Hock process conditions. These results provide valuable insights that have important implications for other efforts that seek to adapt small-molecule reactivity to polymeric feedstocks.

Introduction

Polystyrene (PS) is an inexpensive, large-volume commodity polymer, used in applications ranging from packaging to insulation and consumer goods.[1] Most post-consumer PS, however, ends up in landfills and has a recycling rate of less than 1%.[2–4] Various chemical recycling strategies are being considered for conversion of waste PS into valuable products.[5–7] Much of this effort has focused on thermochemical approaches, such as gasification[8] and pyrolysis[9], or reduction methods, such as hydrogenolysis[10] and hydrocracking.[11] Oxidation methods, particularly those using O_2 as the oxidant, represent an alternative strategy. These thermodynamically favorable reactions require little energy input and can directly access valuable products that can re-enter the chemical value chain.[12]

Industrial methods for hydrocarbon oxidation offer a valuable starting point for consideration of conditions for waste plastics valorization. For example, the Mid-Century (MC) process,[13] an industrial Co/Mn/Br-catalyzed autoxidation method for conversion of *p*-xylene into terephthalic acid (**Figure 1a**), has been applied to individual and mixed polymer feedstocks.[14–17] These and other thermal[18–21] and photochemical[22–31] oxidation conditions typically convert PS into benzoic acid. While these reactions often proceed with high selectivity, the market demand for benzoic acid[31] is relatively small (**Figure 1b**). Biological conversion offers a potential strategy to use benzoic acid as a feedstock for production of value-added products,[15,16] but chemical methods to convert PS into products other than benzoic acid merit attention.[32] Phenol

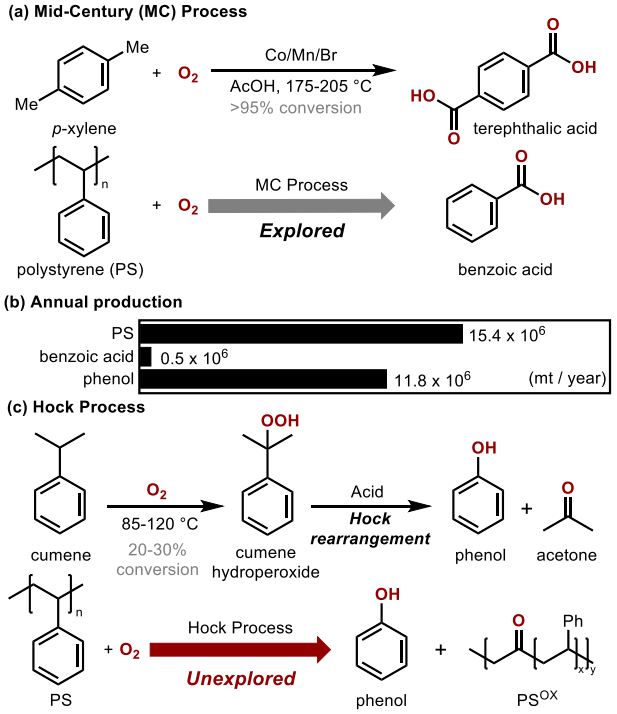

Figure 1. (a) Mid-Century process for production of terephthalic acid from *p*-xylene and its extension to polystyrene conversion to benzoic acid. (b) Market size of relevant chemicals. (c) Cumene oxidation/rearrangement in the Hock process, with targeted adaptation to polystyrene as a feedstock for phenol production.

has a much larger market volume than benzoic acid, but methods for conversion of PS to phenol have not yet been reported. Phenol is currently produced in the multi-step Hock process, which involves autoxidation of cumene and subsequent acid-promoted rearrangement of cumene hydroperoxide to yield phenol and acetone (**Figure 1c**).[33] The structural similarity between the repeat unit in PS and cumene raises the prospect that the Hock process could be adapted to produce phenol from PS. Here, we explore this possibility. The data show that the autoxidation and acid-promoted rearrangement reactivity changes significantly when dimeric and trimeric PS subunits are used instead of cumene. Experimental and computational studies reveal that proximal phenyl groups along the backbone hinder both steps and limit the hydroperoxide and phenol yields. Higher molecular weight derivatives, including pentamers and PS itself, closely resemble the behavior of the trimeric compound. Treatment of PS under Hock process conditions affords phenol and a partially oxidized polymeric byproduct (PS^{OX}, see **Figure 1c**) that retains phenyl groups. The latter material can be used to produce benzoic acid under MC conditions, and the tandem Hock/MC oxidation sequence provides a means to access both phenol and benzoic acid from waste PS. More broadly, this work provides important fundamental insights relevant to adaptation of commodity-scale oxidation conditions to waste-plastic feedstocks.

Results and Discussion

Autoxidation of Dimeric and Trimeric PS Model Compounds. The industrial autoxidation of cumene (**1**) to cumene hydroperoxide (**1a**) is typically carried out in neat cumene around 135 °C, achieving a single-pass conversion of approximately 20-30%.[33–35] These conditions are unsuitable for reactions with PS, as both hydroperoxides and unreacted C–H sites remain on the same polymer chain, complicating the recovery and recycling of unreacted material. Consequently, we considered alternative conditions for cumene autoxidation that use organic solvents and radical initiators, which enable higher conversion to cumene hydroperoxide.[36–40] Ishii and coworkers used acetonitrile as the solvent, with NHPI (*N*-hydroxyphthalimide) and AIBN (azobisisobutyronitrile) as radical initiators, to convert cumene to cumene hydroperoxide in 76% conversion and 75% yield.[36] This method has been the focus of industrial interest and further development.[38–40] Validation of these results in our own lab (see **Figure S5**) motivated us to explore conditions of this type for reactions with PS.

We elected to initiate our study by investigating the dimeric and trimeric PS model compounds, *trans*-**2** and **3** (the latter as a mixture of diastereomers) (**Figure 2**). These compounds provide a structural bridge between cumene and PS and enable more straightforward analysis of autoxidation products relative

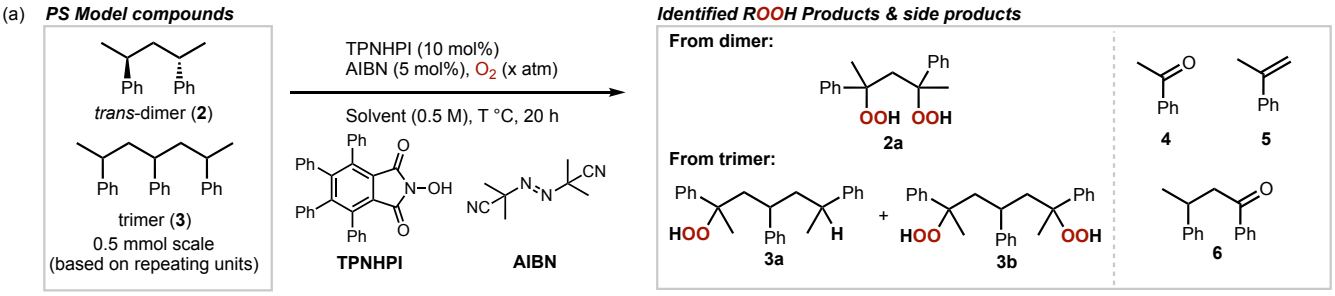

Entry	Substrates	O_2 condition	T [°C]	Conv.[a] [%]	Solvent	ROOH [%][b] 2a	3a	3b	ROOH [%][c] per # of Ph	side products [%] 4	5	6
1	Dimer (**2**)	O_2, 1 atm	70	39	MeCN	31	-	-	31	1.6	0.3	-
2	Dimer (**2**)	O_2, 1 atm	70	45	^{n}BuCN	40	-	-	40	2.0	0.5	-
3	Dimer (**2**)	O_2, 10 atm	70	74	^{n}BuCN	56	-	-	56	3.7	-	-
4	Dimer (**2**)	O_2, 10 atm	100	82	^{n}BuCN	50	-	-	50	8.6	-	-
5	Trimer (**3**)	O_2, 10 atm	70	56	^{n}BuCN	-	23	24	24	1.3	-	2.7

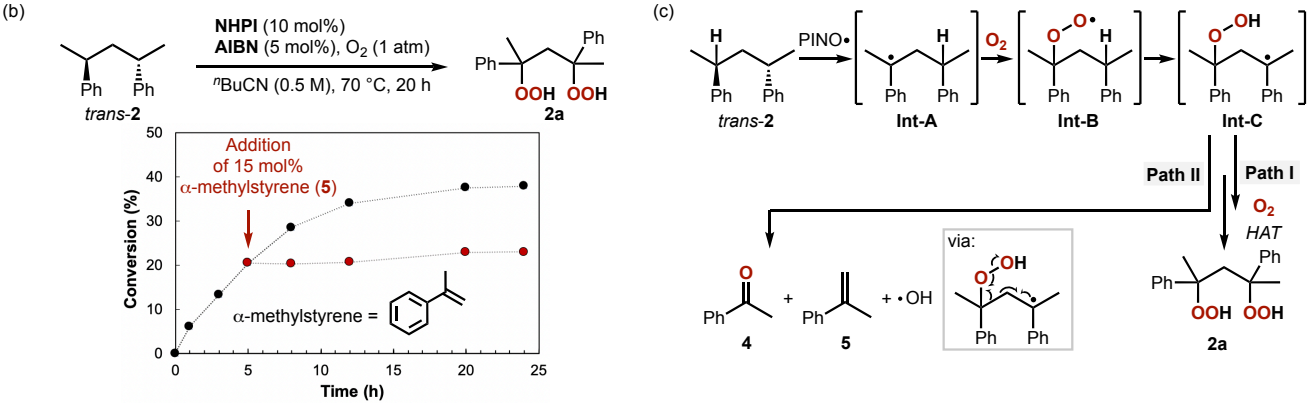

Figure 2. (a) Autoxidation optimization with polystyrene model compounds **2** and **3**. Reaction conditions: 0.5 mmol of Ph-containing subunits (0.25 mmol **2** and 0.167 mmol **3**), 10 mol% TPNHPI (tetraphenyl-*N*-hydroxyphthalimide), 5 mol% AIBN (azobisisobutyronitrile), O_2 (1 or 10 atm), 1 mL valeronitrile (^{n}BuCN) at 70 °C or 100 °C. [a]Conversion of **2** or **3**. [b]Yield of ROOH products **2a**, **3a**, or **3b,** analyzed by UPLC as alcohols obtained by reduction with PMe_3. [c]Yield of ROOH products re-calculated based on peroxides per the number of phenyl rings. (b) Inhibitory effect of α-methylstyrene in the autoxidation reaction of **2**. (c) Proposed mechanisms for O_2-dependent formation of **2** (Path I) and formation of acetophenone **4** and α-methylstyrene **5** (Path II).

to reactions with PS. Reactivity studies began by evaluating the autoxidation of **2** and **3** in acetonitrile in the presence and absence of various hydrogen-atom transfer reagents (e.g., NHPI, tBuOOH, tBuOOtBu) and radical initiators (e.g., AIBN, $Co(OAc)_2$). These screening studies showed that conditions similar to those reported by Ishii afforded the highest yields of hydroperoxides derived from **2** and **3** (see **section 4a** in the Supporting Information for details). The dimeric compound **2** undergoes selective conversion to the bis-hydroperoxide **2a** (as a mixture of diastereomers), with the mono-hydroperoxide forming in only trace amounts (< 1%). Most of the remaining mass balance is present as unreacted dimer **2** (see Supporting Information for analytical details). TPNHPI (tetraphenyl-*N*-hydroxyphthalimide) gives better yields of **2a** than NHPI, while both reactions benefit from the presence of AIBN (31% vs. 20% yield, respectively; see **Figure 2a**, entry 1 and **Figure S12** in the Supporting Information). PS is not soluble in acetonitrile, while NHPI has poor solubility in non-polar solvents. Valeronitrile (^{n}BuCN) offers a suitable compromise and led to an improved yield of *bis*-hydroperoxide **2a** (40%, **Figure 2a**, entry 2).

Small amounts of acetophenone (**4**, 2.0 mol%) and α-methylstyrene (**5**, 0.5 mol%) are observed as side products in these reactions (**Figure 2a**). Control experiments show that α-methylstyrene inhibits autoxidation of the dimeric substrate *trans*-**2** (**Figure 2b**), likely by trapping reactive radical intermediates (see **section 3e** in the Supporting Information for additional details). This observation prompted us to consider the mechanistic origin of α-methylstyrene (and acetophenone) formation during the reaction of **2** (**Figure 2c**). The bis-hydroperoxide is proposed to arise from rapid intramolecular 1,5-hydrogen-atom transfer (HAT) from the initial peroxyl radical intermediate **Int-B**. The resulting tertiary radical intermediate can then react with O_2 (Path I, **Figure 2c**) or undergo the O_2-independent O–O/C–C cleavage step to afford α-methylstyrene and acetophenone (Path II, **Figure 2c**). This hypothesis suggested that improved conversion to the bis-hydroperoxide should be accessible at higher O_2 pressure. With 10 atm O_2,[41] a 56% yield of bis-hydroperoxide **2a** was obtained without α-methylstyrene generation (entry 3). The acetophenone formed under these conditions can arise from decomposition of **2a** (i.e., different from Path II). When the reaction temperature is increased from 70 to 100 °C, the conversion of **2** increased, but the yield of **2a** decreased and the yield of acetophenone increased (**Figure 2a**, entry 4).

The reactivity of trimeric model compound **3** shows the influence of an additional monomer unit. Under conditions optimized with **2**, the reaction of **3** generates hydroperoxides exclusively at the terminal tertiary benzylic positions, yielding mono-hydroperoxide **3a** in 23% yield and bis-hydroperoxide **3b** in 24% yield (**Figure 2a**, entry 5). A small amount of ketone **6** and acetophenone were observed as side products. Overall, these observations indicate that the trimer has lower reactivity than the dimer.

Computational Studies. Density functional theory (DFT) calculations were performed to assess the energetics of the oxidation pathways of dimer and trimer model compounds **2** and **3** in order to gain insight into their different reactivity. **Figure 3** highlights the steps that show significant differences between the two compounds, including (a) PINO-mediated HAT from the tertiary benzylic radical and (b) intramolecular HAT from the intermediate peroxyl radical (see **section 5** of the Supporting Information for the full reaction pathway). Hydrogen-atom transfer (HAT) from a benzylic C–H bond in **2** exhibits an energy barrier of 24.9 kcal/mol (**TS-A**, **Figure 3a**) in the formation benzylic radical intermediate **Int-A**. In the reaction of **3**, two potential PINO-mediated HAT pathways were considered: one from a terminal benzylic C–H bond and

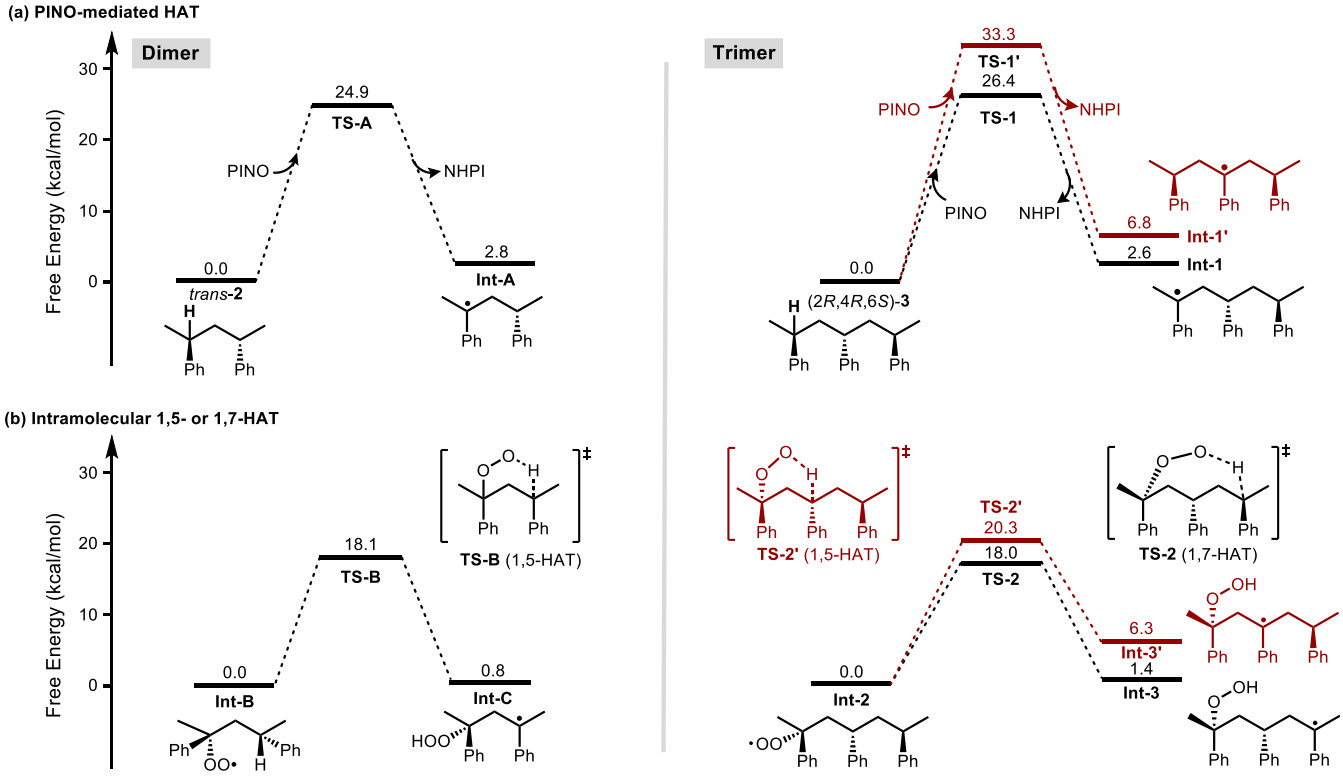

Figure 3. Computational data for the oxidation pathways of dimer and trimer. Density functional theory (DFT) calculations were performed using the B3LYP exchange-correlation functional as implemented in Gaussian 16 using the 6-311++G(df,pd) basis set. The *trans*-dimer **2** and the (2*R*,4*R*,6*S*)-trimer **3** were selected for the calculation among the diastereomers.

the other from the internal benzylic C–H bond. Reaction of PINO with the terminal C–H bond forms the benzylic radical intermediate **Int-1** with an energy barrier of 26.4 kcal/mol (**TS-1**), while reaction with the internal C–H bond for form **Int-1'** has a higher energy barrier of 33.3 kcal/mol (**TS-1'**). Each of these radicals undergoes barrierless reaction with O_2 to afford peroxyl radical species (**Figure S16** in the Supporting Information).

Intramolecular HAT by the dimeric and trimeric peroxyl radical intermediates **Int-B** and **Int-2** (**Figure 3b**) initiates stepwise formation of the bis-hydroperoxide products **2a** and **3b** (cf. **Figure 2**). Comparison of the 1,5-HAT energy barriers for these intermediates shows that reaction of the trimer has a 2.2 kcal/mol higher energy barrier that reaction of the dimer (**TS-2'** versus **TS-B**). The trimer, however, can also undergo 1,7-HAT through transition state **TS-2**. The results show that 1,7-HAT is favored by 2.3 kcal/mol over the 1,5-HAT step. Together, this analysis of inter- and intramolecular HAT energetics rationalizes that lack of C–H oxidation products arising from HAT at the central benzylic C–H bond of the trimer (cf. **Figure 2**).

Optimization of the Acid-Promoted Hock-Rearrangement. Subsequent efforts focused on acid-promoted reaction of hydroperoxides **2a**, **3a**, and **3b** obtained from the autoxidation reaction, without purification. (The hydroperoxides present safety hazards and are insufficiently stable to isolate in pure form.) Each reaction was conducted with 0.2 mmol of total hydroperoxide, and yields were recorded with respect to the hydroperoxide content. Initial tests probed reaction of **2a** with various Brønsted and Lewis acids (**Figure 4** and **Figure S15**). Lewis acids generally led to lower phenol yields compared to reactions with Brønsted acids, and the highest phenol yields were obtained with the strong acids, sulfuric acid (H_2SO_4, 53% yield) and perchloric acid ($HClO_4$, 58% yield) (**Figure 4**, entries 1 and 2). Increased acid concentration enhanced the yield (entries 3 and 4), and the best outcome was observed with 3.6 M perchloric acid ($HClO_4$) in MeCN, affording phenol in 72% yield with respect to the hydroperoxide content (**Figure 4**, entry 4). Similar performance was observed with the mixture of mono- and bis-hydroperoxide species, which afforded a 71% yield of phenol (**Figure 4**, entry 5).

Hock Process Applied to PS. The above studies of model compounds provided the basis for analysis of PS under the same sequential oxidation/acid-promoted rearrangement conditions. Subjecting PS (M_n ~ 73 kDa) to the optimized autoxidation conditions led to incorporation of hydroperoxides at approximately 25 mol% of the benzylic position in the PS backbone (**PS^{OOH}**, **Figure 5a**). The hydroperoxide content was estimated by reducing the hydroperoxides with triphenylphosphine (PPh_3) and quantifying the resulting triphenylphosphine oxide ($Ph_3P{=}O$) by UPLC. This titration method was validated by performing the same assay with bis-hydroperoxide **2a**, which can be independently quantified by other methods (see **section 6b** of the Supporting Information for details). ^{1}H NMR spectroscopic analysis of **PS^{OOH}** does not reveal the presence of alkene or carbonyl groups, similar to the formation of α-methylstyrene and acetophenone with the dimeric model compound (cf. **Figure 2a** and **Figure S18**); however, a small C=O stretching peak at 1716 cm^{-1} is evident in an IR spectrum, suggesting small quantities of terminal benzoyl group may be present (**Figure 5c**).

Subjecting the PS-hydroperoxide material to the optimized acid treatment conditions led to a 52% yield of phenol with

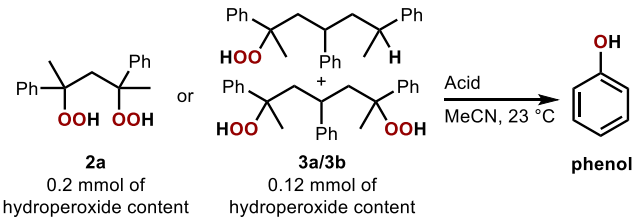

Entry	Substrates	Acid treatment (in 1 mL of MeCN)	Phenol Yield [%] (two-step yield)
1	**2a**	H_2SO_4 0.30 M	53 (21)
2	**2a**	$HClO_4$ 0.30 M	58 (24)
3	**2a**	H_2SO_4 3.6 M	62 (25)
4	**2a**	$HClO_4$ 3.6 M	72 (30)
5	**3a/3b**	$HClO_4$ 3.6 M	71 (17)

Figure 4. Acid-promoted Hock rearrangement conditions with crude **2a** and **3a/3b** obtained from autoxidation of **2** and **3** (cf. **Figure 2a**). The yield of phenol was analyzed by UPLC. The yield in parenthesis is the two-step yield from **2** or **3**.

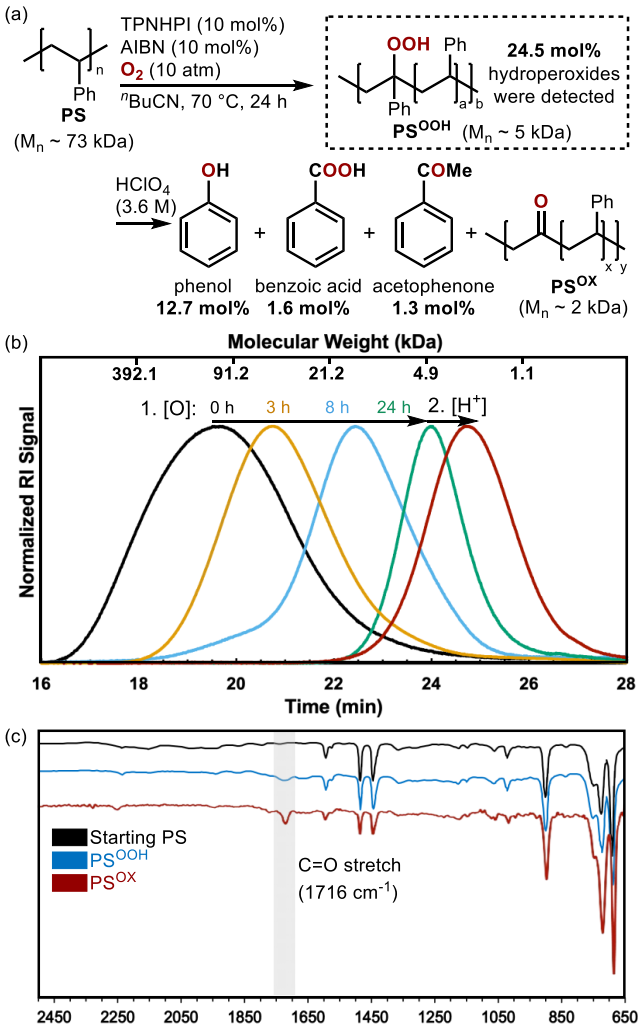

Figure 5. (a) Application of optimized Hock process conditions to polystyrene. Reaction conditions: 1.0 mmol of Ph-containing monomer units in polystyrene, 10 mol% TPNHPI (Tetraphenyl-*N*-hydroxyphthalimide), 10 mol% AIBN (azobisisobutyronitrile), O_2 (10 atm), 2 mL valeronitrile (^{n}BuCN) at 70 °C. (b) Gel permeation chromatographic time-course analysis of polystyrene during the oxidation, [O], and acid-promoted Hock rearrangement, [H$^+$]. (c) IR spectra of starting polystyrene and oxidized polystyrene before/after acid treatment.

respect to the hydroperoxide content (**Figure 5a**), corresponding to a 12.7% yield with respect to phenyl rings in the original PS sample. Other products, including benzoic acid (1.6% yield) and acetophenone (1.3% yield), were formed in only small quantities, showing that phenol is the major product formed upon treating PS under Hock process conditions. The same reaction sequence performed with various sources of post-consumer PS afforded similar yields of phenol (10–12%, **Figure S24**), indicating that this approach could be extended to waste plastic materials.

Gel permeation chromatographic analysis of the polymer during the autoxidation step revealed that the molecular weight of PS progressively decreased from 73 kDa to 2 kDa during the reaction (**Figure 5b**). These observations are consistent with chain scission occurring during the reaction, likely resembling observations made with the well-defined model compounds (cf. compounds **4**–**6** in **Figure 2**). A further decrease in molecular weight is observed upon treating the oxidized polymer with acid, as would be expected from release of phenol from the polymer backbone. IR spectroscopic analysis of the starting PS and solids recovered after acid treatment of the oxidized PS showed the appearance of a new peak at 1716 cm^{-1}, consistent with the introduction of carbonyl groups into the polymer backbone (**Figure 5c**).

Further Conversion of Oxidized PS to Oxygenated Aromatic Monomers. The above data indicate that treatment of PS under Hock process conditions leads to partial conversion to phenol, together with a partially oxidized, low-molecular-weight polymeric byproduct (PS^{OX}). We postulated that the latter material could be subjected to MC oxidation conditions (cf. **Figure 1a**), similar to those used previously to convert PS to benzoic acid (**Figure 6**).[15] To test this hypothesis, the PS^{OX} material obtained from the sequential Hock process conditions described above was separated from phenol by precipitation in pentane and washed with methanol. It was then subjected to the Co/Mn/NHPI-catalyzed oxidation in acetic acid, according to the previously reported conditions. This reaction led to a 48% yield of benzoic acid with respect the phenyl ring present in the original PS (i.e., before the Hock process treatment). This tandem Hock/MC-process sequence afforded 62% total yield of oxygenated aromatic monomers from PS, which may be compared to the 61% yield of benzoic acid obtained when PS is treated directly under the MC conditions (**Figure 6**).[42] These results show that the PS^{OX} byproduct retains aromatic subunits that may be converted to benzoic acid and, further, shows how the Hock process conditions may be used to divert a significant fraction of the phenyl rings in PS into phenol.

Implications for Adaptation of Small-Molecule Transformations to Polymers. The significance of this work goes beyond the possible practical application noted in **Figure 6**, as fundamental insights into the relative reactivity of small molecule and polymeric feedstocks have important implications for waste plastics remediation. To bridge the gap between the dimeric/trimeric PS model compounds and PS, we prepared two PS-like oligomers with an average molecular weight corresponding to pentamers and decamers. Both materials have narrow dispersity ($Đ$ = 1.05 and 1.02, respectively), and they were used as substrates under the Hock process conditions to produce phenol (**Figure 7**). Cumene was also included to establish a benchmark for the reactivity of PS and the PS analogs. The results show that the yield of phenol drops significantly for the dimer, relative to cumene (36% and 70% yield), and another significant decrease is observed between the trimer and dimer (17% and 36%). Further increases in the molecular weight, progressing from trimer to pentamer,

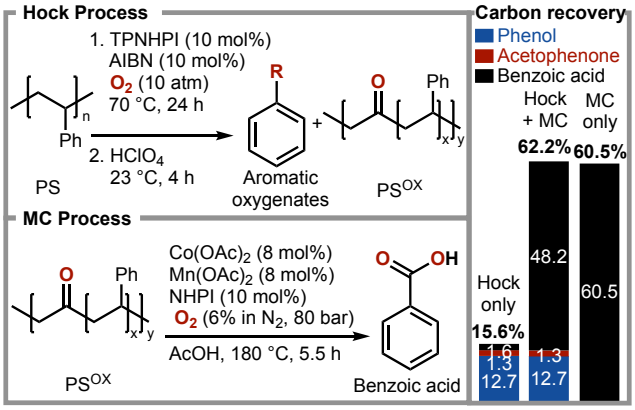

Figure 6. Sequential Hock and MC process. Hock process conditions: 1.0 mmol of PS, 10 mol% TPNHPI (tetraphenyl-*N*-hydroxyphthalimide), 10 mol% AIBN (azobisisobutyronitrile), O_2 (10 atm), 2 mL valeronitrile (^{n}BuCN) at 70 °C. MC process conditions: 1.0 mmol of virgin PS or PS^{OX} after Hock process, 8 mol% of $Co(OAc)_2$, 8 mol% of $Mn(OAc)_2$, 10 mol% of NHPI (*N*-hydroxyphthalimide), 80 bar of 6% O_2 in N_2, 5 mL of AcOH at 180 °C.

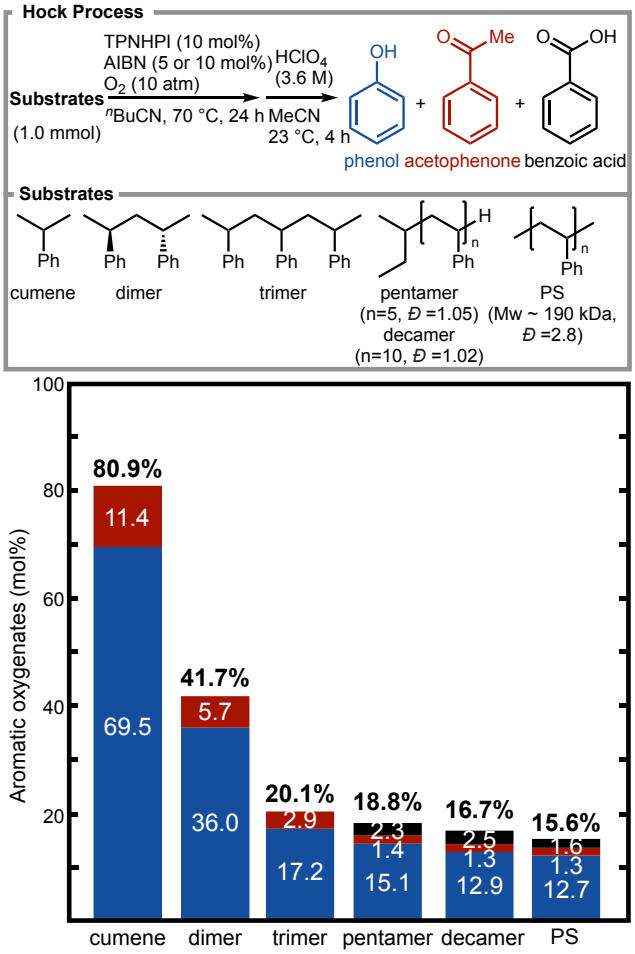

Figure 7. Effectiveness of Hock process on PS-like compounds ranging from cumene to PS. Hock process conditions: For cumene, dimer, and trimer: 1.0 mmol of substrate, 10 mol% TPNHPI (tetraphenyl-*N*-hydroxyphthalimide), 5 mol% AIBN (azobisisobutyronitrile), O_2 (10 atm), 2 mL valeronitrile (^{n}BuCN) at 70 °C. For pentamer, decamer, and PS: 1.0 mmol of substrates, 10 mol% TPNHPI, 10 mol% AIBN, O_2 (10 atm), 2 mL valeronitrile (^{n}BuCN) at 70 °C.

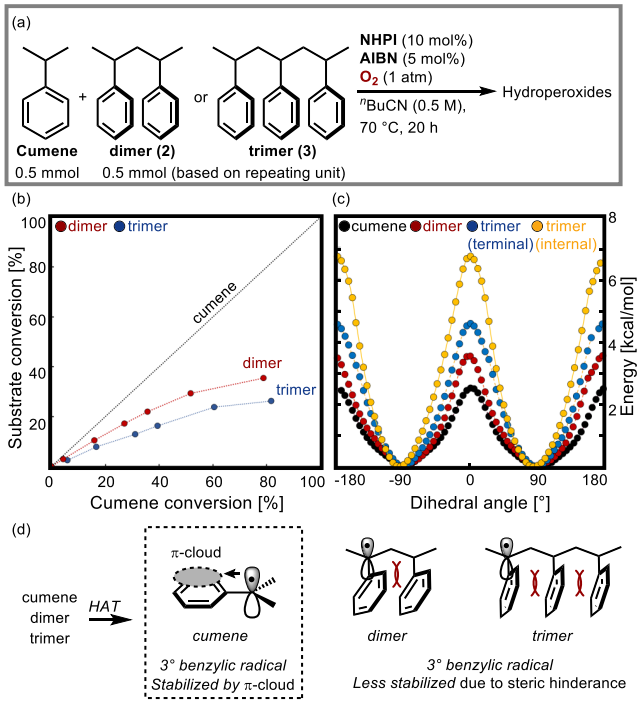

Figure 8. (a) Substrate conversion experiments under the reaction conditions: 0.5 mmol of substrates based on repeating units, 0.5 mmol of cumene, 10 mol% NHPI (*N*-hydroxyphthalimide), 5 mol% AIBN (azobisisobutyronitrile), O_2 (1 atm), 1 mL ^{n}BuCN at 70 °C. (b) The resulting substrate conversion graph under the reaction. (c) Rotational energy barriers for cumene, dimer, and trimer during dihedral angle scans. (d) Benzylic radical stabilization by phenyl group.

decamer, and PS, show relatively modest changes in phenol yield (17% – 13%).

The yield of phenol appears to be influenced most strongly by the yield of hydroperoxide in the initial autoxidation step. Although both autoxidation and acid-promoted rearrangement are influenced by the substrate identity, the major role of the autoxidation step is supported by the significant drop in hydroperoxide yield with cumene (77%), dimer (56%) and trimer (24%) (see above). To probe these differences further, we performed competition experiments in which cumene and the dimer or trimer were combined and subjected to the autoxidation conditions (**Figure 8a**). The conversion of each substrate was monitored, and a plot of the dimer/trimer conversion with respect to cumene conversion is shown in **Figure 8b**. The data confirm that the relative reactivity of the substrate decreases with increasing chain length, consistent with the computational data in **Figure 3a**, which reveal a higher activation barrier PINO-mediated HAT from the trimer relative to the dimer. To explore the origin of these trends, dihedral scans of the phenyl ring were performed with cumene and the dimer and trimer model compounds, and both terminal and internal phenyl rings were evaluated for the trimer (**Figure 8c**). The lowest energy conformer for each of the structures features a 90° (or 270°) dihedral angle between the plane of the phenyl ring and the plane of aliphatic backbone, and the highest energy arises when the phenyl ring and backbone are coplanar (0° and 180°). The data in **Figure 8c** reveal that increasing the number of PS subunits restricts the phenyl ring rotation. The energy of the coplanar conformation increases progressively in the sequence of cumene (2.5 kcal/mol), dimer (3.5 kcal/mol), terminal phenyl rings of the trimer (4.6 kcal/mol), and the internal phenyl ring of the trimer (6.7 kcal/mol). The coplanar conformation stabilizes the benzylic radical generated by HAT, and rotational restrictions will contribute to higher HAT barriers (**Figure 8d**). These insights show that, in spite of the structural similarity between cumene and PS subunits, the presence of adjacent groups in PS has energetic consequences for autoxidation that are not present in cumene. It is reasonable to expect that related considerations could impact other efforts to extend autoxidation reactivity from small molecules to polymers.

Conclusion

Phenol represents an ideal chemical target for valorization of waste PS. The present study introduces a strategy to achieve this goal by subjecting PS to Hock process conditions. Use of well-defined dimeric and trimeric model compounds provides valuable insights into the relationship between cumene, the conventional Hock process substrate, and PS. These compounds permit direct characterization of reaction intermediates and comparison of reaction performance between cumene with PS-like structures. The inclusion of pentameric and decameric PS structures shows progressive reactivity that links the well-defined model compounds to PS. Experimental and computational studies reveal that the phenol yield from PS is limited by restricted rotation of phenyl rings within the extended structure. The conditions outlined herein lead to a 13% yield of phenol from PS, establishing a foundation for future optimization studies that could consider other HAT mediators, initiators, and/or reaction conditions. The partially oxidized PS polymer obtained following treatment of PS under Hock process conditions is an effective substrate for treatment under MC autoxidation condition to convert the remaining phenyl rings into benzoic acid. Collectively, this study has led to important fundamental and practical outcomes relevant to the chemical recycling of waste plastics.

ASSOCIATED CONTENT

The Supporting Information is available free of charge on the ACS Publications website at DOI: xxxx

Experimental details with supplemental notes, characterization data, and NMR spectra (PDF).

AUTHOR INFORMATION

Corresponding Authors

Shannon S. Stahl – Department of Chemistry, University of Wisconsin-Madison, Madison, Wisconsin 53706, United States; The Wisconsin Energy Institute, University of Wisconsin-Madison, Madison, Wisconsin 53726, United States; orcid.org/0000-0002-9000-7665; E-mail: stahl@chem.wisc.edu

Ive Hermans – Department of Chemistry, University of Wisconsin-Madison, Madison, Wisconsin 53706, United States; The Wisconsin Energy Institute, University of Wisconsin-Madison, Madison, Wisconsin 53726, United States; Department of Chemical and Biological Engineering, University of Wisconsin−Madison, Madison, Wisconsin 53706, United States; orcid.org/0000-0001-6228-9928; E-mail: hermans@chem.wisc.edu

Authors

Doohyun Baek – Department of Chemistry, University of Wisconsin-Madison, Madison, Wisconsin 53706, United States; The Wisconsin Energy Institute, University of Wisconsin-Madison, Madison, Wisconsin 53726, United

States;
orcid.org/ 0000-0003-4059-2832

Abdullah J. Al Abdulghani – Department of Chemical and Biological Engineering, University of Wisconsin−Madison, Madison, Wisconsin 53706, United States;
orcid.org/0000-0002-8560-6209

Dylan J. Walsh – Department of Chemistry, University of Wisconsin-Madison, Madison, Wisconsin 53706, United States; The Wisconsin Energy Institute, University of Wisconsin-Madison, Madison, Wisconsin 53726, United States;
orcid.org/0000-0001-7981-2770

Dillon T. Hofsommer – Department of Chemistry, University of Wisconsin-Madison, Madison, Wisconsin 53706, United States; The Wisconsin Energy Institute, University of Wisconsin-Madison, Madison, Wisconsin 53726, United States; orcid.org/0000-0001-8638-2465

James B. Gerken – Department of Chemistry, University of Wisconsin-Madison, Madison, Wisconsin 53706, United States; orcid.org/0009-0000-9294-6300

Changxia Shi – Department of Chemistry, Colorado State University, Fort Collins, Colorado 80523, United States; orcid.org/0000-0002-5858-5692

Eugene Y.-X. Chen – Department of Chemistry, Colorado State University, Fort Collins, Colorado 80523, United States; orcid.org/0000-0001-7512-3484

Notes

The authors declare no competing financial interest.

ACKNOWLEDGMENT

This work was supported by the DOE Office of Science (Office of Basic Energy Sciences) grant DE-SC0023281. The work done at Colorado State University (CSU) was supported by the U.S. Department of Energy, Office of Energy Efficiency and Renewable Energy, Advanced Materials and Manufacturing Technologies Office (AMMTO), and Bioenergy Technologies Office (BETO), performed as part of the BOTTLE Consortium, which includes the members from CSU, and funded under contract no. DE-AC36-08GO28308 with the National Renewable Energy Laboratory, operated by the Alliance for Sustainable Energy. NMR spectrometers were supported by the NSF grant CHE-1048642 and by the Great Lakes Bioenergy Research Center (GLBRC) grant DE-SC0018409. Mass spectrometry was supported by the NIH grant 1S10 OD020022-1. We acknowledge the UW-Madison Department of Chemistry HPC Center and the UW-Madison Center for High Throughput Computing (CHTC) for providing computing resources.

REFERENCES

(1) Hidalgo-Crespo, J.; Moreira, C. M.; Jervis, F. X.; Soto, M.; Amaya, J. L.; Banguera, L. Circular Economy of Expanded Polystyrene Container Production: Environmental Benefits of Household Waste Recycling Considering Renewable Energies. *Energy Rep.* **2022**, *8*, 306–311. https://doi.org/10.1016/j.egyr.2022.01.071.

(2) Tullo, A. H. Plastic Has a Problem; Is Chemical Recycling the Solution? *Chem. Eng. News* **2019**, *97*, 29–34.

(3) Martín, A. J.; Mondelli, C.; Jaydev, S. D.; Pérez-Ramírez, J. Catalytic Processing of Plastic Waste on the Rise. *Chem* **2021**, *7*, 1487–1533. https://doi.org/10.1016/j.chempr.2020.12.006.

(4) Schyns, Z. O. G.; Shaver, M. P. Mechanical Recycling of Packaging Plastics: A Review. *Macromol. Rapid Commun.* **2021**, *42*, 2000415. https://doi.org/10.1002/marc.202000415.

(5) Chen, X.; Wang, Y.; Zhang, L. Recent Progress in the Chemical Upcycling of Plastic Wastes. *ChemSusChem* **2021**, *14*, 4137–4151. https://doi.org/10.1002/cssc.202100868.

(6) Zhang, F.; Wang, F.; Wei, X.; Yang, Y.; Xu, S.; Deng, D.; Wang, Y.-Z. From Trash to Treasure: Chemical Recycling and Upcycling of Commodity Plastic Waste to Fuels, High-Valued Chemicals and Advanced Materials. *J. Energy Chem.* **2022**, *69*, 369–388. https://doi.org/10.1016/j.jechem.2021.12.052.

(7) Xu, Z.; Sun, D.; Xu, J.; Yang, R.; Russell, J. D.; Liu, G. Progress and Challenges in Polystyrene Recycling and Upcycling. *ChemSusChem* **2024**, *17*, e202400474. https://doi.org/10.1002/cssc.202400474.

(8) Lopez, G.; Artetxe, M.; Amutio, M.; Alvarez, J.; Bilbao, J.; Olazar, M. Recent Advances in the Gasification of Waste Plastics. A Critical Overview. *Renew. Sustain. Energy Rev.* **2018**, *82*, 576–596. https://doi.org/10.1016/j.rser.2017.09.032.

(9) Peng, Y.; Wang, Y.; Ke, L.; Dai, L.; Wu, Q.; Cobb, K.; Zeng, Y.; Zou, R.; Liu, Y.; Ruan, R. A Review on Catalytic Pyrolysis of Plastic Wastes to High-Value Products. *Energy Convers. Manag.* **2022**, *254*, 115243. https://doi.org/10.1016/j.enconman.2022.115243.

(10) Musa, A.; Jaseer, E. A.; Barman, S.; Garcia, N. Review on Catalytic Depolymerization of Polyolefin Waste by Hydrogenolysis: State-of-the-Art and Outlook. *Energy Fuels* **2024**, *38*, 1676–1691. https://doi.org/10.1021/acs.energyfuels.3c04109.

(11) Ragaert, K.; Delva, L.; Van Geem, K. Mechanical and Chemical Recycling of Solid Plastic Waste. *Waste Manage.* **2017**, *69*, 24–58. https://doi.org/10.1016/j.wasman.2017.07.044.

(12) Oh, S.; Stache, E. E. Recent Advances in Oxidative Degradation of Plastics. *Chem. Soc. Rev.* **2024**, *53*, 7309–7327. https://doi.org/10.1039/D4CS00407H.

(13) Tomás, R. A. F.; Bordado, J. C. M.; Gomes, J. F. P. P-Xylene Oxidation to Terephthalic Acid: A Literature Review Oriented toward Process Optimization and Development. *Chem. Rev.* **2013**, *113*, 7421–7469. https://doi.org/10.1021/cr300298j.

(14) Partenheimer, W. Valuable Oxygenates by Aerobic Oxidation of Polymers Using Metal/Bromide Homogeneous Catalysts. *Catal. Today* **2003**, *81*, 117–135. https://doi.org/10.1016/S0920-5861(03)00124-X.

(15) Sullivan, K. P.; Werner, A. Z.; Ramirez, K. J.; Ellis, L. D.; Bussard, J. R.; Black, B. A.; Brandner, D. G.; Bratti, F.; Buss, B. L.; Dong, X.; Haugen, S. J.; Ingraham, M. A.; Konev, M. O.; Michener, W. E.; Miscall, J.; Pardo, I.; Woodworth, S. P.; Guss, A. M.; Román-Leshkov, Y.; Stahl, S. S.; Beckham, G. T. Mixed Plastics Waste Valorization through Tandem Chemical Oxidation and Biological Funneling. *Science* **2022**, *378*, 207–211. https://doi.org/10.1126/science.abo4626.

(16) Rabot, C.; Chen, Y.; Lin, S.-Y.; Miller, B.; Chiang, Y.-M.; Oakley, C. E.; Oakley, B. R.; Wang, C. C. C.; Williams, T. J. Polystyrene Upcycling into Fungal Natural Products and a Biocontrol Agent. *J. Am. Chem. Soc.* **2023**, *145*, 5222–5230. https://doi.org/10.1021/jacs.2c12285.

(17) Zhao, B.; Tan, H.; Yang, J.; Zhang, X.; Yu, Z.; Sun, H.; Wei, J.; Zhao, X.; Zhang, Y.; Chen, L.; Yang, D.; Deng, J.; Fu, Y.; Huang, Z.; Jiao, N. Catalytic Conversion of Mixed Polyolefins under Mild Atmospheric Pressure. *The Innovation* **2024**, *5*, 100586. https://doi.org/10.1016/j.xinn.2024.100586.

(18) Luo, X.; Zhan, J.; Mei, Q.; Zhang, S. Selective Oxidative Upgrade of Waste Polystyrene Plastics by Nitric Acid to Produce Benzoic Acid. *Green Chem.* **2023**, *25*, 6717–6727. https://doi.org/10.1039/D3GC00865G.

(19) Ong, A.; Teo, J. Y. Q.; Feng, Z.; Tan, T. T. Y.; Lim, J. Y. C. Organocatalytic Aerobic Oxidative Degradation of Polystyrene to Aromatic Acids. *ACS Sustainable Chem. Eng.* **2023**, *11*, 12514–12522. https://doi.org/10.1021/acssuschemeng.3c01387.

(20) Sun, C.; Guo, Y.; Liu, X.; Wang, Y. Heterogeneous Oxidative Upcycling of Polystyrene Plastics to Benzoic Acid under Air Conditions. *Catal. Sci. Technol.* **2024**, *14*, 6584–6591. https://doi.org/10.1039/D4CY00970C.

(21) Pinsuwan, K.; Phowattanachai, N.; Kaewnoparat, P.; Malakul Na Ayutthaya, A.; Poungboon, T.; Opaprakasit, P.; Petchsuk, A.; Opaprakasit, M. Chemical Recycling of Polystyrene Resin and Its

Single-Used Products *via* Nitric Acid Oxidation: Mechanisms and Effects of Other Plastic Contaminations. *Polymer* **2025**, *316*, 127888. https://doi.org/10.1016/j.polymer.2024.127888.
(22) Wang, M.; Wen, J.; Huang, Y.; Hu, P. Selective Degradation of Styrene-Related Plastics Catalyzed by Iron under Visible Light. *ChemSusChem* **2021**, *14*, 5049–5056. https://doi.org/10.1002/cssc.202101762.
(23) Cao, R.; Zhang, M.-Q.; Hu, C.; Xiao, D.; Wang, M.; Ma, D. Catalytic Oxidation of Polystyrene to Aromatic Oxygenates over a Graphitic Carbon Nitride Catalyst. *Nat. Commun.* **2022**, *13*, 4809. https://doi.org/10.1038/s41467-022-32510-x.
(24) Huang, Z.; Shanmugam, M.; Liu, Z.; Brookfield, A.; Bennett, E. L.; Guan, R.; Vega Herrera, D. E.; Lopez-Sanchez, J. A.; Slater, A. G.; McInnes, E. J. L.; Qi, X.; Xiao, J. Chemical Recycling of Polystyrene to Valuable Chemicals via Selective Acid-Catalyzed Aerobic Oxidation under Visible Light. *J. Am. Chem. Soc.* **2022**, *144*, 6532–6542. https://doi.org/10.1021/jacs.2c01410.
(25) Oh, S.; Stache, E. E. Chemical Upcycling of Commercial Polystyrene via Catalyst-Controlled Photooxidation. *J. Am. Chem. Soc.* **2022**, *144*, 5745–5749. https://doi.org/10.1021/jacs.2c01411.
(26) Qin, Y.; Zhang, T.; Ching, H. Y. V.; Raman, G. S.; Das, S. Integrated Strategy for the Synthesis of Aromatic Building Blocks via Upcycling of Real-Life Plastic Wastes. *Chem* **2022**, *8*, 2472–2484. https://doi.org/10.1016/j.chempr.2022.06.002.
(27) Li, T.; Vijeta, A.; Casadevall, C.; Gentleman, A. S.; Euser, T.; Reisner, E. Bridging Plastic Recycling and Organic Catalysis: Photocatalytic Deconstruction of Polystyrene via a C–H Oxidation Pathway. *ACS Catal.* **2022**, *12*, 8155–8163. https://doi.org/10.1021/acscatal.2c02292.
(28) Ghalta, R.; Bal, R.; Srivastava, R. Metal-Free Photocatalytic Transformation of Waste Polystyrene into Valuable Chemicals: Advancing Sustainability through Circular Economy. *Green Chem.* **2023**, *25*, 7318–7334. https://doi.org/10.1039/D3GC02591H.
(29) Nikitas, N. F.; Skolia, E.; Gkizis, P. L.; Triandafillidi, I.; Kokotos, C. G. Photochemical Aerobic Upcycling of Polystyrene Plastics to Commodity Chemicals Using Anthraquinone as the Photocatalyst. *Green Chem.* **2023**, *25*, 4750–4759. https://doi.org/10.1039/D3GC00986F.
(30) Oh, S.; Stache, E. E. Mechanistic Insights Enable Divergent Product Selectivity in Catalyst-Controlled Photooxidative Degradation of Polystyrene. *ACS Catal.* **2023**, *13*, 10968–10975. https://doi.org/10.1021/acscatal.3c02516.
(31) Ong, A.; Wong, Z. C.; Chin, K. L. O.; Loh, W. W.; Chua, M. H.; Ang, S. J.; Lim, J. Y. C. Enhancing the Photocatalytic Upcycling of Polystyrene to Benzoic Acid: A Combined Computational-Experimental Approach for Acridinium Catalyst Design. *Chem. Sci.* **2024**, *15*, 1061–1067. https://doi.org/10.1039/D3SC06388G.
(32) During preparation of this article, De Vos and coworkers reported an innovative stepwise process for production of terephthalic acid from PS. See: Giakoumakis, N. S.; Marquez, C.; De Oliveira-Silva, R.; Sakellariou, D.; De Vos, D. E. Upcycling of Polystyrene to Aromatic Polyacids by Tandem Friedel–Crafts and Oxidation Reactions. *J. Am. Chem. Soc.* **2024**, jacs.4c13265. https://doi.org/10.1021/jacs.4c13265.
(33) Ghanta, M.; Acharyya, S. S.; Chaudhari, R. V.; Subramaniam, B. Catalytic Aromatic Oxidations. In *Industrial Arene Chemistry*; John Wiley & Sons, Ltd, 2023; pp 1067–1106. https://doi.org/10.1002/9783527827992.ch36.
(34) Suresh, A. K.; Sharma, M. M.; Sridhar, T. Engineering Aspects of Industrial Liquid-Phase Air Oxidation of Hydrocarbons. *Ind. Eng. Chem. Res.* **2000**, *39*, 3958–3997. https://doi.org/10.1021/ie0002733.
(35) Weber, M.; Weber, M.; Kleine-Boymann, M. Phenol. In *Ullmann's Encyclopedia of Industrial Chemistry*; Wiley-VCH, Ed.; Wiley, 2004. https://doi.org/10.1002/14356007.a19_299.pub2.
(36) Fukuda, O.; Sakaguchi, S.; Ishii, Y. Preparation of Hydroperoxides by N-Hydroxyphthalimide-Catalyzed Aerobic Oxidation of Alkylbenzenes and Hydroaromatic Compounds and Its Application. *Adv. Synth. Catal.* **2001**, *343*, 809–813. https://doi.org/10.1002/1615-4169(20011231)343:8<809::AID-ADSC809>3.0.CO;2-1.
(37) Melone, L.; Gambarotti, C.; Prosperini, S.; Pastori, N.; Recupero, F.; Punta, C. Hydroperoxidation of Tertiary Alkylaromatics Catalyzed By N-Hydroxyphthalimide and Aldehydes under Mild Conditions. *Adv. Synth. Catal.* **2011**, *353*, 147–154. https://doi.org/10.1002/adsc.201000786.
(38) Kuhnle, A.; Duda, M.; Tanger, U.; Sheldon, R. A.; Manickam, S.; Arends, I. W. C. E. Method for Producing Aromatic Alcohols, Especially Phenol. US6720462B2, 2004.
(39) Dakka, J. M.; Buchanan, J. S.; Cheng, J. C.; Chen, T.-J.; DeCaul, L. C.; Helton, T. E.; Stanat, J. E.; Benitez, F. M. Process for Producing Phenol and/or Cyclohexanone. US8247627B2, 2012.
(40) Wang, K.; Dakka, J. M. Process for Producing Phenol. US9029612B2, 2015.
(41) All reactions with high pressures of O_2 were limited to small volumes (≤2 mL) with appropriate safety precautions (see section 1c of the Supporting Information). For larger-volume experiments, a dilute oxygen source (6% O_2 in N_2) was used to maintain pO_2 below the limiting oxygen concentrations. See the following for context: Osterberg, P. M.; Niemeier, J. K.; Welch, C. J.; Hawkins, J. M.; Martinelli, J. R.; Johnson, T. E.; Root, T. W.; Stahl, S. S. Experimental Limiting Oxygen Concentrations for Nine Organic Solvents at Temperatures and Pressures Relevant to Aerobic Oxidations in the Pharmaceutical Industry. *Org. Process Res. Dev.* **2015**, *19*, 1537–1543. https://doi.org/10.1021/op500328f.
(42) The MC-like conditions used here were adopted from ref. 15, which achieved a similar yield of benzoic acid when oxidizing PS with a similar M_w. We note that higher benzoic acid yields should be accessible by using the conventional Co/Mn/Br MC conditions, which require specialized equipment (see ref. 14, for context).

TOC Graphic:

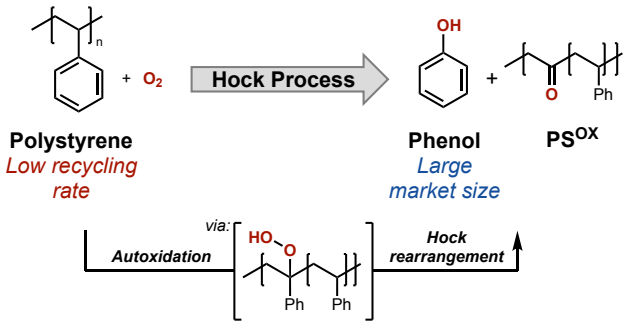
n
+ O2
Hock Process
OH
+
O
Ph
Polystyrene
Low recycling rate
Phenol
Large market size
PSOX
via:
HO
O
Ph
Ph
Autoxidation
Hock rearrangement

Supporting Information

Can the Hock Process Be Used to Produce Phenol from Polystyrene?

Doohyun Baek,[a,b] Abdullah J. Al Abdulghani,[c] Dylan J. Walsh,[a,b] Dillon T. Hofsommer,[a,b] James B. Gerken,[a] Changxia Shi,[d] Eugene Y.-X. Chen,[d] Ive Hermans,[a,b,c] and Shannon S. Stahl[a,b*]*

[a]Department of Chemistry, University of Wisconsin−Madison, Madison, Wisconsin 53706, United States

[b]The Wisconsin Energy Institute, University of Wisconsin−Madison, Madison, Wisconsin 53726, United States

[c]Department of Chemical and Biological Engineering, University of Wisconsin−Madison, Madison, Wisconsin 53706, United States

[d]Department of Chemistry, Colorado State University, Fort Collins, Colorado 80523, United States

*stahl@chem.wisc.edu; hermans@chem.wisc.edu

Table of Contents:

1. General Experimental Considerations

1a. Materials and reagents

All reagents were purchased and used as received unless otherwise noted. Cumene was vacuum-distilled and stored under an N_2 atmosphere before use. Tetrahydrofuran (THF) was distilled from sodium benzophenone ketyl and stored under an N_2 atmosphere before use. Valeronitrile (^{n}BuCN) was purchased from Sigma-Aldrich. Raney nickel was purchased from Sigma-Aldrich (Raney 2800, slurry in H_2O, active catalyst) and thoroughly washed with deionized water before use. Among the low molecular weight oligomers (pentamer and decamer), pentamer was synthesized following a previously reported method.[1] Decamer was synthesized by following the procedure from **Section 2c** in this Supporting Information. For decamer synthesis, initiator *sec*-butyl lithium solution (~1.4 M in cyclohexane) was purchased from Sigma-Aldrich and used as received. Monomer styrene and solvent cyclohexane were purchased from TCI America and VWR Chemicals BDH, respectively. Both the monomer and solvent were dried over CaH_2 while stirring overnight (~12 h) at ambient temperature and freshly distilled under vacuum (CaH_2 was removed via filtration before distillation) prior to performing the styrene oligomerization reactions. Polystyrene was purchased from Sigma Aldrich (M_w ~ 192 kDa). Tetraphenyl-*N*-hydroxyphthalimide (TPNHPI) was synthesized by following a previously reported method.[2] Other *N*-hydroxyphthalimide (NHPI) derivatives were purchased from Sigma Aldrich. 2,2´-Azobis(2-methylpropionitrile) (AIBN), 1,1´-Azobis(cyclohexanecarbonitrile) (ACHN), *tert*-Butyl hydroperoxide (tBuOOH), *tert*-Butyl peroxide (tBuOOtBu) were purchased from Sigma Aldrich. 2,2'-Azobis(2,4-dimethylvaleronitrile) (ADVN) was purchased from Fujifilm Wako chemicals.

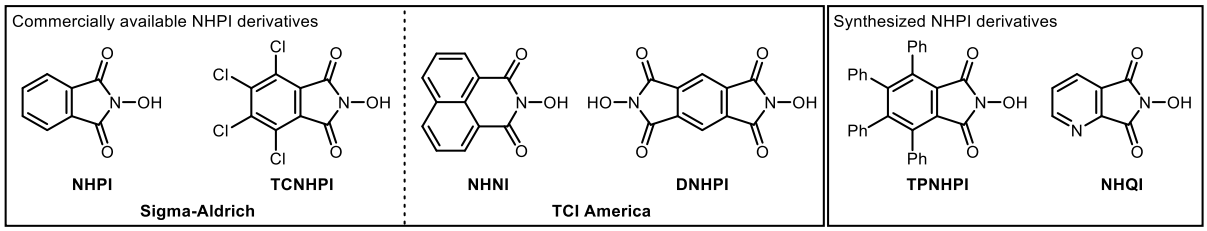

Figure S1. Chemical structures of the commercially available and synthesized *N*-hydroxyphthalimide (NHPI) derivatives.

1b. Equipment and instrumentation

Column chromatography was performed using an automated Combi-Flash with reusable 12 g, 25 g, or 40 g Silicycle cartridges or standard silica cartridges purchased from Teledyne Isco. Thin layer chromatographic (TLC) analysis was performed on Kieselgel 60 F254 aluminum backed silica plates, visualizing with UV light and/or staining with phosphomolybdic Acid (PMA) solution (10% in EtOH). NMR spectra (^{1}H and ^{13}C) were obtained with either a Bruker Avance III 400 MHz spectrometer or a Bruker Avance III 500 MHz spectrometer referenced against the residual solvent peaks: $CDCl_3$ peaks at 7.26 ppm (^{1}H) and 77.16 ppm (^{13}C); multiplicities are described using the following abbreviations: s = singlet, d = doublet, dd = doublet of doublet, m = multiplet. High-resolution mass spectra were obtained using a Thermo Q Exactive™ Plus via (ASAP-MS) by the mass spectrometry facility at the University of Wisconsin-Madison. Low pressure oxidation reactions were performed in a custom-built shaker equipped with a heater and gas manifold (Figure S6). High pressure oxidation reactions were performed with a Hastelloy Parr reactor from a Series 5000 Multiple Reaction System. GPC analysis was performed using a Viscotek GPCmax/VE 2001 instrument fitted with set of two PolyPore columns (molecular weight range: 500-400,000). Polymer samples were prepared with THF (concentration: 2.5 mg/mL) then injected at a flow rate of 1 mL/min at 40 °C. Polymers were characterized by their refractive index (RI) using a Viscotek model 302-050 tetra detector array. Omnisec software (Viscotek, Inc.) was used for initial data processing such as baseline correction and applying molecular weight calibrations. Molecular weight calibrations were determined using polystyrene standards (MW 580–364000 Da). In the case of the PS oligomers (pentamer

and decamer), GPC analysis was performed by the GPC instrument consisted of an Agilent HPLC system equipped with one guard column and two PLgel 5 μm mixed-C gel permeation columns and coupled with a Wyatt DAWN HELEOS II multi (18)-angle light scattering detector and a Wyatt Optilab TrEX dRI detector. The analysis was performed at 40 °C using chloroform as the eluent at a flow rate of 1.0 mL/min, using Wyatt ASTRA 7.1.2 molecular weight characterization software. The refractive index increment (d*n*/d*c*) of 0.1608 was used for polystyrene (PS) in chloroform.

UHPLC/UV analysis was obtained on a Waters Acquity UPLC equipped with a diode array detector and a Waters Acquity UPLC BEH C18 column (50 mm x 2.3 mm ID) at 45 °C. Solvent A was 0.1% formic acid in type 1 water and solvent B was HPLC grade acetonitrile with 0.1% formic acid (flow rate 0.75 mL/min). Calibration curves are shown in **Figure S2**. The reaction mixtures containing hydroperoxides (ROOH) were analyzed by UPLC after treatment with PMe_3, which converts hydroperoxides to the corresponding alcohols (ROH), forming $Me_3P{=}O$ as a byproduct. This treatment avoids complications in quantifying the hydroperoxides due to their instability and safety hazards associated with their handling – both of which limit the ability to generate calibration curves. A sample UPLC trace before/after adding PMe_3 in **Figure S3**. The products were identified by GC/MS and synthesized independently to make calibration curves if the products were not commercially available (compounds **7**, **8**, **9**, **10**). Otherwise, yields were quantified by the calibration curve using a 1,4-dimethoxybenzene as an internal standard with commercially available products without further purification.

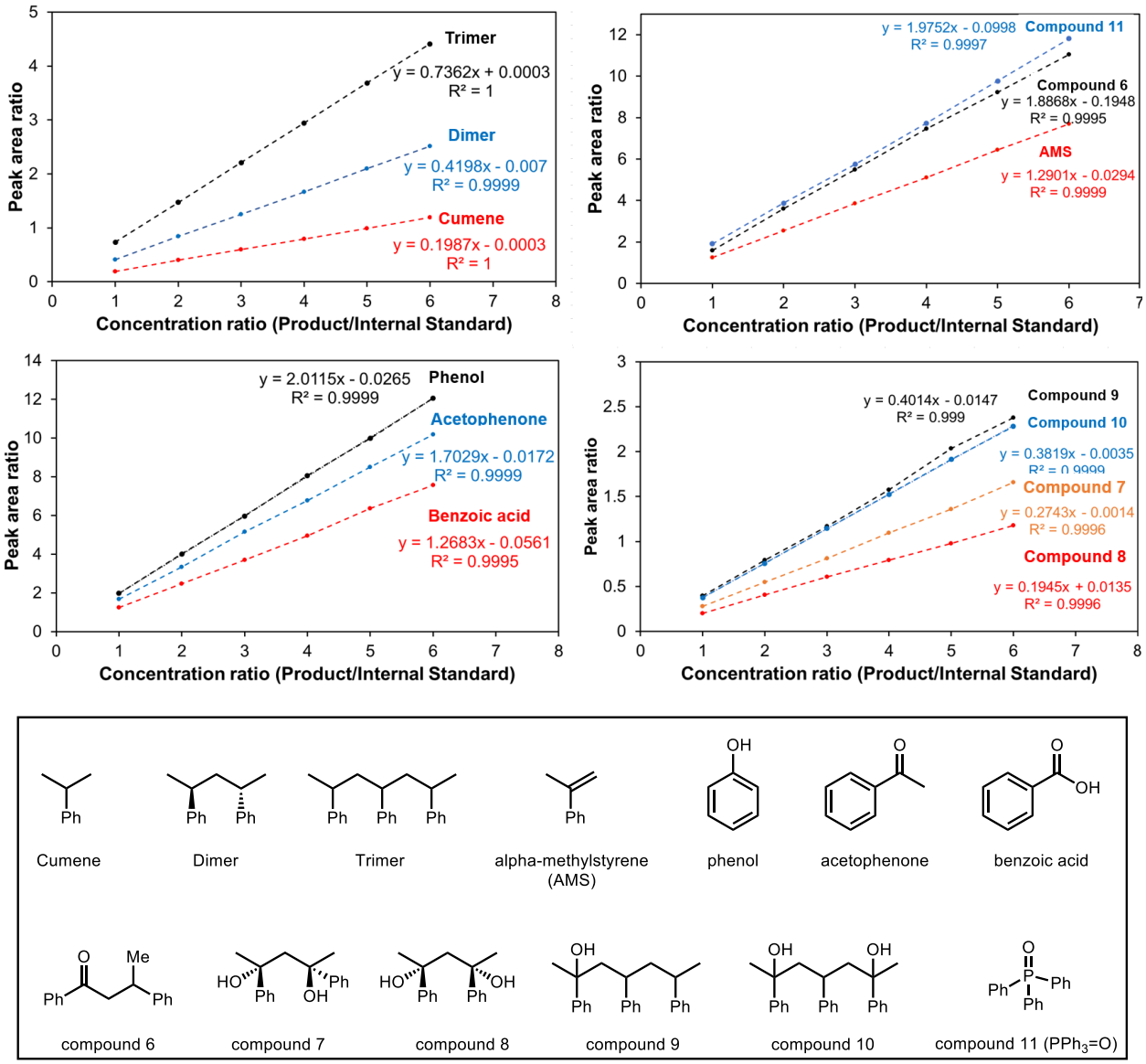

Figure S2. Calibration curves using the different analytes measured in this study by UPLC.

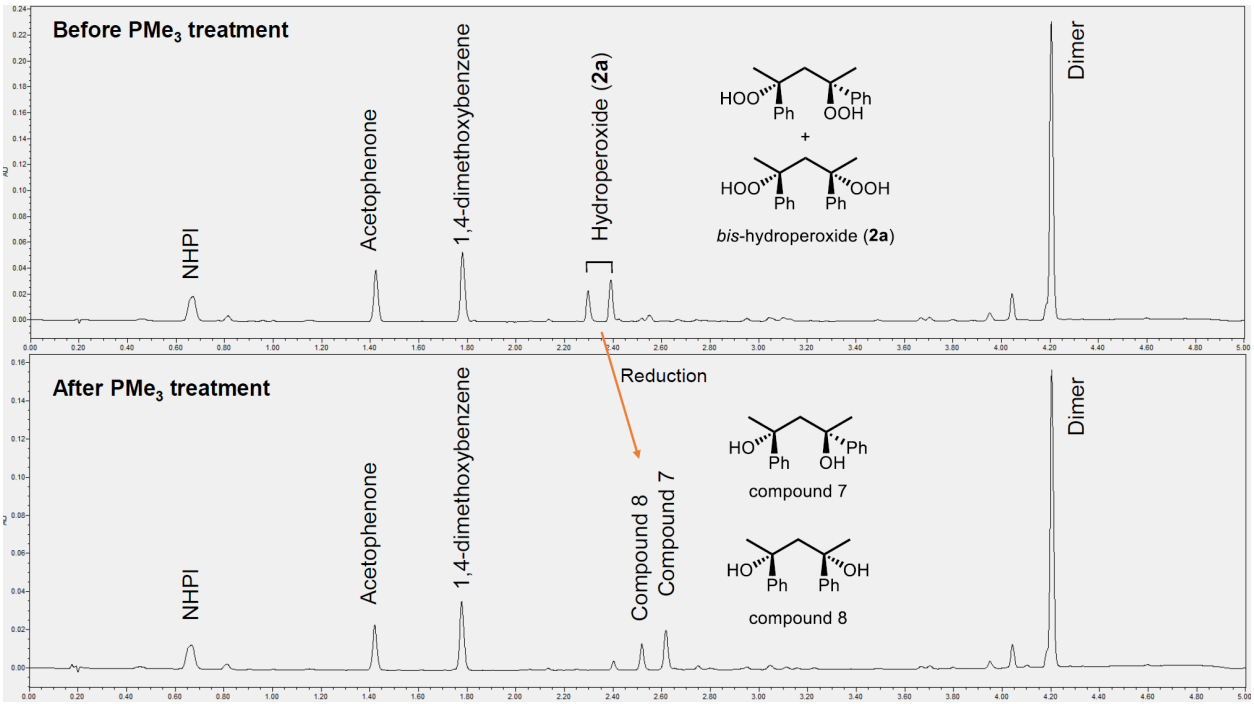

Figure S3. Sample UPLC traces obtained from analysis of the autoxidation reaction of dimer **2**, before (top) and after (bottom) PMe_3 treatment. The PMe_3 treatment avoid the instability and safety hazards associated with handling hydroperoxides, while still allowing quantitation.

1c. Safety considerations

I. Reactions in this paper form benzylic hydroperoxides which could be highly explosive when concentrated.[3a] The reactions should never be concentrated to dryness without ensuring that all remaining peroxides have been removed or quenched with appropriate reagents (e.g. PPh_3, PMe_3 or $Na_2S_2O_3$).

II. Several oxidation conditions in this study (e.g., the 10 atm O_2 condition) exceed the experimental limiting oxygen concentration for aerobic oxidation. To our knowledge, the limiting oxygen concentration of valeronitrile has not be measured, but the limiting oxygen concentration for acetonitrile has been reported.[3b] The limiting oxygen concentration of acetonitrile is 12.1 vol% at 10 bar and 100 °C. We exceeded these limits in our small-scale experiments reported herein, with safety precautions including use of ≤ 2 mL of solvent, double blast shields. For larger scale experiments, a diluted O_2 gas mixture, 6% O_2 in N_2, was used to stay below the limiting oxygen concentration.

III. For the synthesis of PS model compounds, care should be taken when handling Raney nickel, which is a highly pyrophoric solid when dried. It can ignite spontaneously in air.

IV. Perchloric acid is a strong and corrosive inorganic acid that can become explosive at concentrations greater than 85 wt%. It is a powerful oxidizer, especially at elevated temperatures, and may react violently with organic materials, metals, and reducing reagents. When handling perchloric acid, appropriate protective equipment, including gloves, goggles, and a fume hood should be used.

2. Synthesis of polystyrene model compounds

2a. Dimer synthesis

Scheme S1. Synthesis of polystyrene model dimer **2**.

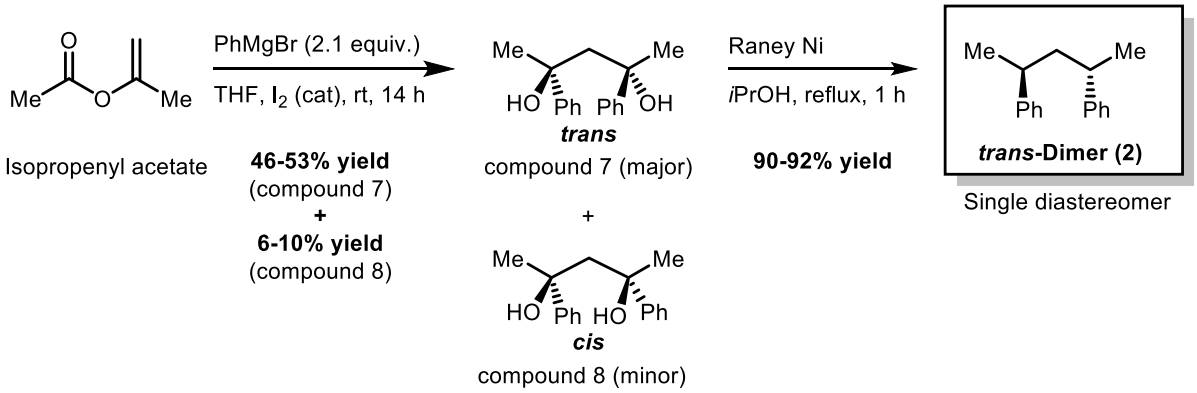

Compounds **7** and **8** were synthesized according to a literature procedure.[4] To a flame-dried Schlenk flask charged with stir bar and isopropenyl acetate (2.50 g, 25.0 mmol, 1 equiv.) in THF (31 mL), was added phenyl magnesium bromide (1.0 M in THF, 52.5 mL, 52.5 mmol, 2.1 equiv.) at -78 °C. The mixture was warmed to 23 °C under vigorous stirring for 12 h. The reaction was quenched with a saturated aqueous NH_4Cl solution and extracted with ethyl acetate. The combined organic layers were dried over $MgSO_4$ and concentrated under reduced pressure. Crude product was purified by flash chromatography (the product can be detected by phosphomolybdic acid (PMA) staining on TLC). Compound **7** was obtained as white solid (3.12 g, 49% yield). Compound **8** was obtained as white solid (510 mg, 8% yield).

(*trans*)-2,4-diphenylpentane-2,4-diol (Compound **7**)

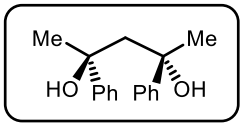

^{1}H-NMR (500 MHz, $CDCl_3$) δ: 7.48 (dd, J = 8.4, 1.3 Hz, 2H), 7.39 – 7.33 (m, 2H), 7.28 – 7.22 (m, 1H), 3.62 (s, 1H), 2.41 (s, 1H), 1.27 (s, 3H).
^{13}C-NMR (126 MHz, $CDCl_3$) δ: 149.30, 128.39, 126.70, 124.63, 76.16, 53.94, 32.05.
HRMS (ESI) calc'd for $C_{17}H_{17}$ $[M\text{-}2(H_2O)+H]^+$: 221.1325, found: 221.1322.

(*cis*)-2,4-diphenylpentane-2,4-diol (Compound **8**)

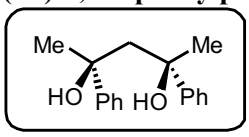

^{1}H-NMR (500 MHz, $CDCl_3$) δ 7.02 (dd, J = 8.2, 1.7 Hz, 4H), 7.00 – 6.92 (m, 6H), 3.22 (s, 2H), 2.62 (d, J = 14.8 Hz, 1H), 2.45 (d, J = 14.8 Hz, 1H), 1.56 (s, 6H).
^{13}C-NMR (126 MHz, $CDCl_3$) δ 147.15, 127.64, 125.82, 124.64, 75.92, 54.05, 33.96.
HRMS (ESI) calc'd for $C_{17}H_{17}$ $[M\text{-}2(H_2O)+H]^+$: 221.1325, found: 221.1322.

The NMR spectra matched with previously reported literature.[4]

(*trans*)-pentane-2,4-diyl)dibenzene (*trans*-dimer, **2**)
The following deoxygenation step was adapted from literature procedures.[5] To a flame-dried Schlenk flask charged with stir bar, 5 g of Raney Ni (Raney 2800, slurry in water, active catalyst) was added under inert atmosphere. The Raney Ni slurry was washed with distilled H_2O (7 times) and *i*PrOH (5 times). After washing, 30 mL of iPrOH and compound **7** (2.56 g, 10 mmol) were added to the flask attached with a condenser. The reaction was refluxed with vigorous stirring for 2 hours. The crude reaction mixture was

filtered through Celite and purified by column chromatography using hexane as an eluent (2.01 g, 93% yield).

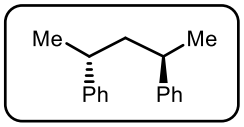

^{1}H-NMR (500 MHz, $CDCl_3$) δ 7.31 (m, 2H), 7.24 – 7.17 (m, 1H), 7.16 – 7.10 (m, 2H), 2.51 (h, J = 6.9 Hz, 1H), 1.89 (t, J = 7.5 Hz, 1H), 1.18 (d, J = 6.9 Hz, 3H).
^{13}C-NMR (126 MHz, $CDCl_3$) δ 146.88, 127.88, 126.79, 125.45, 46.37, 37.24, 22.88.

The NMR spectra matched with previously reported literature.[6]

2b. Trimer synthesis

Scheme S2. Trimer synthesis.

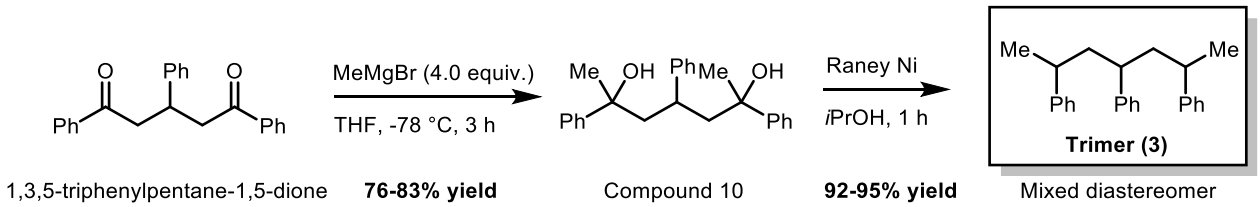

2,4,6-triphenylheptane-2,6-diol (Compound **10**)
1,3,5-triphenylpentane-1,5-dione was synthesized by following previous literature.[7a] To a flame-dried Schlenk flask charged with stir bar and 1,3,5-triphenylpentane-1,5-dione (2.4 g, 7.3 mmol, 1 equiv.) in THF (24 mL), methyl magnesium bromide (3.0 M in THF, 9.7 mL, 29.2 mmol, 4.0 equiv.) were added at -78 °C and stirred for 2 h at -78 °C. The reaction was quenched with a saturated aqueous NH_4Cl solution and extracted with ethyl acetate. The combined organic layers were dried over $MgSO_4$ and concentrated under reduced pressure. Crude product was purified by flash chromatography (the product can be detected by phosphomolybdic acid (PMA) staining on TLC). Compound **10** was obtained as a colorless oil (2.1 g, 81% yield).

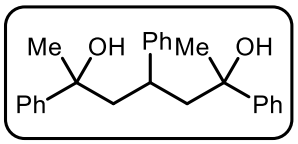

^{1}H-NMR (500 MHz, $CDCl_3$) δ 7.36 – 7.11 (m, 13H), 6.98 – 6.81 (m, 2H), 2.75 – 2.64 (m, 1H), 2.47 (dd, *J* = 14.6, 4.3 Hz, 1H), 2.31 – 2.12 (m, 5H), 1.46 – 1.35 (m, 6H).
^{13}C-NMR (101 MHz, $CDCl_3$) δ 147.80, 147.39, 147.23, 146.86, 145.72, 128.70, 128.31, 127.65, 127.62, 127.54, 127.12, 126.40, 125.97, 125.94, 125.90, 125.70, 124.49, 124.30, 124.26, 75.28, 75.25, 75.14, 51.62, 51.03, 50.90, 37.35, 37.05, 30.84, 30.22.
HRMS (ESI) calc'd for $C_{25}H_{25}$ $[M-2(H_2O)+H]^+$: 325.1951, found: 325.1945.

heptane-2,4,6-triyltribenzene (trimer, **3**; mixed diastereomers)
The following deoxygenation step was adapted from literature procedures.[5] To a flame-dried Schlenk flask charged with stir bar, 5 g of Raney Ni (Raney 2800, slurry in water, active catalyst) was added under inert atmosphere. The Raney Ni slurry was washed with distilled H_2O (7 times) and *i*PrOH (5 times). After washing, 30 mL of iPrOH and compound **10** (1.80 g, 5.1 mmol) were added to the flask attached with a condenser. The reaction was refluxed with vigorous stirring for 2 hours. The crude reaction mixture was filtered through Celite and purified by column chromatography using hexane as an eluent (1.57 g, 94% yield).

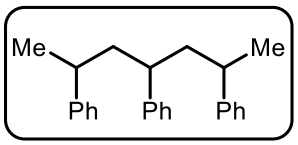

^{1}H-NMR (500 MHz, $CDCl_3$) δ 7.36 – 7.07 (m, 10H), 7.01 (m, 5H), 2.67 – 2.14 (m, 3H), 2.07 – 1.67 (m, 4H), 1.30 – 1.02 (m, 6H).
^{13}C-NMR (101 MHz, $CDCl_3$) δ 148.15, 147.91, 147.24, 146.99, 145.99, 145.62, 145.54, 128.59, 128.46, 128.41, 128.38, 128.36, 128.34, 128.12, 127.95, 127.68, 127.38, 127.20, 126.95, 126.93, 126.18, 126.11, 126.08, 125.97, 125.92, 125.81, 46.53, 45.82, 45.55, 45.23, 41.33, 41.12, 37.63, 37.61, 37.03, 29.86, 23.96, 23.37, 21.36, 21.18.

The NMR spectra matched with previously reported literature.[6]

2c. PS oligomer synthesis (pentamer and decamer)

The synthesis of decamer follows the previous procedures reported for the synthesis of pentamer (M_n = 510 Da, $Đ$ = 1.05).[1] Inside an inert glovebox (typically <1.0 ppm oxygen and moisture), an oven and vacuum dried 1 L round-bottom flask was equipped with a stir bar and charged with 600 mL dry cyclohexane and 55 mL styrene (0.48 mol). Initiator *sec*-BuLi (34 mL, 48 mmol) was placed in a 100 mL beaker first, then poured into the round-bottom flask in seconds to initiate the polymerization. The reaction mixture turned deep red immediately. After 15 min, the polymerization was quenched by addition of 5 mL argon-purged methanol. The flask was removed out of the glovebox, and the quenched solution was filtered through a pad of celite to remove the lithium salt. The filtrate was concentrated under reduced pressure, and the residue was redissolved in a small amount dichloromethane. The resulting solution was precipitated into 2 L cold methanol, filtered, and washed with cold methanol. This procedure was repeated twice, and the resulting product was dried in a vacuum oven at 30 °C for 3 days to a constant weight to give 41 grams of average decamer (76% yield; M_n = 1,010 Da; $Đ$ = 1.02).

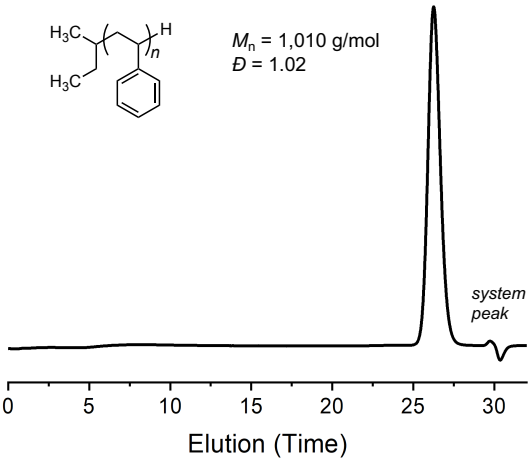

Figure S4. GPC trace of decamer (n=10, M_n = 1,010 Da, $Đ$ = 1.02) from the RI detector.

3. General experimental procedure with polystyrene model compounds

3a. Benchmarking autoxidation reactions with cumene as the substrate.

Reaction setup: The autoxidation of cumene (**1**) to cumene hydroperoxide (**1a**) has been reported by Ishii and coworkers to proceed in acetonitrile. Before initiating reactions with PS model compounds and PS, we benchmarked the previously reported conditions using a "shaker reactor" (see Section 3b) and a high-pressure Parr reactor (see Section 3c). The results, illustrated in Figure S5 validate the previous report provided a foundation for further testing of autoxidation reactions with PS model compounds and PS.

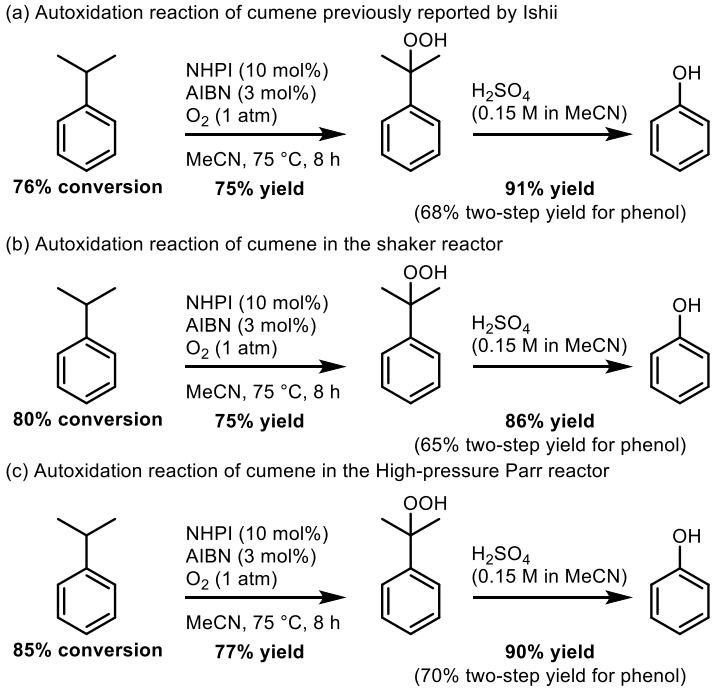

Figure S5. Autoxidation reaction of cumene (a) previously reported by Ishii and coworkers and (b) under the same conditions but using reaction vessels employed in this study.

3b. Reaction optimization at 1 atm O_2

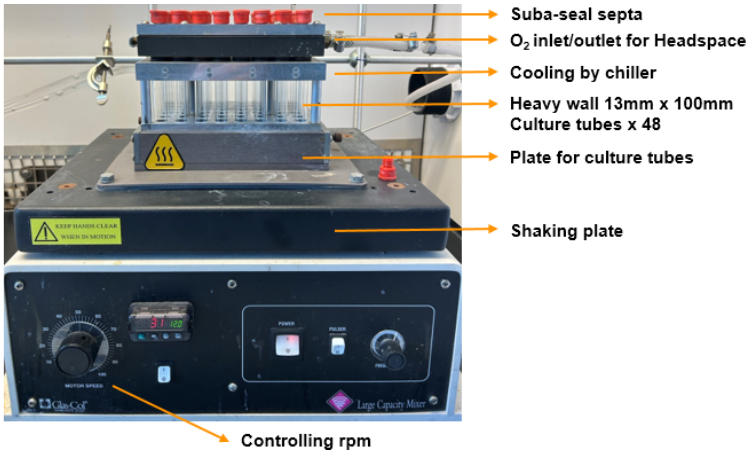

Figure S6. Custom shaker reactor.

Reaction setup: A custom 48 tube shaker equipped with a gas manifold capable of maintaining an O_2 atmosphere was used. Reagents were added sequentially to disposable heavy wall 13 mm x 100 mm culture tubes. First, PS model compound is added (0.5 mmol based on repeating unit: **2,** 56 mg; **3**, 55 mg) to the tubes. TPNHPI (23.4 mg, 0.05 mmol), AIBN (4.1 mg, 0.025 mmol) and C_4H_9CN (1.0 mL) were added sequentially. The test tube was loaded onto the preheated custom parallel shaker reactor. The reactor was purged with O_2 (1 atm) for 3 minutes. The mixture was allowed to shake (60 rpm) at the indicated temperature and time. Then, the reaction mixtures were removed from the parallel reactor and allowed to cool to 23 °C. The resulting mixture was quenched as below.

Quench 1. Phosphine quench to quantify hydroperoxides and other products

Workup with PMe_3: 1 mL of PMe_3 solution (1 mmol, 1.0 M in THF) was added to the reaction mixture under inert atmosphere. The reaction mixture was shaken for 30 minutes to fully reduce the generated hydroperoxides to the corresponding alcohols. To the culture tubes was added 10 mg of 1,4-dimethoxybenzene as an internal standard. The reaction mixture was diluted by adding 4 mL C_4H_9CN and a 50 µL aliquot was removed for UPLC analysis to measure the corresponding alcohols resulting from reduction of the hydroperoxides. Unreacted polystyrene model compounds, benzoic acid, α-methylstyrene, acetophenone, and alcohol products were quantified by comparison to a calibration curve using commercially available compounds or compounds synthesized in section 2.

Quench 2. Acid treatment to quantify phenol and other products

1 mL of $HClO_4$ solution (3.6 M in MeCN) was added to the culture tubes and the mixture was allowed to shake (60 rpm) for 4 h at 23 °C. The tubes were removed from the reactor, and 10 mg of 1,4-dimethoxybenzene was added as an internal standard. The reaction mixture was diluted by adding 4 mL MeCN and 50 µL aliquot was removed for UPLC analysis to measure the products. Unreacted model compounds, phenol, α-methylstyrene, and acetophenone were quantified by comparison to a calibration curve using commercially available compounds.

3c. High pressure oxidation using a Parr reactor

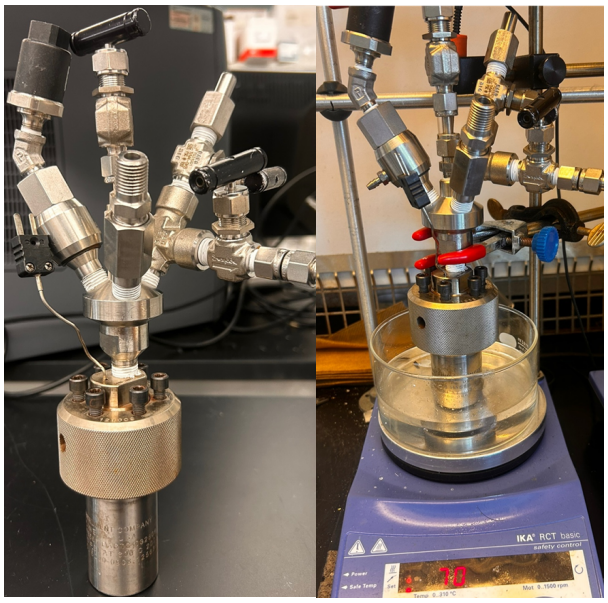

Figure S7. Parr reactor setup.

Reaction setup: High pressure reaction conditions were screened using a stainless steel Parr reactor from Series 5000 Multiple Reaction System. To the reactor vessels were added sequentially: a magnetic stir bar, PS model compounds (1.0 mmol based on repeat unit), TPNHPI (46.8 mg, 0.1 mmol), AIBN (8.2 mg, 0.05 mmol), and C_4H_9CN (2.0 mL). The vessel was pressurized to the desired pressure and loaded onto an oil bath preheated to a set temperature using a hotplate. The mixture was stirred at the indicated temperature and time. Then, the reaction mixture was allowed to cool to 23 °C, the solution was transferred to a 10 mL Schlenk flask, and the Parr reactor was rinsed into the Schlenk flask with 2 mL of C_4H_9CN.

Quench 1. Phosphine quench to quantify hydroperoxides and other products

Workup with PMe_3: To the reaction mixture in a 10 mL Schlenk flask is added 2 mL of PMe_3 solution (2 mmol, 1.0 M in THF) under inert atmosphere to reduce the generated hydroperoxides to the corresponding alcohols. To the reaction mixture was added 10 mg of 1,4-dimethoxybenzene as internal standard. The reaction mixture was diluted by adding 6 mL C_4H_9CN, and a 50 μL aliquot was removed for UPLC analysis to measure the corresponding alcohols produced from reduction of hydroperoxides. Unreacted PS model compounds, α-methylstyrene, acetophenone, and alcohol products were quantified by comparison to a calibration curve using compounds synthesized in section 2.

Quench 2. Acid treatment to quantify phenol and other products

2 mL of $HClO_4$ solution (3.6 M in MeCN) was added to the flask and the mixture was stirred for 4 h at 23 °C. 10 mg of 1,4-dimethoxybenzene was added into the flask. The reaction mixture was diluted by adding 8 mL MeCN and 50 μL aliquot was removed for UPLC analysis to measure the products. Unreacted polystyrene model compounds, phenol, α-methylstyrene, and acetophenone, were quantified by comparison to a calibration curve using commercially available compounds.

3d. Major products identified after phosphine quench (Hock process step 1)

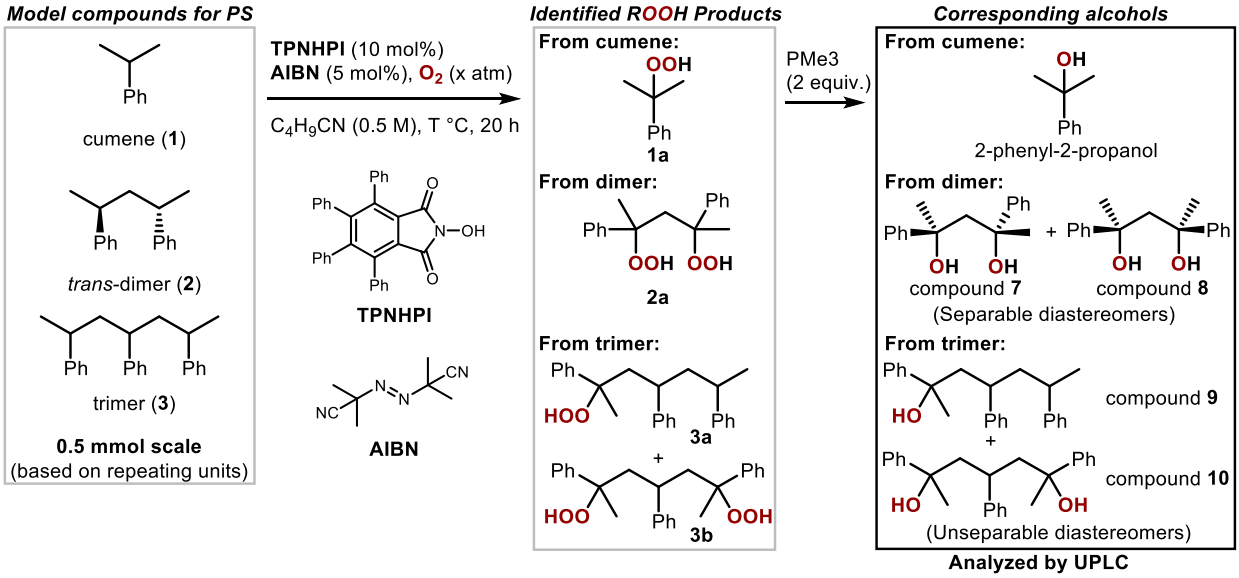

Figure S8. Identified major products after 1st step.

UPLC trace of compound 7 and 8: Compounds **7** and **8** were separable diastereomers by UPLC and flash chromatography. They were Independently synthesized and used to make calibration curve using UPLC. This step is same as compound **7** and **8** synthesis during dimer preparation (**Section 2a** in this Supporting Information).

***trans*-2,4-diphenylpentane-2,4-diol** (Compound **7**)

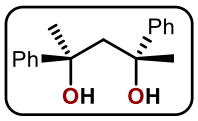

^{1}H-NMR (500 MHz, $CDCl_3$) δ 7.48 (dd, J = 8.4, 1.3 Hz, 2H), 7.39 – 7.33 (m, 2H), 7.28 – 7.22 (m, 1H), 3.62 (s, 1H), 2.41 (s, 1H), 1.27 (s, 3H).
^{13}C-NMR (126 MHz, $CDCl_3$) δ 149.30, 128.39, 126.70, 124.63, 76.16, 53.94, 32.05.
HRMS (ESI) calc'd for $C_{17}H_{17}$ $[M-2(H_2O)+H]^+$: 221.1325, found: 221.1322.

The NMR spectra matched with previously reported literature.[4]

***cis*-2,4-diphenylpentane-2,4-diol** (Compound **8**)

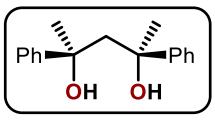

^{1}H-NMR (500 MHz, $CDCl_3$) δ 7.02 (dd, J = 8.2, 1.7 Hz, 4H), 7.00 – 6.92 (m, 6H), 3.22 (s, 2H), 2.62 (d, J = 14.8 Hz, 1H), 2.45 (d, J = 14.8 Hz, 1H), 1.56 (s, 6H).
^{13}C-NMR (126 MHz, $CDCl_3$) δ 147.15, 127.64, 125.82, 124.64, 75.92, 54.05, 33.96.
HRMS (ESI) calc'd for $C_{17}H_{17}$ $[M-2(H_2O)+H]^+$: 221.1325, found: 221.1322.

The NMR spectra matched with previously reported literature.[4]

UPLC trace of compound 9: Compound **9** was independently synthesized and used to make calibration curve using UPLC by following synthetic procedure.

Scheme S3. Compound **9** synthesis.

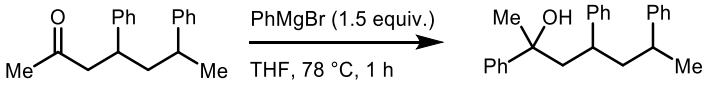

4,6-diphenylheptan-2-one **61% yield** Compound **9**

4,6-diphenylheptan-2-one was prepared by following previous literature.[7b] To a flame-dried Schlenk flask charged with stir bar and 4,6-diphenylheptan-2-one (521 mg, 2.0 mmol, 1 equiv.) in THF (10 mL), phenyl magnesium bromide (1.0 M in THF, 2.9 mL, 2.9 mmol, 1.5 equiv.) were added at -78 °C. The mixture was stirred for 1 h at -78 °C. The reaction was quenched with a saturated aqueous NH_4Cl solution and extracted with ethyl acetate. The combined organic layers were dried over $MgSO_4$ and concentrated under reduced pressure. Crude product was purified by flash chromatography (the product can be detected by phosphomolybdic acid (PMA) staining on TLC). Compound **9** was obtained as a colorless oil (411 mg, 61% yield).

2,4,6-triphenylheptan-2-ol (Compound **9**)

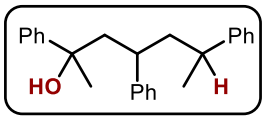

^{1}H-NMR (500 MHz, $CDCl_3$) δ 7.42 – 7.30 (m, 2H), 7.30 – 7.17 (m, 9H), 7.10 – 6.97 (m, 4H), 2.75 – 2.26 (m, 2H), 2.26 – 1.60 (m, 4H), 1.57 (s, 1H), 1.45 (d, J = 26.4 Hz, 3H), 1.15 (dd, J = 29.6, 6.9 Hz, 3H).
^{13}C-NMR (126 MHz, $CDCl_3$) δ 148.19, 147.93, 147.88, 146.77, 146.25, 146.09, 129.04, 128.88, 128.76, 128.60, 128.44, 128.16, 128.08, 128.03, 127.75, 127.40, 127.23, 126.94, 126.80, 126.64, 126.51, 126.42, 126.28, 126.20, 126.00, 125.96, 124.98, 124.94, 124.86, 75.75, 75.38, 75.24, 51.66, 50.98, 49.84, 47.17, 47.06, 46.51, 39.67, 39.45, 37.60, 36.96, 36.80, 32.39, 30.03, 29.92, 23.91, 21.43, 21.12. 33.96.
HRMS (ESI) calc'd for $C_{25}H_{27}O$ $[M-H]^-$: 343.2056, found: 343.2060.

UPLC trace of compound 10: Compound **10** was independently synthesized and used to make calibration curve using UPLC. This step is same as compound **10** synthesis during trimer preparation (**Section 2b** in this Supporting Information).

Scheme S4. Compound **10** synthesis.

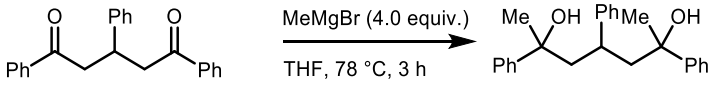

1,3,5-triphenylpentane-1,5-dione **76-83% yield** Compound **10**

2,4,6-triphenylheptane-2,6-diol (compound **10**)

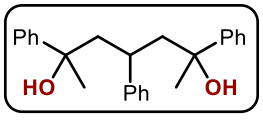

^{1}H-NMR (500 MHz, $CDCl_3$) δ 7.36 – 7.11 (m, 13H), 6.98 – 6.81 (m, 2H), 2.75 – 2.64 (m, 1H), 2.47 (dd, *J* = 14.6, 4.3 Hz, 1H), 2.31 – 2.12 (m, 5H), 1.46 – 1.35 (m, 6H).
^{13}C-NMR (126 MHz, $CDCl_3$) δ 147.80, 147.39, 147.23, 146.86, 145.72, 128.70, 128.31, 127.65, 127.62, 127.54, 127.12, 126.40, 125.97, 125.94, 125.90, 125.70, 124.49, 124.30, 124.26, 75.28, 75.25, 75.14, 51.62, 51.03, 50.90, 37.35, 37.05, 30.84, 30.22.
HRMS (ESI) calc'd for $C_{25}H_{25}$ $[M-2(H_2O)+H]^+$: 325.1951, found: 325.1945.

3e. Inhibitory effect of α-methylstyrene in the autoxidation reaction of dimer

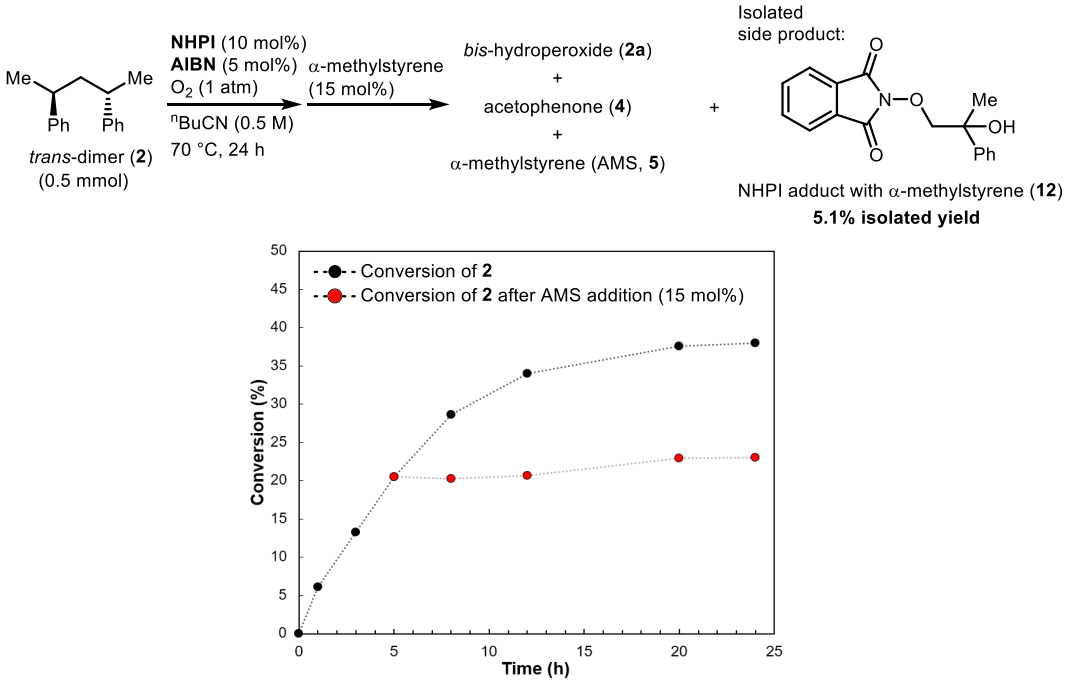

Figure S9. Inhibitory effect of α-methylstyrene in the autoxidation reaction of dimer (**2**).

A custom 48-tube shaker equipped with a gas manifold capable of maintaining an O_2 atmosphere was used. Two disposable heavy-wall 13 mm x 100 mm culture tubes were prepared. Reagents were added sequentially to each of the culture tubes: first, dimer (112 mg, 0.5 mmol; 1.0 mmol based on the repeating unit) was added to the tubes. Then, NHPI (16.4 mg, 0.10 mmol), AIBN (8.2 mg, 0.050 mmol), and valeronitrile (nBuCN, 2.0 mL) were added. The test tubes were loaded onto the preheated custom parallel shaker reactor. The reactor was purged with O_2 (1 atm) for 3 minutes. The mixture was allowed to shake (60 rpm). After 5 hours, 15 mol% of α-methylstyrene (9.7 μL, 0.075 mmol) was added to one of the test tubes. For each time point, a 20 μL aliquot was removed from the test tubes and mixed with 20 μL of a stock solution (691 mg of 1,4-dimethoxybenzene in 10 mL of MeCN) of the internal standard for UPLC analysis. Conversion was calculated based on the consumed starting substrates. After the reaction, TLC analysis (hexane:ethyl acetate 4:1) with phosphomolybdic acid (PMA) staining showed a clear spot that could be isolated. The crude residue was purified by flash chromatography, and compound **12** was isolated (7.6 mg, 5.1% yield).

The observation of compound **12** suggests that the inhibitory effect of α-methylstyrene (**5**) is attributed to its reactivity with the PINO radical, ultimately terminating the radical chain reaction by trapping the PINO radical.

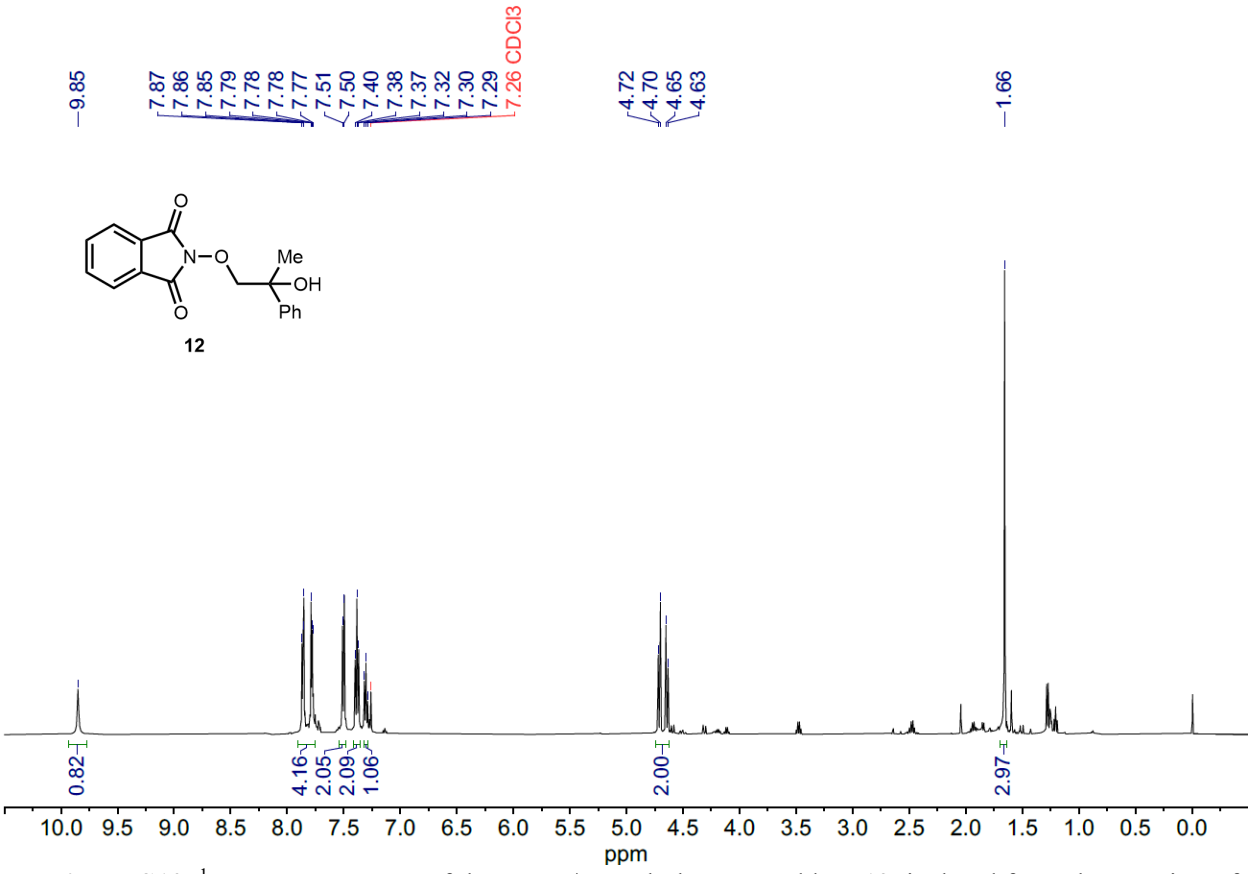

Figure S10. [1]H NMR spectrum of the PINO/α-methylstyrene adduct **12**, isolated from the reaction of *trans*-**2** under NHPI-initiated autoxidation conditions.

2-(2-hydroxy-2-phenylpropoxy)isoindoline-1,3-dione (compound **12**)

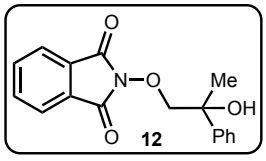

[1]H-NMR (500 MHz, $CDCl_3$) δ 9.85 (s, 1H), 7.90 – 7.76 (m, 4H), 7.50 (d, J = 7.1 Hz, 2H), 7.38 (t, J = 7.7 Hz, 2H), 7.30 (t, J = 7.3 Hz, 1H), 4.74 – 4.63 (m, 2H), 1.66 (s, 3H)

The NMR spectra matched the previously reported literature.[7c]

4. Reaction optimization

4a. Peroxidation step (1st step) optimization

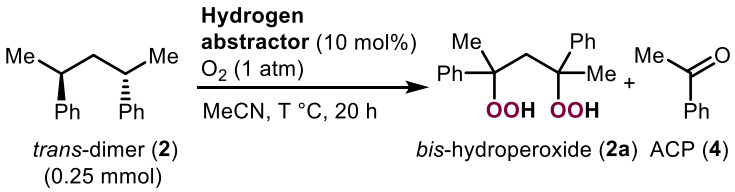

Entry	Hydrogen Abstractor	Solvent	T [°C]	Conv. [%]	**2a** [%]	**4** [%]
1	-	MeCN	120	6	1.0	4.2
2	-	MeCN	100	4	0.6	1.3
3	AIBN	MeCN	100	7	0.5	3.1
4	ACHN	MeCN	100	6	0.6	2.8
5	ADVN	MeCN	100	9	0.8	3.5
6	tBuOOH	MeCN	100	2	-	0.8
7	tBuOOtBu	MeCN	100	3	-	0.5
8	NHPI	MeCN	100	21	10	5.8
9	NHPI	MeCN	70	17	13	2.0

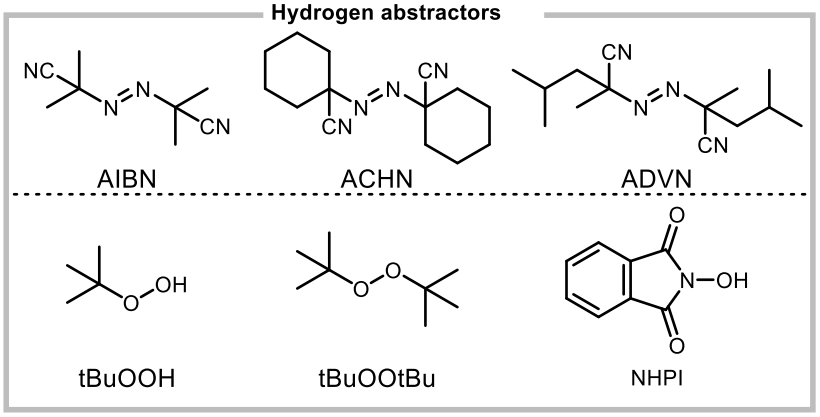

Figure S11. Hydrogen abstractor screening for autoxidation reaction of *trans*-**2**.

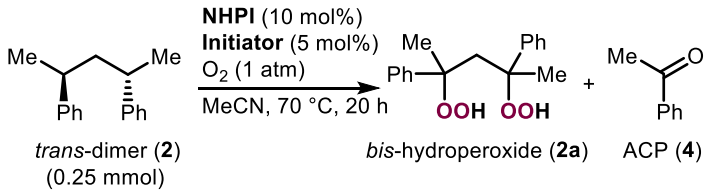

Entry	Hydrogen Abstractor	Initiator for NHPI	Solvent	Conv. [%]	**2a** [%]	**4** [%]
1	NHPI	-	MeCN	17	13	-
2	NHPI	$Co(OAc)_2$	MeCN	35	-	16
3	NHPI	AIBN	MeCN	31	20	1.5
4	NHQI	AIBN	MeCN	11	4.1	0.2
5	DNHPI	AIBN	MeCN	6	3.5	0.5
6	NHNI	AIBN	MeCN	3	-	-
7	TCNHPI	AIBN	MeCN	28	15	1.2
8	TPNHPI	AIBN	MeCN	39	31	1.6

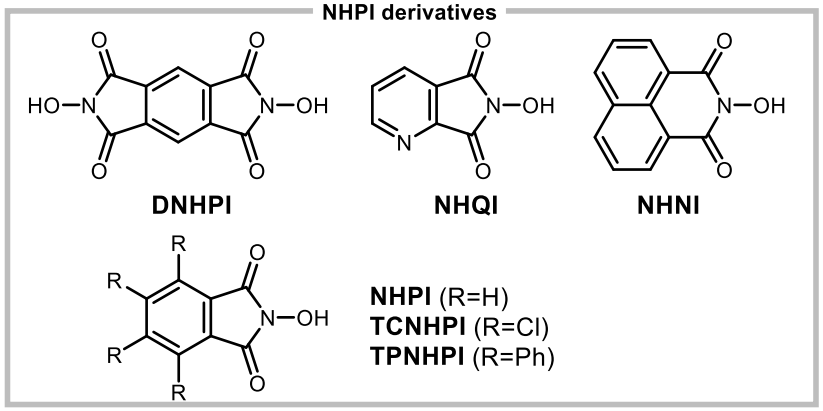

Figure S12. *N*-hydroxyphthalimide (NHPI) and NHPI derivatives screening with radical initiators for autoxidation reaction of *trans*-**2**.

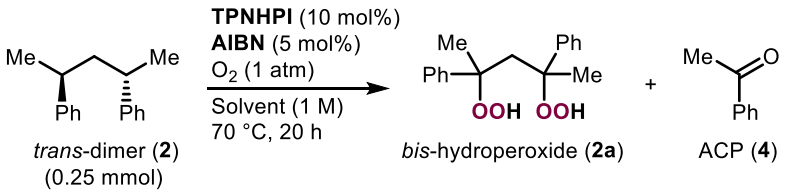

Entry	Solvent	Conv. [%]	**2a** [%]	**4** [%]
1	MeCN	39	31	1.6
2	^{n}PrCN	36	27	1.8
3	^{n}BuCN	45	40	2.0

Figure S13. Nitrile solvent screening for autoxidation reaction of *trans*-**2**. *n*-Alkyl nitrile solvents were favored because the nitrile solvent is known to provide the lowest rate of phthalimide-*N*-oxyl (PINO) radical decay.[8]

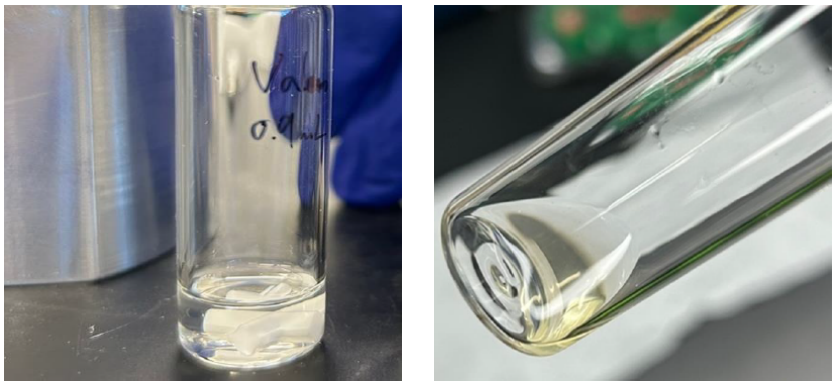

Figure S14. Polystyrene dissolved in ^{n}BuCN (left) and polystyrene + TPNHPI in ^{n}BuCN (right).

4b. Optimization of the Hock rearrangement (2nd step)

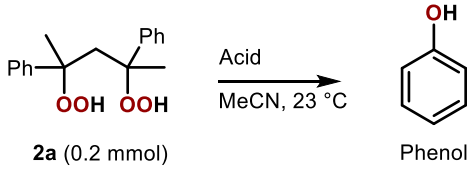

2a (0.2 mmol) Phenol

Entry	Acid treatment	Phenol Yield [%] (two-step yield)
1	B_2O_3 (30 mol%)	N.D.
2	$B(OTf)_3$ (30 mol%)	N.D.
3	$B(OH)_3$ (30 mol%)	N.D.
4	$TiCl_3$ (30 mol%)	N.D.
5	$InCl_3$ (30 mol%)	23 (9)
6	$AlCl_3$ (30 mol%)	25 (10)
7	TFA 0.30 M	21 (8.0)
8	MsOH 0.30 M	48 (19)
9	$PhSO_3H$ 0.30 M	50 (20)
10	H_2SO_4 0.30 M	53 (21)
11	$HClO_4$ 0.30 M	58 (24)
12	H_2SO_4 3.6 M	62 (25)
13	$HClO_4$ 3.6 M	72 (30)
14	$HClO_4$ 3.6 M	71 (17)
15	TfOH 3.6 M	13 (5)

Figure S15. Hock rearrangement step (2nd step) screening with various Lewis/Brønsted acids.

5. DFT calculation studies

Density functional theory (DFT) calculations were performed using the B3LYP exchange-correlation functional as implemented in Gaussian 16.[9-13] The 6-311++G(df,pd) basis set was utilized unless otherwise noted. Frequency calculations were performed to estimate zero-point vibrational energy (ZPE) corrections and verify the number of imaginary frequencies to be zero for local minima and one for transition states. Multiple possible conformers were sampled by means of dihedral angle scans. The energies of all identified conformers of transition states were thermally averaged in the reported reaction activation barriers.[14] Gibbs free energies were computed at 70 °C using the ideal gas approximation, as implemented in the Python Multiscale Thermochemistry Toolbox (pMuTT).[15] As a reference of potential computational errors, single point energies of the dimer pathway were computed using the domain-based local pair natural orbital coupled cluster method (DLPNO-CCSD(T)) and the aug-cc-pVDZ basis set as implemented in ORCA 5.0.3.[16,17] The *trans*-dimer and the (2*R*,4*R*,6*S*)-trimer were selected for the calculation among the diastereomers. For dihedral angle scans of terminal phenyl rings of trimer, two dihedral scans were performed for each terminal phenyl rings and the two energy profiles were arithmetically averaged.

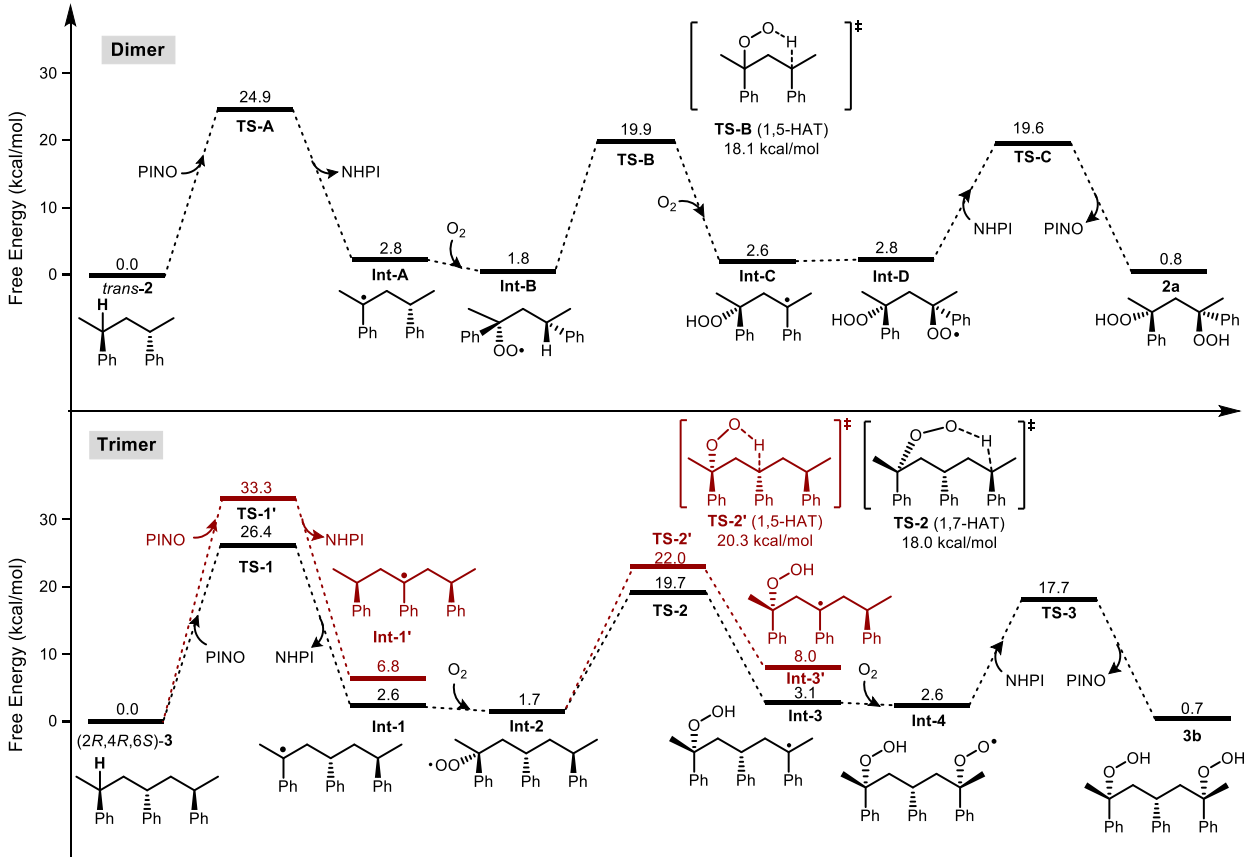

Figure S16. Full energy diagram for the oxidation pathways of dimer and trimer. Density functional theory (DFT) calculations were performed using the B3LYP exchange-correlation functional as implemented in Gaussian 16. The 6-311++G(df,pd) basis set was utilized. The *trans*-dimer and the (2*R*,4*R*,6*S*)-trimer were selected for the calculation among the diastereomers.

5a. Evaluation of the calculated energy barrier

I. Estimation of the experimental free energy barrier using Eyring equation

The Eyring equation [$\Delta G^{\ddagger} = -RT \ln(kh/k_bT)$; R = 8.314 J/mol K, T = 343 K, $h = 6.63\times10^{-34}$ J·s, $k_b = 1.38\times10^{-23}$ J/K] was used to estimate the experimental free energy barriers and compare them to the calculated barrier (k is the rate constant in s^{-1}). The rate constant k was estimated using the reaction time-course data shown in **Figure 2b**. The initial rate data (first two data points) were used to obtain the pseudo first-order rate constant k', based on the assumption of a bimolecular rate law: Rate = k [dimer][PINO] = k'[dimer], where Rate = 4.23×10^{-6} M·s^{-1}, [dimer] = 0.25 M, and [PINO] = 0.05 M). This analysis results in a standard-state adjusted pseudo first-order rate constant k' of 3.4×10^{-4} s^{-1}, which corresponds $\Delta G^{\ddagger}$ = 25.6 kcal/mol. This value is quite close to that estimated by DFT calculations ($\Delta G^{\ddagger}$ = 24.9 kcal/mol, shown in Figure 3a).

II. Benchmarking calculations with reported experimental values

For a quantitative experimental benchmarking, we computed the activation energy barrier ($TS_{cumeneHAT}$) for cumene autoxidation (R-H + R-OO• → R• + R-OOH) since it is relevant to the HAT reactions reported in our study and the experimental value for this reaction is available in the literature. We calculate this value to be 14.1 kcal/mol at 0 K using our computational method. This value is in close agreement with the reported experimental values of 13.3 kcal/mol[18] and 14.8 kcal/mol.[19]

5b. Cartesian coordinates

Cumene (1)

E = -350.301131 Eh
ZPVE = 0.184268 Eh
G = -350.1573029847871 Eh

C	0.40186100	1.09727700	0.00020700
C	1.77701200	1.30073400	0.00025000
C	2.64703500	0.21385000	0.00004800
C	2.12736100	-1.07528700	-0.00019600
C	0.74902600	-1.27242000	-0.00024000
C	-0.13658200	-0.19349700	-0.00003800
H	-0.25813500	1.95689000	0.00036700
H	2.17109000	2.31001000	0.00044100
H	3.71844400	0.37191000	0.00008000
H	2.79331100	-1.92987200	-0.00035500
H	0.35395800	-2.28240800	-0.00043300
C	-1.63858700	-0.42634600	-0.00008600
H	-1.79040200	-1.51073000	-0.00030000
C	-2.30639800	0.13145400	-1.26733700
H	-1.85621700	-0.28927800	-2.16839800
H	-3.37299900	-0.10622000	-1.27593200
H	-2.20789100	1.21835000	-1.32152300
C	-2.30640100	0.13095900	1.26737700
H	-3.37300700	-0.10669600	1.27587000
H	-1.85623800	-0.29013600	2.16827700
H	-2.20787500	1.21783200	1.32199900

Cumyl peroxyl radical (1a)

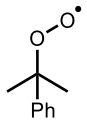

E = -500.061547 Eh
ZPVE = 0.179753 Eh
G = -499.9259123743523 Eh

C	-0.93260700	-1.16465000	0.11192100
C	-2.30806500	-1.33875400	0.02897500
C	-3.14690600	-0.23725900	-0.11216800
C	-2.59657400	1.03662800	-0.17636500
C	-1.21698100	1.20941900	-0.10414500
C	-0.36715100	0.11304200	0.04383700
H	-0.29170900	-2.03041200	0.21433000
H	-2.72537600	-2.33714100	0.07453800

H	-4.21958300	-0.37238600	-0.17381500
H	-3.23860500	1.90168600	-0.28815100
H	-0.81226400	2.21056200	-0.16322000
C	1.13806800	0.27703500	0.17606800
C	1.61771600	-0.02252800	1.59572000
H	1.27379300	-1.00295400	1.92521000
H	2.70626800	0.00628700	1.64020800
H	1.21459200	0.72701400	2.27805200
C	1.69092600	1.59878200	-0.34040900
H	2.77919200	1.55055100	-0.34730400
H	1.34064100	1.80616400	-1.35175200
H	1.39258900	2.41980100	0.31204200
O	1.67881500	-0.80584500	-0.72942200
O	2.98492300	-0.90783800	-0.70317100

$TS_{cumeneHAT}$

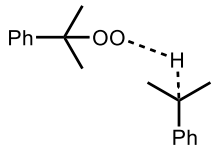

E = -850.335307 Eh
ZPVE = 0.359022 Eh
G = -850.0399550394591 Eh

C	3.02573900	1.17184200	0.87650100
C	2.74214200	2.51920500	1.06087300
C	1.94449700	3.20201500	0.14788900
C	1.43474300	2.52042200	-0.95439500
C	1.72504100	1.17765200	-1.14417700
C	2.53336100	0.46788900	-0.23604900
H	3.65238400	0.66825600	1.59953000
H	3.14847200	3.03823300	1.92073300
H	1.72061200	4.25143200	0.29406300
H	0.80170600	3.03606100	-1.66606700
H	1.29694500	0.66487100	-1.99426000
C	2.81374400	-0.97468400	-0.44253900
C	3.66091700	-1.68068100	0.59975100
H	3.66596400	-2.75587200	0.41377500
H	3.29359600	-1.52105900	1.61407700
C	3.15861800	-1.39788700	-1.86355100
H	3.16025000	-2.48545800	-1.95011200
H	2.45943800	-1.00764300	-2.60128600
H	4.15924800	-1.03639600	-2.12977400
H	1.62850800	-1.54929800	-0.29853700
O	0.59452800	-2.23043800	-0.25730600
O	-0.47132000	-1.35906800	-0.48013400
C	-1.27467800	-1.15363300	0.73597800
C	-1.80288000	-2.51177600	1.21497400

H	-0.97270300	-3.15576800	1.50499200
H	-2.46037600	-2.37184400	2.07457200
H	-2.37006900	-3.00499100	0.42560100
C	-0.41500500	-0.49600100	1.81113800
H	-0.05207400	0.47962200	1.49002200
H	-0.97877900	-0.37874200	2.73747900
H	0.43997300	-1.13607500	2.02433500
C	-2.41899200	-0.27936700	0.22919400
C	-3.06087600	-0.61095700	-0.96923000
C	-2.87909700	0.82829200	0.94150600
C	-4.12714400	0.14495800	-1.43977800
H	-2.71194100	-1.45925400	-1.54234000
C	-3.95379400	1.58155200	0.47558900
H	-2.40367700	1.11711300	1.86870900
C	-4.58120700	1.24444400	-0.71705200
H	-4.60557200	-0.12629000	-2.37314200
H	-4.29593600	2.43551500	1.04765200
H	-5.41484100	1.83209100	-1.08150200
H	4.70243500	-1.33817600	0.56126600

Dimer (2)

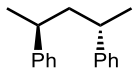

E = -660.064950 Eh
ZPVE = 0.322092 Eh
G = -659.7979521055805 Eh

C	2.77947300	-0.70936100	-1.06904200
C	3.87807000	-1.55856300	-0.99951200
C	4.73731700	-1.50637100	0.09444400
C	4.48617100	-0.59745900	1.11578000
C	3.38432000	0.25016900	1.04048400
C	2.51319100	0.21047800	-0.04976400
H	2.12350400	-0.76666400	-1.92961700
H	4.06421100	-2.26296500	-1.80143800
H	5.59355200	-2.16731700	0.14848600
H	5.14761300	-0.54569400	1.97231300
H	3.19834500	0.95622900	1.84248400
C	1.30897400	1.13713800	-0.10885100
H	1.37677900	1.78738400	0.76821300
C	0.00000800	0.32204700	0.00008400
H	0.07689000	-0.33651600	0.87086600
H	-0.07686700	-0.33679100	-0.87049200
C	1.34544100	2.03552100	-1.35613500
H	0.55423500	2.78703400	-1.33003000
H	2.30008000	2.56002600	-1.42554300
H	1.21847100	1.45202400	-2.27124300
C	-1.30896800	1.13716100	0.10873800
H	-1.37670500	1.78721800	-0.76847200

C	-1.34555700	2.03581400	1.35582600
H	-2.30023100	2.56027800	1.42506300
H	-1.21860800	1.45252300	2.27106900
H	-0.55439500	2.78736700	1.32960400
C	-2.51317600	0.21048400	0.04974500
C	-3.38420500	0.24993200	-1.04059200
C	-2.77955100	-0.70913000	1.06920300
C	-4.48604700	-0.59771600	-1.11580200
H	-3.19815800	0.95581400	-1.84273200
C	-3.87813900	-1.55834900	0.99976000
H	-2.12366100	-0.76624000	1.92985100
C	-4.73728600	-1.50640100	-0.09428800
H	-5.14741000	-0.54614300	-1.97240800
H	-4.06435400	-2.26257300	1.80182500
H	-5.59351300	-2.16736200	-0.14826200

TS-A

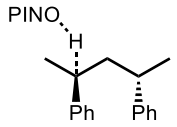

E = -1247.844554 Eh
ZPVE = 0.424363 Eh
G = -1247.495630336596 Eh

C	-0.57085900	2.57765300	0.78440600
C	-1.22667100	2.75074900	1.99588700
C	-1.22471700	1.73696200	2.94928500
C	-0.55957100	0.54375500	2.67530500
C	0.10116900	0.37139400	1.46884300
C	0.12201600	1.38834100	0.49268200
H	-0.58973600	3.38076100	0.06135800
H	-1.74174600	3.68244500	2.19597100
H	-1.73864800	1.87244700	3.89279200
H	-0.56025900	-0.25801200	3.40357900
H	0.59027200	-0.57269800	1.27002600
C	0.81216800	1.18134500	-0.80440400
C	2.08556000	0.32721700	-0.79069100
H	2.45561500	0.25702700	-1.81669300
H	1.83573200	-0.69528500	-0.49938200
C	0.79910000	2.33678400	-1.79494000
H	1.26876500	2.03088900	-2.73012900
H	-0.21864900	2.65075200	-2.02959200
H	1.34415100	3.20867000	-1.42144800
C	3.24474600	0.80035800	0.13443900
H	2.84784000	0.84578200	1.15212800
C	3.78276700	2.19714000	-0.20972400
H	4.64425800	2.43506500	0.41696700
H	4.10089600	2.26444100	-1.25257100
H	3.02738300	2.96449000	-0.03856200

C	4.34947000	-0.24353200	0.13731700
C	4.60171400	-1.00187400	1.28206800
C	5.13297600	-0.48290200	-0.99588800
C	5.60416400	-1.96747500	1.30055300
H	4.00690100	-0.83226900	2.17282700
C	6.13513500	-1.44630700	-0.98336500
H	4.96328400	0.08840000	-1.90093600
C	6.37520200	-2.19356400	0.16620600
H	5.78164900	-2.54184100	2.20183800
H	6.72991300	-1.61468100	-1.87311400
H	7.15568100	-2.94429700	0.17617600
H	0.00740200	0.36119900	-1.40064600
C	-3.55199500	-1.47674100	-0.06552800
C	-4.07338300	-0.33928800	-0.68177100
C	-5.37771000	0.06397700	-0.46398500
C	-6.15919400	-0.71119900	0.39560900
C	-5.63790300	-1.84962700	1.01141900
C	-4.31841800	-2.24883900	0.78754400
C	-2.13493300	-1.65164100	-0.48726000
C	-3.02007800	0.27584900	-1.53507600
H	-5.77309700	0.94804300	-0.94686100
H	-7.18602300	-0.42650000	0.58768600
H	-6.26793700	-2.43161800	1.67224200
H	-3.90528700	-3.13049000	1.25990800
O	-1.33381600	-2.49332400	-0.17686000
O	-3.05660400	1.26552100	-2.21800200
N	-1.89392000	-0.57179900	-1.37548700
O	-0.76776100	-0.41861300	-2.04748300

IntA

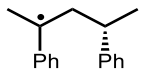

E = -659.421545 Eh
ZPVE = 0.308541 Eh
G = -659.1685504964211 Eh

C	-3.06776100	0.35851500	0.50886300
C	-4.02682000	-0.64294000	0.40850800
C	-3.90173400	-1.63938600	-0.55560100
C	-2.81015100	-1.62228100	-1.41611600
C	-1.85298100	-0.61679300	-1.31075300
C	-1.96354500	0.38872500	-0.34870900
H	-3.18536800	1.12525400	1.26581500
H	-4.87487200	-0.64474100	1.08289900
H	-4.64949900	-2.41874900	-0.63561000
H	-2.70196900	-2.39057800	-2.17231100
H	-1.00470500	-0.61312200	-1.98578200
C	-0.90385400	1.47173800	-0.24350000
H	-0.23340700	1.34521600	-1.09801200

C	-0.03281300	1.32554000	1.04359200
H	-0.69335000	1.40257600	1.91206600
H	0.63074500	2.19442800	1.08814900
C	-1.50148100	2.88418700	-0.32301300
H	-0.70930800	3.63649900	-0.34235600
H	-2.10490000	3.00254900	-1.22481500
H	-2.14016300	3.10058800	0.53640000
C	0.75911500	0.05190600	1.13242900
C	0.18617000	-1.08497200	1.92799500
H	-0.00598600	-1.96716500	1.30699400
H	0.86580000	-1.40564500	2.72644100
H	-0.75942000	-0.80524700	2.38963200
C	2.00875100	-0.09537600	0.46085400
C	2.59612600	0.95471200	-0.29859700
C	2.74009800	-1.31452100	0.51739200
C	3.81001500	0.79429700	-0.94175000
H	2.09096100	1.90731300	-0.37869100
C	3.95340400	-1.46446100	-0.12975200
H	2.34223900	-2.14884600	1.07820000
C	4.50333800	-0.41463200	-0.86627200
H	4.22501300	1.61910000	-1.50903900
H	4.47992900	-2.40916700	-0.06171600
H	5.45298100	-0.53581700	-1.37166900

IntB

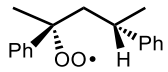

E = -809.822490 Eh
ZPVE = 0.317554 Eh
G = -809.5635251714355 Eh

C	2.66661800	1.07294600	0.91055700
C	3.71004500	1.88651000	0.48186600
C	4.58553500	1.44302000	-0.50473800
C	4.40936700	0.17744100	-1.05308400
C	3.36299900	-0.63135900	-0.62020800
C	2.47044300	-0.19766600	0.36232600
H	2.00258700	1.43795400	1.68553700
H	3.84088900	2.86821800	0.92118600
H	5.39728200	2.07657200	-0.83997700
H	5.08524700	-0.18179900	-1.81973600
H	3.23479800	-1.61636900	-1.05574600
C	1.36610100	-1.12194800	0.85439500
H	1.32703000	-1.97672500	0.17445400
C	-0.04326100	-0.48824200	0.89684000
H	0.00239200	0.51853900	1.31773600
H	-0.65923500	-1.06982700	1.58724100
C	1.72302100	-1.66782000	2.25138300
H	1.00119100	-2.42445200	2.56690800

H	2.71527800	-2.12168400	2.24793300
H	1.72515900	-0.86923900	2.99748400
C	-0.83661700	-0.39669600	-0.42152800
C	-0.10196000	0.28460900	-1.56894100
H	-0.74526400	0.34666300	-2.44490500
H	0.21113300	1.28759300	-1.28220500
H	0.79351100	-0.27458400	-1.83095300
C	-2.21915200	0.18591000	-0.13949400
C	-3.20553200	-0.60149400	0.46187700
C	-2.51122500	1.52319500	-0.41011600
C	-4.44899200	-0.06782700	0.77630600
H	-3.00791200	-1.64491600	0.66923100
C	-3.75458100	2.06083200	-0.08899700
H	-1.77263300	2.16017100	-0.87736800
C	-4.72885200	1.26765200	0.50393700
H	-5.20227100	-0.69883000	1.23189800
H	-3.96007600	3.10109300	-0.30998000
H	-5.69823200	1.68378700	0.74848100
O	-1.00548400	-1.84236500	-0.79101400
O	-1.61384400	-2.02970300	-1.93917500

TS-B

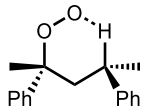

E = -809.790275 Eh
ZPVE = 0.312147 Eh
G = -809.5345601107173 Eh

C	-2.79941900	-1.28899000	-0.70707500
C	-4.09488900	-1.50323900	-1.16252700
C	-5.10713200	-0.60506600	-0.83926100
C	-4.81038500	0.50306700	-0.05493400
C	-3.51410000	0.71592400	0.40627500
C	-2.49135300	-0.17666200	0.08121500
H	-2.02571700	-1.99993700	-0.97075700
H	-4.31232300	-2.37225600	-1.77147700
H	-6.11653700	-0.76890500	-1.19560100
H	-5.59005500	1.20927300	0.20350100
H	-3.29541500	1.58032000	1.01673600
C	-1.07332800	0.01080600	0.60869900
C	0.00061200	-0.17376600	-0.53058200
H	-0.49601100	0.03407100	-1.47930100
H	0.30264800	-1.22012900	-0.54898700
C	-0.82955800	-0.92994300	1.79593000
H	0.16105900	-0.78150400	2.22096000
H	-1.57034300	-0.73787200	2.57286600
H	-0.93215800	-1.96665000	1.47308300

C	1.22733200	0.74560900	-0.43391700
H	0.99509600	1.26649700	0.72556600
C	1.10598300	1.96608900	-1.33395300
H	1.84123100	2.73412500	-1.09432200
H	1.23042000	1.68977400	-2.38750500
H	0.11614000	2.40892600	-1.22081500
C	2.56667900	0.11188500	-0.31026100
C	3.70970000	0.68537000	-0.89274900
C	2.74838200	-1.06793800	0.43428600
C	4.96336300	0.10408600	-0.74844600
H	3.62169400	1.58977500	-1.47775600
C	4.00053300	-1.64475000	0.58382600
H	1.89996600	-1.53671600	0.91409800
C	5.11855700	-1.06318600	-0.00886000
H	5.82263000	0.56643200	-1.21890500
H	4.10574900	-2.55126100	1.16740400
H	6.09622400	-1.51420600	0.10552000
O	-0.99998400	1.38806300	1.04227000
O	0.22746400	1.61624700	1.66269300

IntC

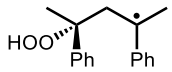

E = -809.819122 Eh
ZPVE = 0.315693 Eh
G = -809.5622249728759 Eh

C	3.85907900	0.61832000	-0.29599800
C	4.97033500	-0.14347100	0.01690400
C	4.85214800	-1.51320700	0.25336700
C	3.59157900	-2.10608800	0.16971600
C	2.47409200	-1.35281800	-0.14003700
C	2.55886200	0.04572900	-0.38765800
H	3.98860000	1.67660500	-0.47352900
H	5.94190000	0.33257300	0.07714300
H	5.72386100	-2.10692700	0.49709400
H	3.48315500	-3.16946700	0.34754700
H	1.51845500	-1.85427700	-0.19693000
C	1.42597400	0.85004100	-0.71569300
C	0.04114000	0.28291800	-0.83256900
H	0.05898300	-0.79208000	-1.00635200
H	-0.45773300	0.72305600	-1.70131000
C	1.59814100	2.31319300	-1.01132200
H	0.64907500	2.77286000	-1.27693900
H	1.99588500	2.86441100	-0.15159700
H	2.29965700	2.47603400	-1.83785900
C	-0.92997700	0.50595300	0.38010900
C	-0.29884100	0.10192100	1.71178500
H	-1.01118200	0.22805400	2.52575500
H	0.02773400	-0.93673300	1.69944600

H	0.58078100	0.71728300	1.90244400
C	-2.24481400	-0.21522700	0.08077600
C	-3.23977600	0.42335100	-0.66299900
C	-2.45824700	-1.53753700	0.47597900
C	-4.41487100	-0.23951800	-0.99757400
H	-3.09709700	1.45247700	-0.96249500
C	-3.63271700	-2.20382100	0.13867900
H	-1.71047000	-2.06300100	1.05540500
C	-4.61684100	-1.55716900	-0.59969600
H	-5.17710200	0.27789500	-1.56758100
H	-3.77762700	-3.22871500	0.45831000
H	-5.53292400	-2.07314800	-0.85943700
O	-1.12574100	1.93645800	0.34452400
O	-2.03251500	2.33396600	1.41037900
H	-1.44949500	2.90426900	1.92904900

IntD

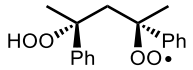

E = -960.217768 Eh
ZPVE = 0.324612 Eh
G = -959.9551745913187 Eh

C	-1.36588100	-0.83347800	0.03129500
C	-0.01472900	-0.08463600	-0.00361500
H	-0.01550400	0.61712200	0.83250800
H	-0.01642000	0.52865900	-0.90658500
C	-1.50364800	-2.00472900	-0.93469200
H	-1.28213300	-1.68610400	-1.95132300
H	-0.79711300	-2.79117400	-0.68160700
H	-2.51428700	-2.40643000	-0.89239500
C	1.35110200	-0.82636700	0.03407700
C	1.48640200	-1.86137100	1.15382000
H	2.50543200	-2.24372600	1.18655400
H	1.24484600	-1.42834400	2.12236100
H	0.79918700	-2.69072200	0.99489200
C	2.43759000	0.25609400	0.10261200
C	2.94806000	0.81533800	-1.07019700
C	2.89104500	0.75040300	1.32730300
C	3.89117900	1.83568700	-1.01944900
H	2.61703300	0.43501900	-2.02656000
C	3.83207200	1.77414600	1.37937600
H	2.51432300	0.34191500	2.25589800
C	4.33725200	2.32072600	0.20535200
H	4.28119600	2.24943300	-1.94152500
H	4.17101200	2.14126000	2.34050000
H	5.07258900	3.11483600	0.24451300
O	1.38576200	-1.47780000	-1.25653300
O	2.64771900	-2.18018400	-1.41666400
H	2.33394100	-3.09193400	-1.48503700

C	-2.48043400	0.20462100	-0.11374500
C	-2.88735200	0.96646300	0.98488000
C	-3.06461300	0.46259700	-1.35468600
C	-3.85863200	1.95072200	0.84694000
H	-2.45695300	0.77984600	1.95957000
C	-4.03358600	1.45167400	-1.49428400
H	-2.77110000	-0.10629100	-2.22641000
C	-4.43593100	2.19872600	-0.39395400
H	-4.16640900	2.52278400	1.71358900
H	-4.47558700	1.63294000	-2.46633300
H	-5.19322000	2.96528200	-0.50111300
O	-1.42361200	-1.37733700	1.42595000
O	-2.48864600	-2.10768900	1.66503400

TS-C

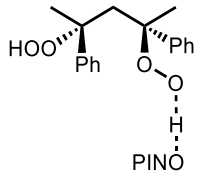

E = -1548.648971 Eh
ZPVE = 0.439574 Eh
G = -1548.291177860369 Eh

C	-4.10291500	-2.31552100	-1.31449800
C	-5.17229900	-3.20418000	-1.28353400
C	-5.37350000	-4.01788700	-0.17358300
C	-4.49720700	-3.93058200	0.90223700
C	-3.43088900	-3.03679300	0.87353800
C	-3.21792000	-2.21885400	-0.23664200
H	-3.96469600	-1.69621900	-2.19195400
H	-5.84588700	-3.26214500	-2.13007500
H	-6.20271400	-4.71421300	-0.14966700
H	-4.63905500	-4.56367400	1.76992800
H	-2.75099000	-2.98009300	1.71138200
C	-2.06604300	-1.20360500	-0.25727400
C	-2.68506300	0.21981500	-0.07636500
H	-3.54652000	0.13543300	0.58610700
H	-3.07300600	0.51443800	-1.05153600
C	-1.24383700	-1.33623400	-1.54566500
H	-0.36303600	-0.70067400	-1.51815600
H	-0.92952100	-2.36829900	-1.68484900
H	-1.84754100	-1.04518400	-2.40526800
C	-1.81352800	1.38175100	0.49376000
C	-1.68848800	1.35153400	2.01765800
H	-1.10864200	2.20010000	2.37399300
H	-2.69169400	1.42429200	2.43847800
H	-1.23221800	0.42667300	2.35899600

C	-2.39140200	2.73230700	0.04772600
C	-1.59198900	3.70881000	-0.54689000
C	-3.74187500	3.01852900	0.27125400
C	-2.13124100	4.93983900	-0.91123200
H	-0.54560600	3.51145500	-0.72960900
C	-4.27816000	4.24800700	-0.09156500
H	-4.38661700	2.28344800	0.73620000
C	-3.47413200	5.21520100	-0.68697500
H	-1.49380100	5.68417600	-1.37266400
H	-5.32617500	4.44985000	0.09323300
H	-3.89185800	6.17285500	-0.97152800
O	-0.51172500	1.22890900	-0.16843500
O	0.56550400	1.50836000	0.62541700
O	-1.24134700	-1.35371700	0.91055700
O	-0.39501800	-2.52215000	0.80826600
H	0.47533300	-2.08309600	0.78737900
H	1.10619600	0.52700300	0.75989200
C	5.24593300	-0.13393900	0.47480600
C	4.83064700	-0.48410500	-0.81157000
C	5.73304500	-0.59985000	-1.85347300
C	7.07802000	-0.35393100	-1.57290200
C	7.49334000	-0.00398300	-0.28662700
C	6.57692600	0.11119000	0.75992200
C	4.06567700	-0.08679800	1.37743900
C	3.35863900	-0.68295100	-0.81367300
H	5.40166500	-0.87159400	-2.84703700
H	7.81254000	-0.43522900	-2.36401500
H	8.54363400	0.18050200	-0.09995700
H	6.88921700	0.38171400	1.75998900
O	3.98529800	0.17218400	2.54557300
O	2.61038900	-0.99048700	-1.70150000
N	2.96531700	-0.42975700	0.53299900
O	1.73231500	-0.55183000	0.96443900

2a

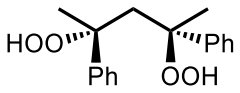

E = -960.859119 Eh
ZPVE = 0.336545 Eh
G = -960.5832277561693 Eh

C	-1.34921000	-0.82588900	0.03012100
C	0.01319700	-0.08260500	-0.02111200
H	0.01648000	0.64073000	0.79575500
H	0.01952000	0.50342100	-0.94230400
C	-1.47652000	-1.98479500	-0.95813900
H	-1.22497200	-1.66606500	-1.96851300
H	-0.78780100	-2.78004500	-0.68525300

H	-2.48942600	-2.38308500	-0.94728700
C	1.37418500	-0.83139500	0.04532300
C	1.49321900	-1.84214700	1.18825400
H	2.51041600	-2.22781100	1.24127800
H	1.24164300	-1.38564300	2.14343200
H	0.79764900	-2.66587100	1.04161100
C	2.46587400	0.24736300	0.09935500
C	2.98214500	0.78507500	-1.08111700
C	2.91946900	0.75989100	1.31646900
C	3.92975900	1.80187400	-1.04528600
H	2.65172200	0.38973200	-2.03162400
C	3.86505400	1.78020200	1.35391500
H	2.53915700	0.36741300	2.25045400
C	4.37538800	2.30531000	0.17232200
H	4.32388900	2.19834400	-1.97326100
H	4.20404000	2.16117700	2.30971200
H	5.11442900	3.09653200	0.20006000
O	1.42104400	-1.51003100	-1.23136100
O	2.68070000	-2.22176100	-1.36307200
H	2.36577100	-3.13547400	-1.38202200
C	-2.44719800	0.23479000	-0.14644300
C	-2.75984300	1.08335700	0.92108200
C	-3.12925600	0.41177100	-1.35073600
C	-3.73092700	2.07010700	0.79218500
H	-2.23490300	0.96890000	1.86186800
C	-4.09674000	1.40401400	-1.48471200
H	-2.91338900	-0.22501000	-2.19764000
C	-4.40383900	2.23537900	-0.41420700
H	-3.95850400	2.71285200	1.63400300
H	-4.61295300	1.52278400	-2.42958100
H	-5.15919100	3.00431000	-0.51811800
O	-1.39887200	-1.32534700	1.39090400
O	-2.61951500	-2.07148100	1.59986300
H	-3.21897400	-1.38204300	1.92310700

(2*R*,4*R*,6*S*)-trimer (**3**)

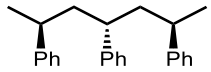

E = -969.830802 Eh
ZPVE = 0.459896 Eh
G = -969.4400555464813 Eh

C	0.55239700	2.90036300	0.86942900
C	1.03052200	4.19490900	0.69886500
C	1.76710000	4.52716500	-0.43448400
C	2.01831600	3.55254800	-1.39354700
C	1.53802200	2.25792300	-1.21655200
C	0.79889200	1.90787600	-0.08468000
H	-0.02173100	2.66518400	1.75788000

H	0.82599400	4.94676800	1.45177100
H	2.13942400	5.53539600	-0.56793800
H	2.58959500	3.79793800	-2.28091500
H	1.74287900	1.50442000	-1.96861400
C	0.25769400	0.49458400	0.07573800
H	0.66170000	-0.09035400	-0.75447100
C	-1.28513500	0.50991100	-0.05402100
H	-1.54705500	1.11156300	-0.92966600
H	-1.70679300	1.03574800	0.80846700
C	0.72238900	-0.16865300	1.38765000
H	0.24781800	-1.14898700	1.48316100
H	0.36105100	0.42219300	2.23572700
C	-1.98378800	-0.86413000	-0.17996100
H	-1.71189100	-1.46820200	0.69040900
C	-1.54555100	-1.63670800	-1.43506900
H	-2.09407100	-2.57668000	-1.51909800
H	-1.73375800	-1.05911900	-2.34336700
H	-0.48091500	-1.87371700	-1.40660500
C	-3.49368700	-0.69177500	-0.12423600
C	-4.22288800	-1.18294200	0.96025900
C	-4.19340000	-0.03392300	-1.14086200
C	-5.60428100	-1.02586100	1.03271900
H	-3.70182200	-1.69779600	1.76011700
C	-5.57283100	0.12628100	-1.07418200
H	-3.65857500	0.35908000	-1.99733200
C	-6.28533900	-0.36952500	0.01405700
H	-6.14674000	-1.41790700	1.88472100
H	-6.09332900	0.63922100	-1.87412300
H	-7.35999000	-0.24552400	0.06571000
C	2.24803400	-0.34484300	1.53329900
H	2.70952300	0.63762500	1.39891300
C	2.59995600	-0.82791300	2.95077100
H	2.14444900	-1.79777500	3.16572500
H	3.67956300	-0.93410000	3.07149200
H	2.24205100	-0.11719600	3.69961400
C	2.84002800	-1.26334400	0.47568200
C	3.83499500	-0.80240400	-0.38856600
C	2.42658100	-2.59358400	0.34879700
C	4.39934700	-1.63671500	-1.34988000
H	4.17065200	0.22524300	-0.30850500
C	2.98536600	-3.43131100	-0.60993800
H	1.66089000	-2.98615200	1.00789700
C	3.97543000	-2.95561800	-1.46517800
H	5.17069600	-1.25456400	-2.00788100
H	2.64939900	-4.45846100	-0.68810900
H	4.41198300	-3.60770200	-2.21163700

TS-1

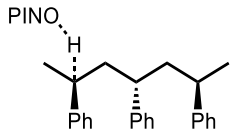

E = -1557.610658 Eh
ZPVE = 0.562084 Eh
G = -1557.1370322797136 Eh

C	3.27172900	2.56415300	1.41710700
C	4.23324800	3.53149000	1.68802300
C	5.31563700	3.70437900	0.83020900
C	5.42515100	2.90130100	-0.29935000
C	4.45969800	1.93419800	-0.56507500
C	3.36865800	1.74752200	0.28599000
H	2.43848300	2.44571800	2.09970100
H	4.13727100	4.15166800	2.57126300
H	6.06511000	4.45720000	1.04124500
H	6.26316800	3.02494300	-0.97490600
H	4.55725500	1.30974600	-1.44596100
C	2.30792500	0.70336700	-0.03862600
H	2.67886500	0.14550200	-0.90149300
C	1.00619000	1.42945800	-0.45510200
H	1.27902200	2.21146900	-1.17643600
H	0.61698500	1.96198100	0.41465700
C	2.08646600	-0.29438300	1.11443900
H	1.26783700	-0.96955100	0.86097600
H	1.74900700	0.25014700	2.00150600
C	-0.11502900	0.61216400	-1.11246100
C	0.34106500	-0.41164000	-2.13570600
H	-0.48003700	-1.04930900	-2.46067400
H	0.76721900	0.08174000	-3.01810000
H	1.10953900	-1.06388600	-1.72516400
C	-1.32628900	1.40641200	-1.45782000
C	-1.84201900	2.36518700	-0.56312700
C	-2.01457500	1.22229400	-2.67096600
C	-2.96848000	3.11129500	-0.87443200
H	-1.37177100	2.51209800	0.39931200
C	-3.13809400	1.97563600	-2.98447500
H	-1.66046900	0.49513200	-3.38725300
C	-3.62215700	2.92527400	-2.09013700
H	-3.34106200	3.83730700	-0.16229000
H	-3.63641400	1.82036800	-3.93369600
H	-4.49988200	3.51044100	-2.33484800
C	3.32176900	-1.13581800	1.49542400
H	4.14678900	-0.44793900	1.70272400
C	3.04870600	-1.92994600	2.78456300
H	2.20839900	-2.61625900	2.65754600
H	3.92131100	-2.51876500	3.07357700
H	2.80485800	-1.25409900	3.60762200
C	3.77729600	-2.05246200	0.37073000

C	5.06977000	-1.95335300	-0.14821500
C	2.92963400	-3.03013800	-0.16164700
C	5.50586900	-2.79793700	-1.16582500
H	5.74369200	-1.20330700	0.25011100
C	3.35944600	-3.87559500	-1.17850100
H	1.92165800	-3.13812800	0.22160900
C	4.65088400	-3.76277300	-1.68619200
H	6.51437100	-2.70131900	-1.55023200
H	2.68472100	-4.62557200	-1.57382700
H	4.98638500	-4.42199100	-2.47743200
H	-0.60466900	-0.16176300	-0.15556500
C	-4.56079400	-0.39084900	1.31179100
C	-4.62067200	-1.30561600	0.26066800
C	-5.82992500	-1.76964500	-0.22242600
C	-6.99432400	-1.29046100	0.38199000
C	-6.93448100	-0.37614000	1.43419100
C	-5.70835800	0.08877000	1.91511600
C	-3.13395700	-0.08225300	1.60596300
C	-3.23522400	-1.63551600	-0.17361100
H	-5.86601500	-2.47991600	-1.03807700
H	-7.95930500	-1.63376500	0.03087500
H	-7.85393500	-0.02326100	1.88410800
H	-5.65181000	0.79705900	2.73134800
O	-2.65540300	0.65240700	2.42975100
O	-2.85077700	-2.37286300	-1.04352500
N	-2.40475200	-0.86632000	0.67784900
O	-1.08280500	-0.95575500	0.68224500

TS-1’

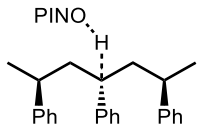

E = -1557.600924 Eh
ZPVE = 0.562383 Eh
G = -1557.1254371743626 Eh

C	-0.95421600	-1.97665700	1.63319300
C	-2.06346300	-2.49701000	2.28488400
C	-2.81358200	-1.70346100	3.14719700
C	-2.43637000	-0.37856900	3.34717800
C	-1.32577400	0.14121700	2.69931900
C	-0.54180900	-0.64246500	1.82837200
H	-0.40583600	-2.62309400	0.96490100
H	-2.34188300	-3.53019000	2.11665900
H	-3.67863400	-2.11059200	3.65565600
H	-3.00979800	0.25511600	4.01271100
H	-1.06562100	1.17306100	2.87943200
C	0.64711100	-0.07064200	1.12970700

C	1.67476300	-1.11462400	0.66292300
H	1.16789700	-1.87821300	0.07226900
H	2.04108200	-1.62596500	1.56365100
C	1.24015800	1.19609200	1.76883400
H	2.30551400	1.23240600	1.55117200
H	1.16858900	1.07044300	2.85407600
C	2.90786700	-0.65945500	-0.15352700
H	3.44776500	0.10057800	0.41686400
C	2.54916700	-0.05133400	-1.51754700
H	3.45821700	0.17867600	-2.07600800
H	1.94556400	-0.73658300	-2.11447400
H	1.98236200	0.87201000	-1.40741400
C	3.86319100	-1.83667600	-0.29515800
C	5.08588300	-1.84135600	0.37839600
C	3.54508100	-2.94456400	-1.08722400
C	5.96639500	-2.91424000	0.26935900
H	5.35499800	-0.99116900	0.99584500
C	4.42036600	-4.01908600	-1.19942500
H	2.60684300	-2.96959500	-1.62862200
C	5.63588800	-4.00897200	-0.52103000
H	6.91068400	-2.89201700	0.80017500
H	4.15369100	-4.86581300	-1.82065300
H	6.31833200	-4.84525700	-0.61020000
C	0.62781000	2.58195400	1.39904500
H	-0.42372600	2.44414300	1.14176900
C	0.69357800	3.53015100	2.61115000
H	1.72478600	3.68301400	2.93883900
H	0.27598600	4.50657000	2.36086700
H	0.13275400	3.12720200	3.45868900
C	1.29165100	3.23550800	0.19431800
C	0.52710400	3.62837400	-0.90530800
C	2.66216000	3.51377200	0.17916000
C	1.11413700	4.27164900	-1.99137600
H	-0.53405400	3.41361000	-0.91357600
C	3.25255200	4.15521500	-0.90369500
H	3.28237400	3.23280700	1.02310600
C	2.47889800	4.53668300	-1.99614200
H	0.50200900	4.56256800	-2.83671200
H	4.31671400	4.35916000	-0.89409300
H	2.93706500	5.03482500	-2.84185100
H	0.05823800	0.29110400	-0.00720200
C	-3.66032800	-1.18727900	-1.37936700
C	-4.07637400	0.04854700	-0.88422900
C	-5.41478200	0.33125800	-0.68504400
C	-6.33984000	-0.66714600	-0.99847000
C	-5.92379500	-1.90324200	-1.49413700
C	-4.56926900	-2.18071100	-1.69203000
C	-2.17563800	-1.19077300	-1.48718100
C	-2.88074500	0.90427400	-0.65453700
H	-5.72795200	1.29380000	-0.30231800
H	-7.39689400	-0.48021000	-0.85700800

H	-6.66417500	-2.65709600	-1.73050100
H	-4.23726300	-3.13549200	-2.07841000
O	-1.42896600	-2.05376400	-1.86862200
O	-2.80456400	2.03728600	-0.25298900
N	-1.78336100	0.09139700	-1.02611900
O	-0.53756400	0.53545300	-1.08219600

Int-1

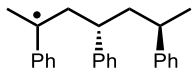

E = -969.187677 Eh
ZPVE = 0.446282 Eh
G = -968.8110554641595 Eh

C	1.70065900	2.82257700	0.60905000
C	2.77645100	3.70333400	0.62916400
C	3.85814900	3.50893700	-0.22495200
C	3.85110300	2.42715300	-1.09818800
C	2.77121900	1.54886700	-1.11367700
C	1.67913500	1.72834200	-0.26185000
H	0.86930000	2.99353900	1.28286300
H	2.77017400	4.54388600	1.31280600
H	4.69652200	4.19434600	-0.20935600
H	4.68678300	2.26435400	-1.76829700
H	2.77754700	0.70619400	-1.79578000
C	0.49655100	0.77614000	-0.31597900
H	0.76454900	-0.02854700	-1.00635900
C	-0.75168200	1.50130300	-0.91567100
H	-0.41608300	2.02166700	-1.82025700
H	-1.07006500	2.27966200	-0.22190100
C	0.17307600	0.13508900	1.04562800
H	-0.75285700	-0.43856900	0.95171400
H	-0.03518100	0.92260900	1.77697600
C	-1.87929300	0.58461900	-1.29104100
C	-1.65284500	-0.27730800	-2.50146500
H	-1.68530200	-1.34676300	-2.26558900
H	-2.41263900	-0.10303000	-3.27174400
H	-0.68101700	-0.07415000	-2.95132700
C	-3.11083900	0.51346600	-0.57756600
C	-3.38672800	1.30329300	0.57395400
C	-4.14743800	-0.37151900	-0.99144500
C	-4.59181400	1.21301100	1.24562200
H	-2.64238300	1.99409200	0.94303100
C	-5.34903600	-0.45420800	-0.31170200
H	-3.99790800	-0.99838000	-1.85944900
C	-5.58768900	0.33537400	0.81364700
H	-4.76168300	1.83320200	2.11787800
H	-6.11157000	-1.14065600	-0.66054100
H	-6.52947400	0.26864400	1.34319700

C	1.27741400	-0.77630300	1.61837300
H	2.20201000	-0.19284400	1.66118300
C	0.93203200	-1.19776700	3.05709000
H	-0.00281000	-1.76229500	3.09217000
H	1.71735200	-1.82694100	3.48003400
H	0.81655800	-0.32029500	3.69796400
C	1.55538900	-1.98767100	0.74211000
C	2.83291800	-2.21307200	0.22598800
C	0.55412800	-2.91800800	0.44428900
C	3.10670400	-3.32757900	-0.56262200
H	3.62423500	-1.50481600	0.44414700
C	0.82130300	-4.03232300	-0.34307200
H	-0.44775900	-2.77546400	0.83216400
C	2.10037900	-4.24210900	-0.85126100
H	4.10705200	-3.48013400	-0.94998800
H	0.02991300	-4.74046000	-0.55839600
H	2.30925400	-5.11067200	-1.46366700

Int-1'

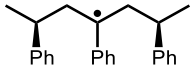

E = -969.183041 Eh
ZPVE = 0.446971 Eh
G = -968.8042550652932 Eh

C	3.62337800	0.90566900	0.58029000
C	4.73330200	1.56552800	0.08395300
C	4.59045800	2.69260100	-0.72516900
C	3.30602200	3.15066000	-1.02060400
C	2.19076000	2.50049600	-0.52481000
C	2.29842300	1.34340600	0.29616200
H	3.77993900	0.04755400	1.21809900
H	5.72330000	1.20196300	0.33303000
H	5.46100300	3.20494600	-1.11439300
H	3.17618300	4.02545700	-1.64677000
H	1.21464600	2.88182700	-0.78539700
C	1.15271900	0.66588300	0.81944200
C	-0.22766100	1.26460800	0.76773400
H	-0.18007900	2.34192600	0.59970700
H	-0.67969800	1.13738100	1.75779400
C	1.31696600	-0.60603500	1.61622100
H	0.37466600	-0.83939000	2.11756200
H	2.04104900	-0.42560000	2.42121700
C	-1.21929900	0.64347200	-0.26556000
H	-1.19942500	-0.43923400	-0.12574400
C	-0.80594800	0.92903200	-1.71579100
H	-1.48344800	0.42979400	-2.41060600
H	-0.83314700	1.99848500	-1.93800800
H	0.20523800	0.56994200	-1.91132400
C	-2.63923100	1.10248200	0.01919700
C	-3.61146500	0.18284100	0.41788800
C	-3.01469400	2.44475000	-0.09733200
C	-4.91593400	0.58492000	0.69142400
H	-3.34272600	-0.86339100	0.50994200
C	-4.31551700	2.85249900	0.17619800
H	-2.28618300	3.18482200	-0.40715100
C	-5.27319800	1.92313300	0.57220600
H	-5.65268700	-0.14878000	0.99623100
H	-4.58291000	3.89800000	0.07901500
H	-6.28695300	2.24003300	0.78402400
C	1.79241500	-1.88077500	0.85172600
H	2.58416800	-1.57885200	0.16314200
C	2.39737000	-2.89250100	1.83989100
H	1.67380400	-3.18896600	2.60297000
H	2.72461800	-3.79603700	1.32265400
H	3.26060800	-2.46200100	2.35330200
C	0.69986000	-2.51985400	0.01224700

C	0.81064100	-2.56818600	-1.37816100
C	-0.42763100	-3.10216200	0.60131300
C	-0.17129400	-3.17152900	-2.15971300
H	1.67839200	-2.12790700	-1.85621100
C	-1.41041300	-3.70737200	-0.17329900
H	-0.54252200	-3.08702100	1.67902400
C	-1.28685300	-3.74360300	-1.55984300
H	-0.06213500	-3.19432600	-3.23733200
H	-2.27307200	-4.15502300	0.30580000
H	-2.05168200	-4.21539400	-2.16424400

Int-2

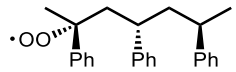

E = -1119.588243 Eh
ZPVE = 0.455305 Eh
G = -1119.2057002731933 Eh

C	0.70673400	3.02049400	0.90157700
C	1.12023700	4.32932500	0.67905300
C	1.74321700	4.67441600	-0.51677700
C	1.94644200	3.69870500	-1.48596700
C	1.53010000	2.39003800	-1.25770400
C	0.90531100	2.02757000	-0.06286300
H	0.22413400	2.77429100	1.84009200
H	0.95525500	5.08175000	1.44092600
H	2.06609100	5.69350400	-0.69013300
H	2.43071300	3.95399300	-2.42092100
H	1.69770100	1.63589100	-2.01834700
C	0.43164700	0.59615800	0.15656700
H	0.78079900	0.02061000	-0.70381700
C	-1.11848500	0.57665200	0.14934400
H	-1.46084400	1.23762000	-0.65022900
H	-1.49881700	1.01397000	1.07693500
C	1.04179900	-0.03252700	1.42611300
H	0.59439600	-1.01233400	1.59562100
H	0.76110900	0.57295100	2.29380300
C	-1.85914400	-0.75957100	-0.07868500
C	-1.27392300	-1.60300500	-1.20527600
H	-1.88290200	-2.48866000	-1.37577400
H	-1.22491600	-1.02341500	-2.12731300
H	-0.26285800	-1.92111600	-0.95608500
C	-3.35363600	-0.47874000	-0.22245800
C	-4.11899100	-0.16971000	0.90581000
C	-3.97423700	-0.45850300	-1.47163400
C	-5.46704800	0.14411000	0.78734700
H	-3.66331400	-0.19257900	1.88696700
C	-5.32354200	-0.13799200	-1.59224200
H	-3.41288900	-0.69458000	-2.36543100

C	-6.07561300	0.16334000	-0.46372300
H	-6.04385200	0.37078100	1.67564300
H	-5.78544700	-0.13032700	-2.57190900
H	-7.12649500	0.40763100	-0.55651800
C	2.57733600	-0.17436200	1.40446700
H	3.00390200	0.80991800	1.18996200
C	3.09318600	-0.60830500	2.78734300
H	2.67910700	-1.57603200	3.08015400
H	4.18111600	-0.69672400	2.78927900
H	2.80936000	0.12096100	3.54990200
C	3.06289400	-1.11806700	0.31504800
C	3.95253900	-0.67437000	-0.66536200
C	2.65287800	-2.45508000	0.27190000
C	4.41819900	-1.53164700	-1.65902500
H	4.28507100	0.35742000	-0.65018900
C	3.11381400	-3.31548700	-0.71843200
H	1.96848600	-2.83484700	1.02160400
C	3.99900800	-2.85672700	-1.69017000
H	5.10957300	-1.16279000	-2.40735900
H	2.78349200	-4.34735300	-0.72958000
H	4.35945000	-3.52691000	-2.46086600
O	-1.66128800	-1.51632200	1.20120000
O	-2.17768000	-2.72416800	1.18355700

TS-2

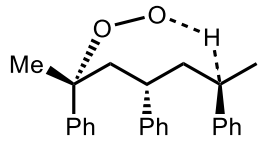

E = -1119.557217 Eh
ZPVE = 0.449330 Eh
G = -1119.1770970560133 Eh

C	3.49470800	-1.43893300	-0.91210300
C	4.24660800	-2.40944700	-1.56531000
C	4.03857400	-3.75674500	-1.29111900
C	3.07622900	-4.11889200	-0.35585600
C	2.32522200	-3.14703600	0.29854200
C	2.51977500	-1.79230000	0.02573800
H	3.68292800	-0.39694500	-1.13927800
H	4.99599700	-2.11002400	-2.28806500
H	4.62125900	-4.51472300	-1.79992200
H	2.90414400	-5.16473700	-0.13172100
H	1.57888800	-3.44499300	1.02003800
C	1.73551900	-0.70800300	0.77405200
C	1.10455400	0.29911600	-0.21302300
H	0.56234600	-0.27461200	-0.96578600
H	1.92576100	0.78753700	-0.73547200
C	2.64390600	-0.04005700	1.81342600

H	2.11149400	0.72929300	2.37265800
H	3.01228800	-0.78722600	2.51673600
H	3.50095200	0.41714300	1.31947100
C	-1.31456300	1.16339500	0.02868600
H	-1.36453000	1.03363500	-1.05408500
H	-1.86220000	2.08748000	0.25555400
C	0.59305300	2.79221100	0.00553000
C	0.80625200	3.77187900	0.97651800
C	0.74351700	3.15373800	-1.33740500
C	1.16153000	5.07110300	0.62397900
H	0.69504700	3.51550500	2.02436400
C	1.09556800	4.45020500	-1.69530800
H	0.58668200	2.41559200	-2.11570400
C	1.30726000	5.41542200	-0.71479800
H	1.32620100	5.81217400	1.39686400
H	1.20631300	4.70755100	-2.74188700
H	1.58431300	6.42467700	-0.99294400
O	0.70281900	-1.30425500	1.60264800
O	-0.31469100	-1.86788700	0.82600900
C	-2.02425500	0.01107800	0.72965400
C	0.17705600	1.38514100	0.40611500
H	0.25561200	1.33510400	1.49254300
H	-1.16485000	-0.98333100	0.71374600
C	-3.21022500	-0.57647100	0.03913900
C	-3.76076700	-1.78300200	0.50691200
C	-3.81126000	0.01896700	-1.08015100
C	-4.85908500	-2.36194500	-0.11029900
H	-3.30194400	-2.28526500	1.34915500
C	-4.92064000	-0.55521500	-1.69126200
H	-3.42967700	0.95268700	-1.46957300
C	-5.44927800	-1.74850800	-1.21288700
H	-5.25339500	-3.29818900	0.26556000
H	-5.37335800	-0.06472800	-2.54453800
H	-6.30897600	-2.19801000	-1.69399300
C	-2.19540500	0.21377400	2.22991600
H	-2.83134000	1.08818300	2.41334300
H	-2.66851300	-0.64400000	2.70489200
H	-1.23958900	0.38052100	2.72668300

TS-2’

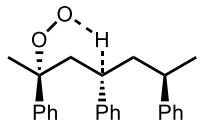

E = -1119.553106 Eh
ZPVE = 0.449663 Eh
G = -1119.1743106143683 Eh

C	4.01315500	-0.61432000	-1.21133200

C	4.99402200	-1.47981800	-1.68024300
C	5.51063700	-2.46761300	-0.84763500
C	5.03672900	-2.57750200	0.45386200
C	4.05314400	-1.71140800	0.92430700
C	3.52786800	-0.71844700	0.09558800
H	3.62858900	0.14979100	-1.87590600
H	5.35572500	-1.38042400	-2.69642200
H	6.27577900	-3.14249000	-1.21073300
H	5.43298600	-3.34043200	1.11291900
H	3.69385300	-1.80666000	1.93860400
C	2.45709900	0.25161000	0.58418600
C	1.16460000	0.12086000	-0.30375000
H	1.02539100	-0.94451200	-0.47753900
H	1.38508000	0.57195500	-1.27221500
C	3.00732600	1.67931200	0.65548300
H	2.25590600	2.38257100	1.00545800
H	3.85571600	1.70526800	1.34043200
H	3.35288100	1.99642800	-0.32854300
C	-0.10175000	0.69398200	0.32843700
H	0.34030800	0.77543400	1.54743700
C	-1.25737100	-0.30153300	0.49835900
H	-1.88824500	0.01333700	1.33214400
H	-0.84154600	-1.27029700	0.78589000
C	-0.51082500	2.09816200	0.01689700
C	-1.48292200	2.72467700	0.81779500
C	0.03091600	2.84726800	-1.03707200
C	-1.89442900	4.02619400	0.57381700
H	-1.90752700	2.18879800	1.65733400
C	-0.38628000	4.14991100	-1.28844800
H	0.77979700	2.41358900	-1.68512600
C	-1.35004700	4.74809300	-0.48555600
H	-2.63763300	4.48215100	1.21650700
H	0.04529300	4.69765000	-2.11749900
H	-1.67077400	5.76407300	-0.67867000
O	2.07387800	-0.21562900	1.89556600
O	1.17943800	0.68658700	2.47347500
C	-2.19012200	-0.47868300	-0.73366100
C	-1.47484100	-1.02760700	-1.97700000
H	-1.01301800	-1.99852800	-1.78420000
H	-2.18573500	-1.15604100	-2.79528500
H	-0.69419000	-0.34715700	-2.31959300
H	-2.57234800	0.51423800	-0.98699700
C	-3.38944900	-1.33073500	-0.35265900
C	-4.66579000	-0.76780900	-0.29451200
C	-3.25369800	-2.68701000	-0.04016700
C	-5.77446100	-1.53109400	0.06063400
H	-4.79395200	0.28221100	-0.53333500
C	-4.35726100	-3.45368500	0.31652900
H	-2.27679900	-3.15483400	-0.07508600
C	-5.62373500	-2.87841000	0.36817500
H	-6.75508000	-1.07186400	0.09590400

H	-4.22846000	-4.50269800	0.55470400
H	-6.48362200	-3.47561200	0.64529000

Int-3

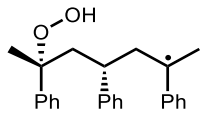

E = -1119.584435 Eh
ZPVE = 0.453629 Eh
G = -1119.2035066061185 Eh

C	-0.54372700	3.17168400	-0.62248100
C	-1.04970200	4.44691100	-0.39832300
C	-1.92569900	4.67740100	0.65896100
C	-2.28760700	3.62150500	1.48745100
C	-1.77691600	2.34650700	1.25887100
C	-0.89832900	2.09935200	0.20282900
H	0.13672600	3.01295000	-1.45144200
H	-0.75969900	5.26280800	-1.04961300
H	-2.31975200	5.67074400	0.83477200
H	-2.96750000	3.78789800	2.31440400
H	-2.06754800	1.52941300	1.90926800
C	-0.36045600	0.69962400	-0.04109900
H	-0.66394500	0.09062700	0.81070500
C	1.18784800	0.69185300	-0.13815500
H	1.59160700	1.57302800	0.36435000
H	1.48984200	0.77483200	-1.18511200
C	-1.00275400	0.05214000	-1.31140600
H	-0.49123500	-0.89547700	-1.48581500
H	-0.77347400	0.69480900	-2.16659100
C	1.93596300	-0.51486300	0.48622700
C	1.67231600	-0.63949800	1.98803300
H	2.26706800	-1.44124600	2.42115900
H	1.90612600	0.29253200	2.50318600
H	0.62272300	-0.86856400	2.16379600
C	3.42476800	-0.40004500	0.13749700
C	3.84798500	-0.70767000	-1.16051600
C	4.38069400	0.03352200	1.05649700
C	5.18462000	-0.59441200	-1.52483400
H	3.11990100	-1.03880800	-1.89130600
C	5.71899200	0.15682100	0.69154100
H	4.09177000	0.27823600	2.06940400
C	6.12737500	-0.15886800	-0.59849100
H	5.48921300	-0.84286900	-2.53432800
H	6.44289200	0.49662000	1.42217700
H	7.16895700	-0.06739500	-0.88017200
C	-2.48898000	-0.15210100	-1.22670700
C	-3.38653800	0.87551000	-1.85330400

H	-4.06516500	0.42806800	-2.58897600
H	-4.01755500	1.38053100	-1.11284000
H	-2.80843800	1.64627600	-2.36095200
C	-3.04322200	-1.27772800	-0.54770200
C	-4.45014000	-1.44512500	-0.41916100
C	-2.22944800	-2.28923600	0.03581000
C	-4.99382600	-2.53431700	0.23805700
H	-5.11649800	-0.70589600	-0.84201900
C	-2.78564800	-3.37396100	0.69001400
H	-1.15242500	-2.22432200	-0.03407100
C	-4.17039300	-3.51059900	0.80022900
H	-6.07088000	-2.62706200	0.31500700
H	-2.13289800	-4.12574900	1.11774200
H	-4.59952900	-4.36205800	1.31323800
O	1.37385600	-1.65877800	-0.20446100
O	1.93535600	-2.88322800	0.32436600
H	2.68295900	-3.03031400	-0.27424600

Int-3'

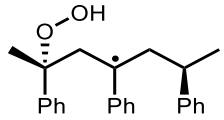

E = -1119.579486 Eh
ZPVE = 0.453938 Eh
G = -1119.195741832245 Eh

C	2.64787000	2.47547000	0.78075300
C	3.33788200	3.54460300	0.23527700
C	2.81709600	4.24937800	-0.84894200
C	1.57915300	3.87059200	-1.36763500
C	0.87817100	2.81098500	-0.81933500
C	1.38857700	2.05999400	0.27218600
H	3.06673500	1.97547100	1.64238300
H	4.28820100	3.83920500	0.66466800
H	3.36187000	5.08095800	-1.27747200
H	1.15943700	4.40733900	-2.21013000
H	-0.07106900	2.53776700	-1.25866600
C	0.66498100	0.95969900	0.84694300
C	-0.84002100	0.93326300	0.76640600
H	-1.21158800	1.86807900	0.34842800
H	-1.22941100	0.89469100	1.79164400
C	1.32974100	-0.00532100	1.79834100
H	0.59229500	-0.74243200	2.11767800
H	1.61807500	0.54178800	2.70984800
C	-1.57308000	-0.20725300	-0.01202500
C	-0.96311700	-0.45201000	-1.38759500
H	-1.49400200	-1.24499000	-1.91111000
H	-0.99685400	0.45211800	-1.99584000
H	0.07874000	-0.74463600	-1.27746400

C	-3.07092300	0.11681600	-0.04068100
C	-3.81982700	-0.00618200	1.13560900
C	-3.72289700	0.56199800	-1.19144500
C	-5.17536200	0.30186200	1.15931900
H	-3.33372800	-0.34964600	2.04068700
C	-5.07904000	0.87727100	-1.16900900
H	-3.17928000	0.66204800	-2.12074000
C	-5.81142600	0.74775700	0.00490700
H	-5.73425000	0.19606500	2.08133000
H	-5.56307300	1.21989600	-2.07552300
H	-6.86680900	0.98978900	0.02069200
C	2.59833200	-0.76320200	1.31208000
C	3.22568200	-1.52129900	2.49429200
H	2.53494400	-2.26103900	2.90552100
H	4.12957700	-2.04748600	2.18281200
H	3.49256000	-0.83220200	3.29976700
C	2.35851700	-1.68588100	0.12890000
C	2.99125700	-1.43642500	-1.09109200
C	1.54264900	-2.81602400	0.22808000
C	2.81852100	-2.28659800	-2.17997300
H	3.62701300	-0.56378500	-1.19033200
C	1.36654400	-3.66823200	-0.85540800
H	1.02062300	-3.02813000	1.15220600
C	2.00566800	-3.40864600	-2.06448600
H	3.32020900	-2.07127800	-3.11593100
H	0.72010600	-4.53146400	-0.75664000
H	1.86823900	-4.07357600	-2.90852800
O	-1.36457500	-1.36017200	0.84213700
O	-1.96502500	-2.53479000	0.24885600
H	-2.85903900	-2.50653500	0.62210100
H	3.32757800	-0.02400200	0.97787100

Int-4

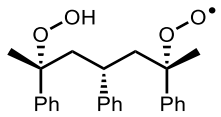

E = -1269.985063 Eh
ZPVE = 0.462515 Eh
G = -1269.5975353182957 Eh

C	0.70613600	3.03848600	0.67097600
C	1.16520300	4.31351600	0.36313000
C	1.76187300	4.56557000	-0.86882300
C	1.89173600	3.53101200	-1.78786000
C	1.42879400	2.25644400	-1.47429700
C	0.83349300	1.98798400	-0.24136500
H	0.25080800	2.86420300	1.63889200
H	1.06036300	5.11201100	1.08780600

H	2.12378700	5.55802500	-1.10731700
H	2.35678600	3.71328300	-2.74928900
H	1.54075500	1.45492200	-2.19573600
C	0.29388100	0.59610200	0.06148700
H	0.58249100	-0.04035300	-0.77600400
C	-1.25755100	0.66265100	0.10367600
H	-1.58821700	1.38498600	-0.64537000
H	-1.58057100	1.06417700	1.06801700
C	0.86436200	-0.02927100	1.35366400
H	0.25569100	-0.89618000	1.60663000
H	0.76088500	0.67419100	2.18428600
C	-2.07693100	-0.62504400	-0.18268100
C	-1.65030800	-1.31014900	-1.48141100
H	-2.32138800	-2.13100500	-1.72638000
H	-1.64295900	-0.60212400	-2.31103900
H	-0.64684500	-1.71748500	-1.37267200
C	-3.56597800	-0.25763200	-0.14791800
C	-4.18973700	-0.04318000	1.08603200
C	-4.32391700	-0.09155900	-1.30755500
C	-5.53099900	0.31591000	1.15840900
H	-3.61612200	-0.15869300	1.99776000
C	-5.66494900	0.27640700	-1.23812800
H	-3.87541100	-0.24925400	-2.27897500
C	-6.27501800	0.47874700	-0.00594000
H	-5.99372100	0.47267600	2.12530200
H	-6.23319300	0.40041900	-2.15192600
H	-7.31914200	0.76075200	0.04741300
C	2.32577000	-0.51777000	1.33811200
C	2.67575500	-1.18532100	2.66926500
H	2.07918700	-2.08676500	2.80198900
H	3.72899100	-1.45671800	2.69311600
H	2.46484400	-0.50584500	3.49686600
C	2.63271500	-1.42263500	0.14641600
C	3.50848600	-1.05616300	-0.87631400
C	1.99183100	-2.66346600	0.06075900
C	3.74410100	-1.91305000	-1.94859900
H	4.01661300	-0.10390300	-0.84315100
C	2.22613400	-3.51675300	-1.01078700
H	1.29456600	-2.97102700	0.82986300
C	3.10722000	-3.14552700	-2.02146900
H	4.43280300	-1.61059400	-2.72812300
H	1.71837900	-4.47256200	-1.05305600
H	3.29434500	-3.81047200	-2.85552600
O	-1.78335500	-1.48832200	0.94586300
O	-2.44271400	-2.76556500	0.78025800
H	-3.29258600	-2.60678100	1.21847400
O	3.12193900	0.73602200	1.23754200
O	4.40616000	0.57889800	1.47202100

TS-3

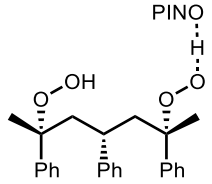

E = -1858.419633 Eh
ZPVE = 0.577902 Eh
G = -1857.9355251660809 Eh

C	-3.59355600	1.20736700	1.86232400
C	-4.16953400	1.45753800	3.10329800
C	-3.47868100	1.14717700	4.27091200
C	-2.21013700	0.58334600	4.18268600
C	-1.64037900	0.33358700	2.93832800
C	-2.31993100	0.64126300	1.75788600
H	-4.15414400	1.45151600	0.96696600
H	-5.15977900	1.89388500	3.15860000
H	-3.92528600	1.34210200	5.23811800
H	-1.66217600	0.33546500	5.08379600
H	-0.65619100	-0.11577300	2.87907300
C	-1.68411900	0.34835000	0.40636400
H	-0.66459700	0.00919000	0.58839600
C	-1.61544000	1.60295800	-0.50653000
H	-2.55430200	2.15765500	-0.45483300
H	-1.51913700	1.27747400	-1.54491800
C	-2.40734100	-0.76251000	-0.40167000
H	-1.90162100	-0.83206500	-1.36532200
H	-3.42978200	-0.43633400	-0.60989200
C	-0.47962100	2.62623000	-0.27902500
C	-0.31765600	3.10569300	1.16179600
H	0.42632900	3.89861900	1.21689600
H	-1.26384400	3.48031500	1.54856100
H	-0.00444700	2.28338500	1.80055400
C	-0.64444600	3.77018300	-1.28262000
C	-0.20016400	3.62677600	-2.59931400
C	-1.30190200	4.94869400	-0.92704200
C	-0.40177800	4.63746300	-3.53173400
H	0.32189000	2.72629900	-2.89345800
C	-1.50909600	5.95901300	-1.86166700
H	-1.65795700	5.09210800	0.08428000
C	-1.05861500	5.80835800	-3.16760600
H	-0.04081800	4.50980600	-4.54501400
H	-2.01903700	6.86686500	-1.56321200
H	-1.21456600	6.59636800	-3.89386800
C	-2.46887400	-2.19941900	0.17895200
C	-3.47592600	-2.37163400	1.32945700
H	-4.47533700	-2.11543900	0.97696400
H	-3.48457300	-3.41281400	1.65221900

H	-3.22918200	-1.73976300	2.17845100
C	-2.82474700	-3.21657300	-0.91719300
C	-2.25376600	-4.49072600	-0.90330300
C	-3.77513600	-2.92923400	-1.89963200
C	-2.61562400	-5.44459300	-1.84778000
H	-1.51235700	-4.72661900	-0.15319800
C	-4.14103700	-3.88397500	-2.84417600
H	-4.24605900	-1.95559400	-1.93823300
C	-3.56112600	-5.14682800	-2.82381000
H	-2.15415400	-6.42464600	-1.82149800
H	-4.88094900	-3.63702800	-3.59612000
H	-3.84252000	-5.89017900	-3.55960900
O	-1.23007100	-2.55748900	0.81251900
O	-0.15412700	-2.50538500	-0.16937600
H	0.51282000	-2.01300100	0.34124900
O	0.71419600	1.84022500	-0.64548300
O	1.87471500	2.55035000	-0.49365400
H	2.42852500	2.09822500	0.40393200
O	3.02072300	1.58277800	1.35067000
N	3.64221000	0.51663100	0.91225800
C	5.01791600	0.50453400	0.50524200
C	3.04018000	-0.75930900	0.82695000
C	5.27769000	-0.91369800	0.14433600
O	5.73618900	1.46241300	0.48489100
C	4.10918700	-1.65666300	0.32898400
O	1.89088000	-0.99513900	1.11395300
C	6.43969400	-1.50394800	-0.31656600
C	4.06406300	-3.01236400	0.05653000
C	6.40282600	-2.87240400	-0.59195300
H	7.34033900	-0.92116900	-0.45792100
C	5.23431000	-3.61406100	-0.40924900
H	3.15342500	-3.58008700	0.19638900
H	7.29399800	-3.36799100	-0.95547400
H	5.23657600	-4.67274500	-0.63488400

3b

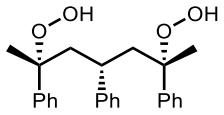

E = -1270.624904 Eh
ZPVE = 0.474155 Eh
G = -1270.225440122063 Eh

C	-0.67775300	3.08550500	-0.71786400
C	-1.08077200	4.38394100	-0.42692900
C	-1.60341600	4.69194200	0.82549900
C	-1.71538800	3.68903000	1.78205400
C	-1.30925900	2.39202200	1.48466000
C	-0.78941900	2.06654300	0.23133400

H	-0.27737200	2.86866700	-1.70128000
H	-0.98677600	5.15736600	-1.18002400
H	-1.91961100	5.70269500	1.05236100
H	-2.12249500	3.91452800	2.76051800
H	-1.40850500	1.61599100	2.23516000
C	-0.30468100	0.65030100	-0.05288900
H	-0.59327100	0.04234400	0.80584300
C	1.24669300	0.67699200	-0.12166200
H	1.60527500	1.35058000	0.65961000
H	1.56387000	1.12377700	-1.06807800
C	-0.92468700	0.01771700	-1.31716100
H	-0.33400500	-0.85575900	-1.58866900
H	-0.85154600	0.71628500	-2.15469500
C	2.04303900	-0.64182400	0.07604500
C	1.56653500	-1.43689500	1.29134100
H	2.22020500	-2.28600700	1.48114300
H	1.54008600	-0.80760700	2.18199100
H	0.56248100	-1.81774200	1.11405800
C	3.53586300	-0.29032700	0.12233800
C	4.19998000	0.03548400	-1.06528100
C	4.25863400	-0.24597300	1.31504400
C	5.54566400	0.38550300	-1.06156500
H	3.65443200	0.01409300	-2.00093700
C	5.60408700	0.11205500	1.32259000
H	3.77835600	-0.49238500	2.25222500
C	6.25413700	0.42665200	0.13513700
H	6.03966800	0.63021600	-1.99415500
H	6.14450700	0.14016100	2.26097200
H	7.30166600	0.70105000	0.14133100
C	-2.39415400	-0.46821800	-1.23572000
C	-2.80723200	-1.04338600	-2.59722800
H	-2.16248700	-1.87511200	-2.87866500
H	-3.83521200	-1.39963100	-2.56965200
H	-2.71754400	-0.27090200	-3.36374300
C	-2.58270400	-1.48386500	-0.10484100
C	-3.25599800	-1.14708800	1.07051300
C	-2.04420800	-2.76953400	-0.21550600
C	-3.39448700	-2.07261500	2.10094300
H	-3.68261900	-0.16008800	1.17359200
C	-2.17915100	-3.69368500	0.81484000
H	-1.50247700	-3.05982600	-1.10685300
C	-2.85830000	-3.34945600	1.97892500
H	-3.92812100	-1.79221900	3.00130900
H	-1.75085600	-4.68269700	0.70574600
H	-2.96830600	-4.06905300	2.78095500
O	1.78229500	-1.39437200	-1.13719900
O	2.42840000	-2.68730300	-1.06826800
H	3.29237500	-2.49622200	-1.46372100
O	-3.12780400	0.74305500	-0.97424200
O	-4.56259900	0.47947800	-1.02740900
H	-4.82218100	1.13572200	-1.68708300

5c. Dihedral angle scans

Table S1. Dihedral angle scans of cumene, dimer, and trimer.

cumene		dimer		trimer (internal Ph)		trimer (terminal Ph)	
dihedral angle	Relative energy (kcal/mol)	dihedral angle	Relative energy (kcal/mol)	dihedral angle	Relative energy (kcal/mol)	dihedral angle	Relative energy (kcal/mol)
0.0	2.5	0.0	3.5	0.1	4.5	0.0	6.7
5.0	2.4	5.0	3.3	5.1	4.4	5.0	6.6
10.0	2.3	10.0	2.9	10.1	4.2	10.0	6.3
15.0	2.0	15.0	2.6	15.1	3.9	15.0	5.9
20.0	1.8	20.0	2.3	20.1	3.5	20.0	5.4
25.0	1.5	25.0	2.0	25.1	3.2	25.0	4.6
30.0	1.3	30.0	1.7	30.1	2.9	30.0	3.8
35.0	1.1	35.0	1.4	35.1	2.4	35.0	3.2
40.0	0.9	40.0	1.2	40.1	2.0	40.0	2.6
45.0	0.8	45.0	1.0	45.1	1.7	45.0	2.1
50.0	0.7	50.0	0.9	50.1	1.4	50.0	1.6
55.0	0.5	55.0	0.7	55.1	1.1	55.0	1.2
60.0	0.5	60.0	0.6	60.1	0.9	60.0	0.9
65.0	0.4	65.0	0.5	65.1	0.6	65.0	0.6
70.0	0.3	70.0	0.3	70.1	0.4	70.0	0.3
75.0	0.2	75.0	0.2	75.1	0.3	75.0	0.1
80.0	0.1	80.0	0.1	80.1	0.1	80.0	0.0
85.0	0.0	85.0	0.0	85.1	0.0	85.0	0.0
90.0	0.0	90.0	0.0	90.1	0.0	90.0	0.1
95.0	0.0	95.0	0.0	95.1	0.0	95.0	0.2
100.0	0.1	100.0	0.1	100.1	0.1	100.0	0.4
105.0	0.2	105.0	0.2	105.1	0.3	105.0	0.6
110.0	0.3	110.0	0.2	110.1	0.4	110.0	0.8
115.0	0.4	115.0	0.4	115.1	0.6	115.0	1.1
120.0	0.5	120.0	0.5	120.1	0.8	120.0	1.5
125.0	0.5	125.0	0.6	125.1	1.0	125.0	1.8
130.0	0.7	130.0	0.8	130.1	1.3	130.0	2.2
135.0	0.8	135.0	1.0	135.1	1.6	135.0	2.6
140.0	0.9	140.0	1.3	140.1	1.9	140.0	3.1
145.0	1.1	145.0	1.5	145.1	2.2	145.0	3.6
150.0	1.3	150.0	1.9	150.1	2.7	150.0	4.1
155.0	1.5	155.0	2.3	155.1	3.1	155.0	4.7
160.0	1.8	160.0	2.6	160.1	3.5	160.0	5.3

165.0	2.0	165.0	3.0	165.1	3.9	165.0	5.8
170.0	2.3	170.0	3.3	170.1	4.3	170.0	6.3
175.0	2.4	175.0	3.5	175.1	4.5	175.0	6.6
180.0	2.5	180.0	3.5	180.1	4.6	180.0	6.7
185.0	2.5	185.0	3.4	185.1	4.5	185.0	6.6
190.0	2.4	190.0	3.1	190.1	4.3	190.0	6.3
195.0	2.1	195.0	2.8	195.1	4.0	195.0	5.9
200.0	1.9	200.0	2.4	200.1	3.7	200.0	5.4
205.0	1.6	205.0	2.0	205.1	3.4	205.0	4.6
210.0	1.3	210.0	1.7	210.1	2.9	210.0	3.8
215.0	1.1	215.0	1.4	215.1	2.5	215.0	3.1
220.0	0.9	220.0	1.2	220.1	2.0	220.0	2.5
225.0	0.8	225.0	1.0	225.1	1.7	225.0	2.0
230.0	0.6	230.0	0.8	230.1	1.3	230.0	1.5
235.0	0.5	235.0	0.7	235.1	1.0	235.0	1.1
240.0	0.4	240.0	0.5	240.1	0.8	240.0	0.8
245.0	0.3	245.0	0.4	245.1	0.6	245.0	0.5
250.0	0.2	250.0	0.3	250.1	0.4	250.0	0.3
255.0	0.1	255.0	0.2	255.1	0.2	255.0	0.1
260.0	0.1	260.0	0.1	260.1	0.1	260.0	0.0
265.0	0.0	265.0	0.0	265.1	0.0	265.0	0.0
270.0	0.0	269.2	0.0	268.8	0.0	271.1	0.0
275.0	0.0	274.2	0.0	273.8	0.0	276.1	0.1
280.0	0.0	279.2	0.1	278.8	0.1	281.1	0.3
285.0	0.1	284.2	0.1	283.8	0.2	286.1	0.5
290.0	0.1	289.2	0.2	288.8	0.3	291.1	0.7
295.0	0.2	294.2	0.3	293.8	0.5	296.1	1.0
300.0	0.3	299.2	0.4	298.8	0.7	301.1	1.3
305.0	0.4	304.2	0.6	303.8	0.9	306.1	1.7
310.0	0.5	309.2	0.7	308.8	1.2	311.1	2.1
315.0	0.6	314.2	1.0	313.8	1.5	316.1	2.6
320.0	0.8	319.2	1.3	318.8	1.8	321.1	3.2
325.0	0.9	324.2	1.6	323.8	2.2	326.1	3.7
330.0	1.1	329.2	2.0	328.8	2.7	331.1	4.3
335.0	1.3	334.2	2.4	333.8	3.2	336.1	5.0
340.0	1.6	339.2	2.8	338.8	3.7	341.1	5.6
345.0	1.9	344.2	3.0	343.8	4.1	346.1	5.9
350.0	2.1	349.2	3.2	348.8	4.2	351.1	6.3
355.0	2.4	354.2	3.4	353.8	4.4	356.1	6.5

6. Polystyrene autoxidation and characterization

6a. General experimental procedure of polystyrene autoxidation

Scheme S5. Two different quenches after polystyrene autoxidation.

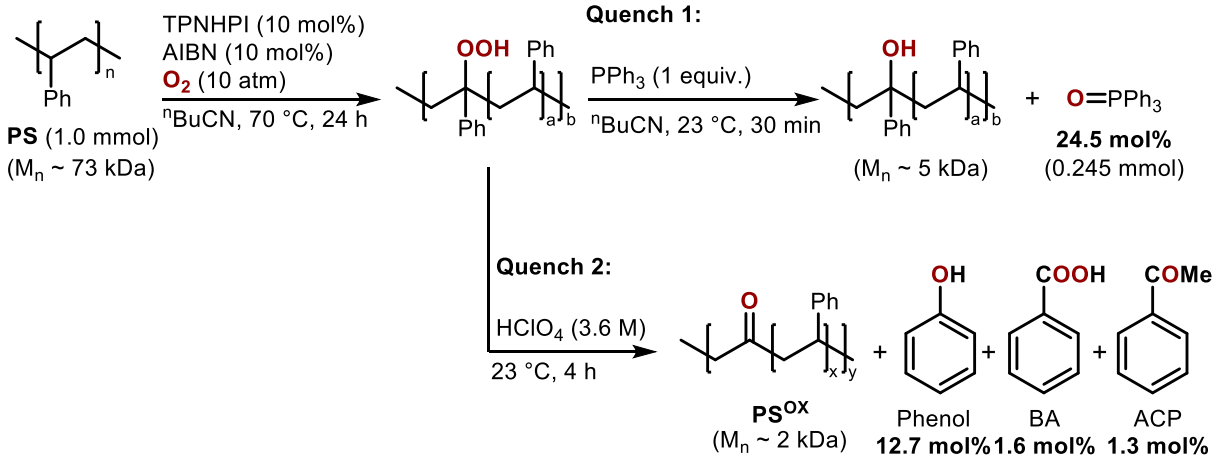

Reaction setup: To the Parr reactor vessels were added sequentially: a magnetic stir bar, PS (104 mg, 1.0 mmol based on repeat unit) and ^{n}BuCN (2.0 mL). After PS completely dissolved into ^{n}BuCN, TPNHPI (46.8 mg, 0.10 mmol), AIBN (8.2 mg, 0.10 mmol) were added into the vessels. The vessel was pressurized to the 10 atm with oxygen gas and loaded onto an oil bath preheated to a set temperature using a hotplate. The mixture was stirred for 24 h. Then, the reaction mixture was allowed to cool to 23 °C, the solution was transferred to a 10 mL Schlenk flask, and the Parr reactor was rinsed into the Schlenk flask with 3 mL of C_4H_9CN.

Quench 1. Phosphine quench to quantify hydroperoxides and other products

Workup with PPh_3: To the reaction mixture in a 10 mL Schlenk flask is added 1 mL of PPh_3 solution (1 mmol, 1.0 M in THF) and stirred for 30 min under inert atmosphere to reduce the generated hydroperoxides to the corresponding alcohols. To the reaction mixture was added 10 mg of 1,4-dimethoxybenzene as internal standard. The reaction mixture was diluted by adding 4 mL C_4H_9CN, and a 50 µL aliquot was removed for UPLC analysis to measure the corresponding triphenylphosphine oxide. 24.5 mol% of triphenylphosphine oxide were quantified by comparison to a calibration curve using commercially available triphenylphosphine oxide.

Quench 2. Acid treatment to quantify phenol and other products

1 mL of $HClO_4$ solution (3.6 M in MeCN) was added to the flask and the mixture was stirred for 4 h at 23 °C. 10 mg of 1,4-dimethoxybenzene was added into the flask. The reaction mixture was diluted by adding 4 mL MeCN and 50 µL aliquot was removed for UPLC analysis to measure the products. 12.7 mol% of phenol, 1.6 mol% of benzoic acid, and 1.3 mol% of acetophenone were quantified by comparison to a calibration curve using commercially available compounds. The remaining crude mixture was precipitated in 100 mL of pentane, filtered, and washed with MeOH, yielding PS^{OX} as a brown solid. The PS^{OX} was dried under reduced pressure for overnight and 71 mg of PS^{OX} was obtained.

6b. Assessment of the triphenylphosphine quenching method

To evaluate the accuracy of the triphenylphosphine quenching method (Quench 1 in **Section 6a**) for quantifying hydroperoxides on the polystyrene backbone, the method was applied to dimer (**2**) and compared with the hydroperoxide concentration of bis-hydroperoxide (**2a**). The yield detected with triphenylphosphine oxide ($Ph_3P=O$) showed good agreement with the hydroperoxide content.

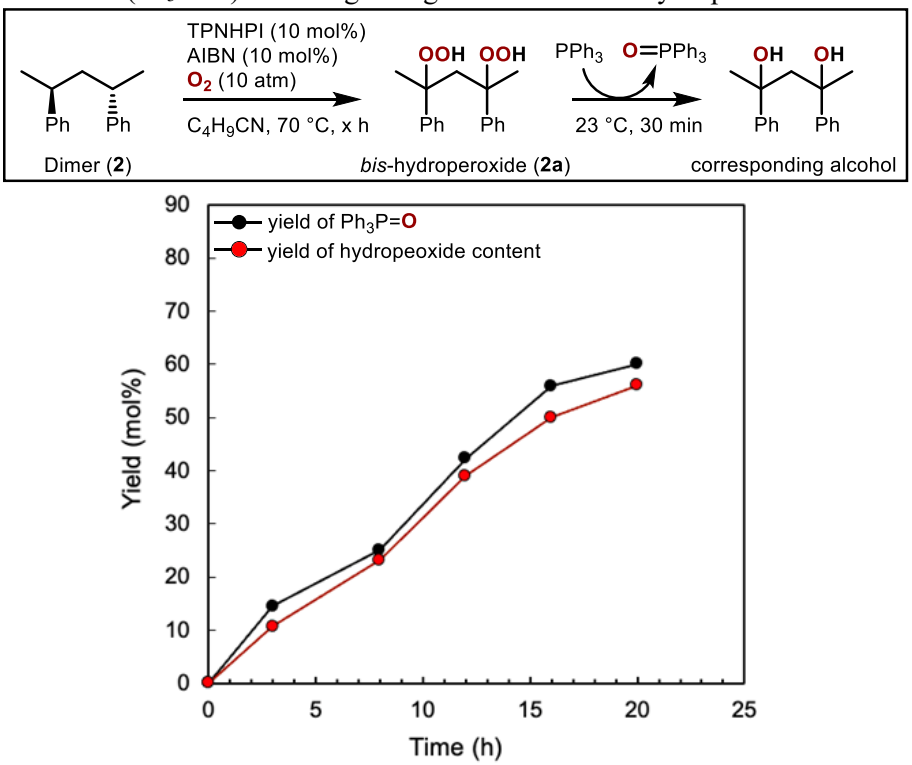

Figure S17. The detected yield of triphenylphosphine oxide ($Ph_3P=O$, black) and the hydroperoxide content (red) by triphenylphosphine quenching method after autoxidation reaction of **2**.

6c. NMR spectra of oxidatively degraded polystyrene

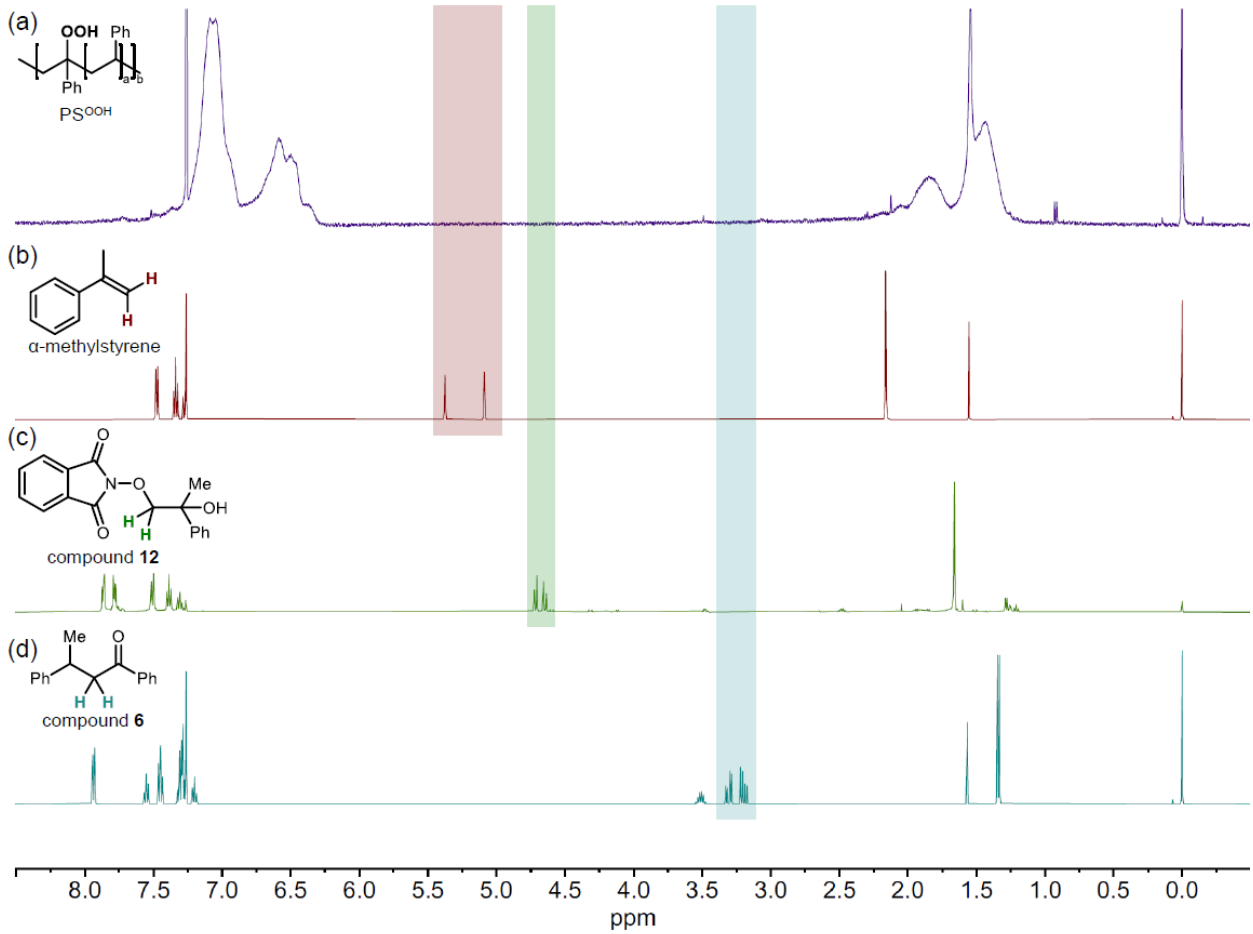

Figure S18. Stacked NMR spectra of (a) PS^{OOH} after 1st step and potential side products such as (b) α-methylstyrene, (c) compound **12** and (d) compound **6**.

Based on the generation of a small amount of α-methylstyrene during the dimer autoxidation step, we investigated whether similar side products are generated during the oxidation of PS. The ^{1}H NMR spectrum of oxidized PS after the first step (**PS^{OOH}**) was compared with potential side products detected during the autoxidation of the dimeric PS model compound **2**. We searched for proton peaks corresponding to potential side products, including α-methylstyrene-like alkene moieties, benzoyl terminal group of the compound **6** observed in **Figure 2**, and the methylene peak of the PINO radical adduct (**12**) observed in **Figure S9**. However, no proton peaks for such species were detected in the spectrum (**Figure S19**). While this analysis does not completely rule out the presence of alkene-like products, it suggests that their concentration is too low to be detected.

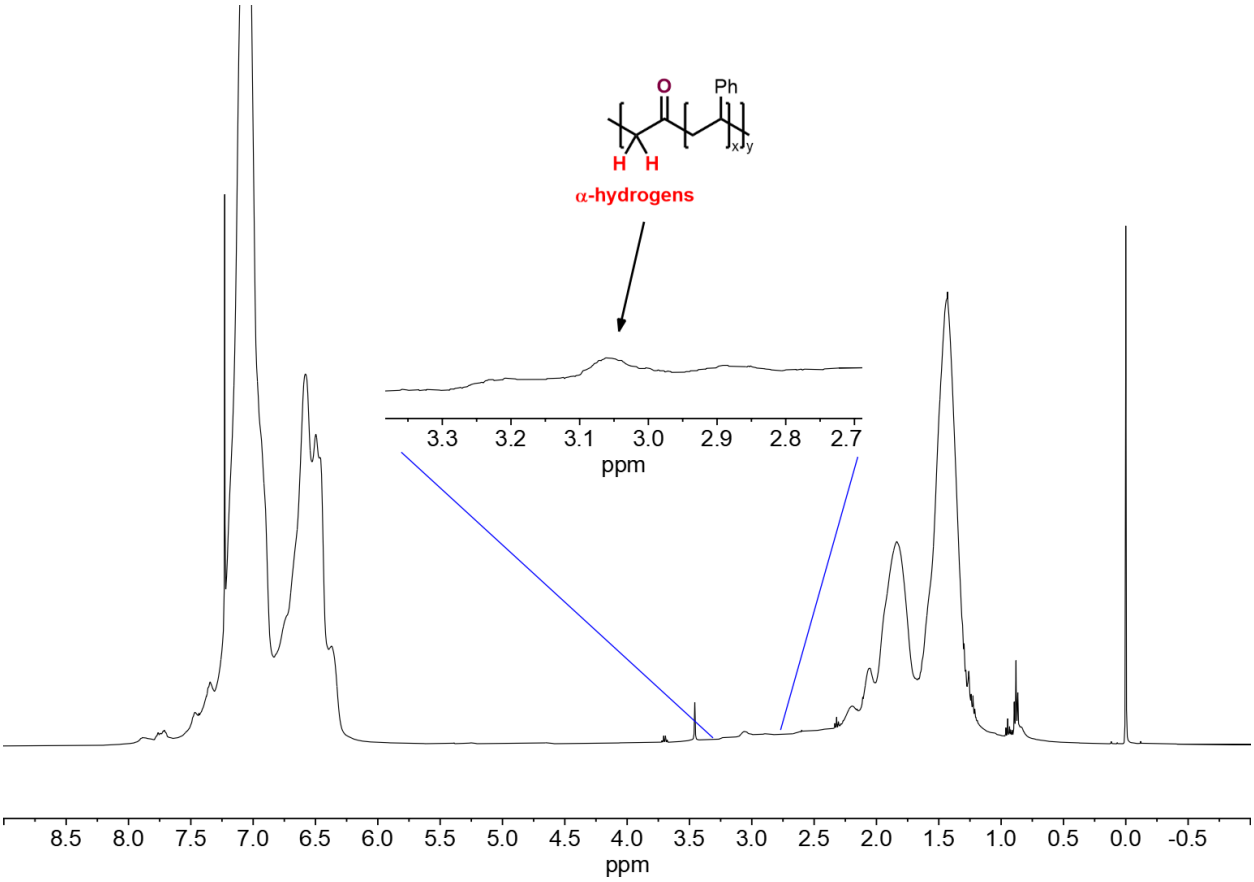

Figure S19. NMR spectra of oxidatively degraded polystyrene after Hock process.

The NMR spectra showed small α-hydrogen peaks around 3.05 ppm that are matched with previously reported NMR of polystyrene after oxidative degradation.[20]

6d. IR spectra of oxidatively degraded polymers

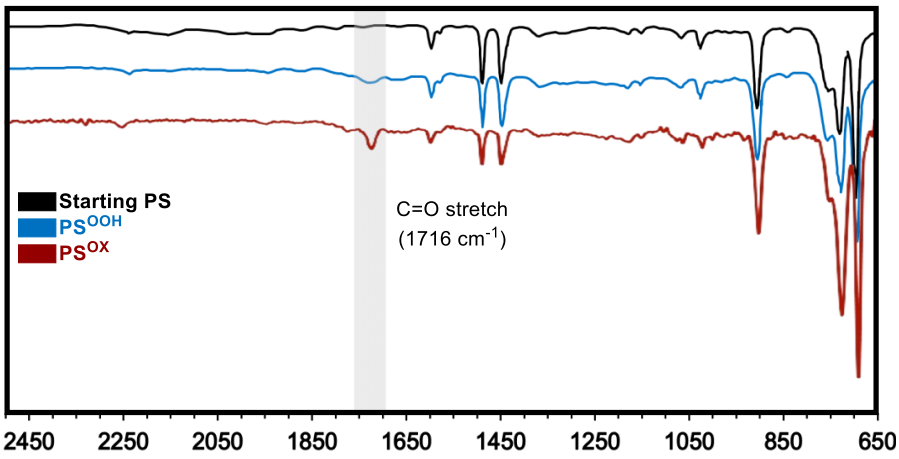

Figure S20. IR spectra of oxidatively degraded polystyrene after Hock process

After the autoxidation step (1st step), the precipitated **PS^{OOH}** exhibited a small C=O stretching peak, indicating the presence of a small amount of carbonyl groups. This feature could be attributed to the formation of terminal benzoyl groups, similar to the formation of acetophenone (**4**) and compound **6** in the reactions of the PS model compounds **2** and **3** (cf. Figure 2a of the manuscript). The benzoyl group could arise from O–O bond cleavage of hydroperoxide and chain scission, evident in GPC the time-course (Figure 5b). After acid treatment, the precipitated **PS^{OX}** showed clear C=O stretch at 1716 cm^{-1}.

6e. GPC analysis of oxidatively degraded polymers

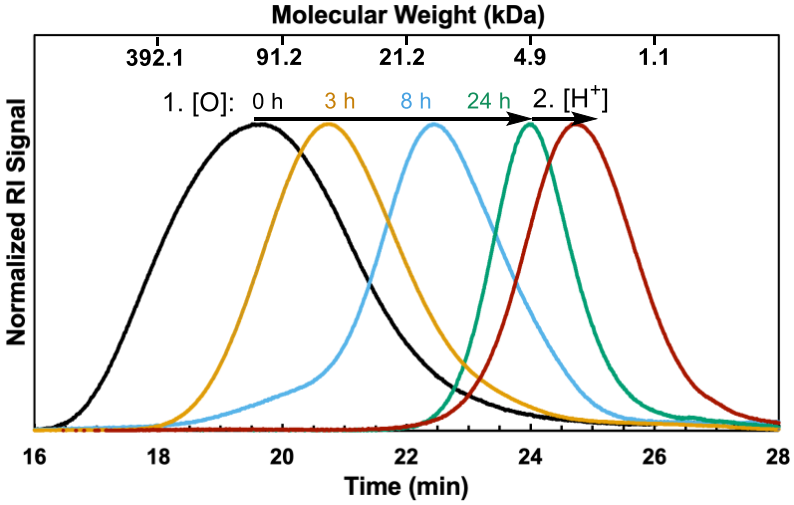

Reaction time (h)	Peak position (min)	M_n (kDa)	M_w (kDa)	PDI (M_w/M_n)
0	19.53	73	192	2.76
3	20.74	19	65	3.42
8	22.44	9.3	26	2.79
24	24.29	5.3	8.0	1.58
After 2nd step	24.72	2.1	3.1	1.51

Figure S21. Time-course of polystyrene oxidation monitored by gel-phase chromatography.

6f. GPC Calibration curve

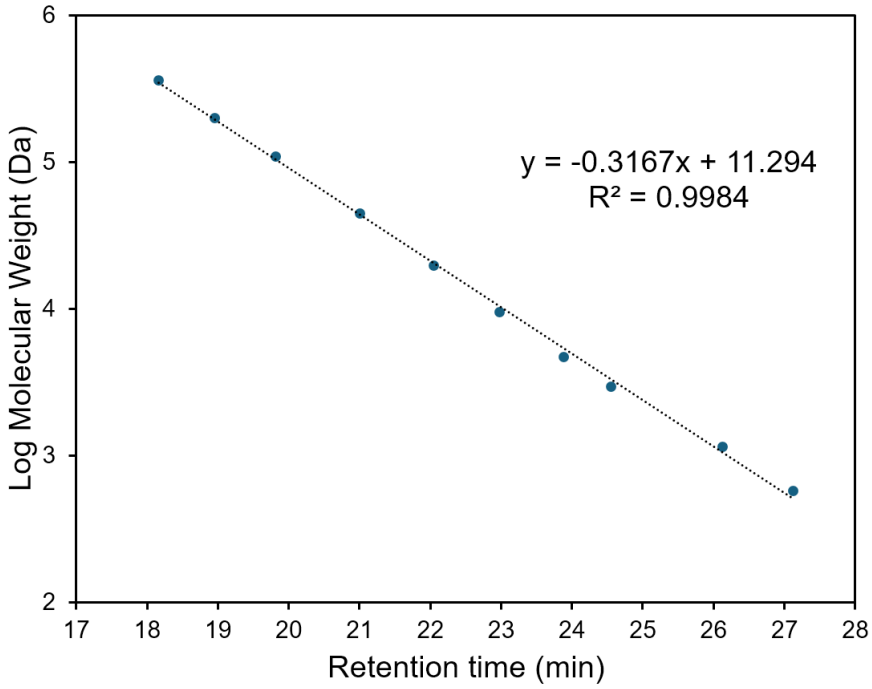

Figure S22. GPC Calibration curve.

Table S2. Molecular weight of polystyrene (PS) standard and their retention time.

Retention Time (min)	M_w of PS standard (Da)
18.2	364000
19.0	202100
19.8	110500
21.0	45120
22.0	19920
23.0	9590
23.9	4730
24.5	2970
26.1	1150
27.1	580

6g. Experimental procedure of sequential Hock and MC process

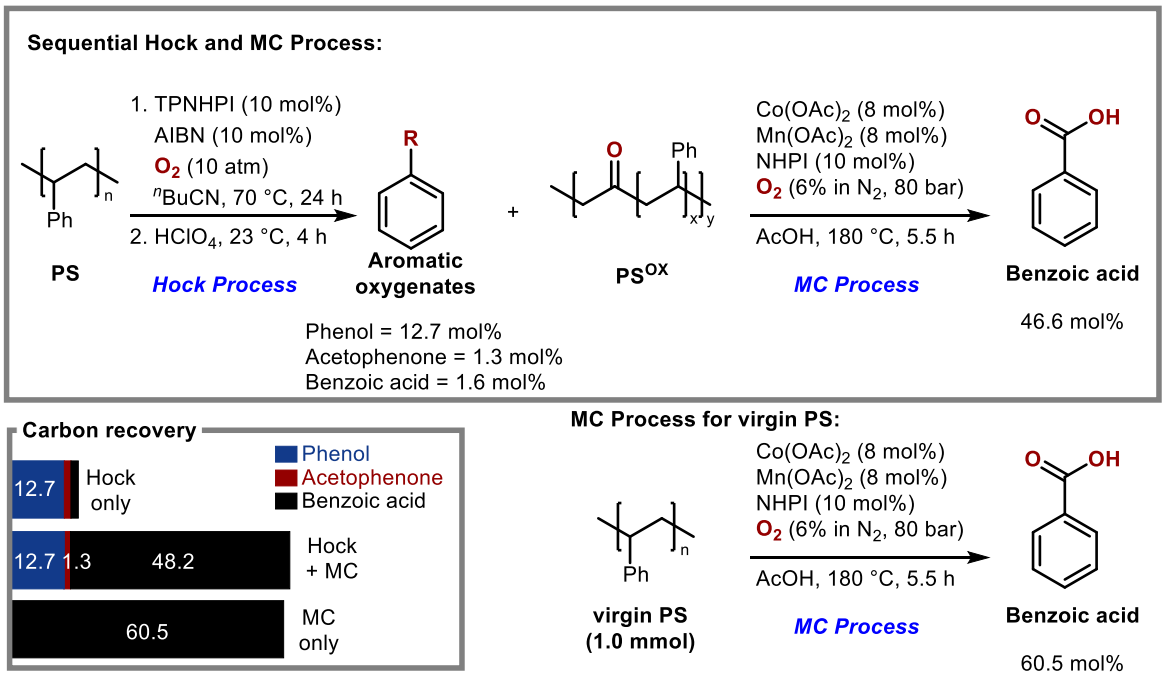

Figure S23. Sequential Hock and Mid-Century (MC) process of polystyrene (PS) for better carbon recovery.

1. Hock process

Reaction setup: To the Parr reactor vessels were added sequentially: a magnetic stir bar, PS (104 mg, 1.0 mmol based on repeat unit) and ^{n}BuCN (2.0 mL). After PS completely dissolved into ^{n}BuCN, TPNHPI (46.8 mg, 0.10 mmol), AIBN (8.2 mg, 0.10 mmol) were added into the vessels. The vessel was pressurized to the 10 atm with oxygen gas and loaded onto an oil bath preheated to a set temperature using a hotplate. The mixture was stirred for 24 h. Then, the reaction mixture was allowed to cool to 23 °C, the solution was transferred to a 10 mL Schlenk flask, and the Parr reactor was rinsed into the Schlenk flask with 3 mL of C_4H_9CN.

Acid treatment to quantify phenol and other products: 1 mL of $HClO_4$ solution (3.6 M in MeCN) was added to the flask and the mixture was stirred for 4 h at 23 °C. 10 mg of 1,4-dimethoxybenzene was added into the flask. The reaction mixture was diluted by adding 4 mL MeCN and 50 µL aliquot was removed for UPLC analysis to measure the products (12.7 mol% of phenol, 1.6 mol% of benzoic acid, and 1.3 mol% of acetophenone). The remaining crude mixture was precipitated in 100 mL of pentane, filtered, and washed with MeOH, yielding PS^{OX} as a brown solid.

2. MC process

Reaction setup: The following MC oxidation reaction condition was adapted from the previous literature procedure.[21] To the Parr reactor vessels were added sequentially: a magnetic stir bar, PS^{OX} from Hock process or virgin PS (104 mg, 1.0 mmol based on repeat unit), $Co(OAc)_2$ (14.1 mg, 0.080 mmol, 8 mol% of starting PS), $Mn(OAc)_2$ (13.8 mg, 0.080 mmol, 8 mol% of starting PS), 10 mol% of NHPI (16.3 mg, 0.10 mmol of starting PS) and AcOH (5.0 mL). The vessel was placed into Series 5000 Multiple Reaction System and pressurized to the 80 atm of 6% O_2 in N_2. The mixture was stirred at 500 rpm and heated to 180 °C. After 5.5 h, 10 mg of 1,4-dimethoxybenzene was added into the crude mixture. 50 µL aliquot was removed for UPLC analysis to measure the product.46.6 mol% of benzoic acid (yield based on 1.0 mmol

of starting PS). From the virgin PS substrate (1.0 mmol), 60.5 mol% of benzoic acid was obtained under the same MC oxidation reaction condition.

6h. Application to post-consumer polystyrene wastes

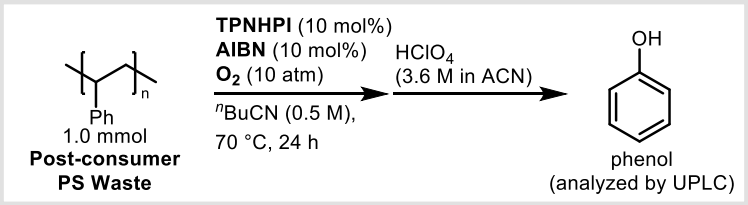

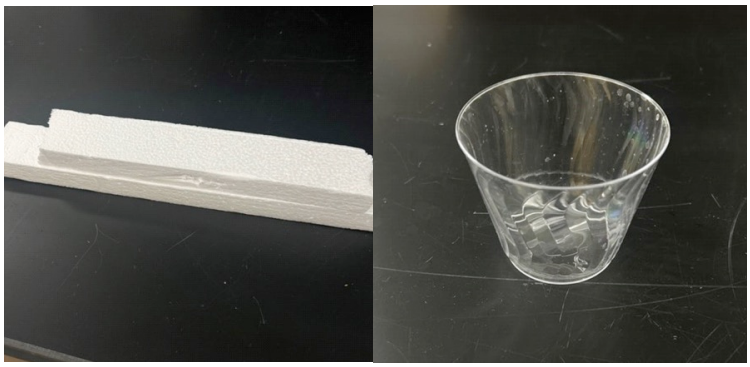

Styrofoam **Clear disposable cup**

12.3% phenol yield **9.8% phenol yield**

Figure S24. Autoxidation of post-consumer polystyrene (PS) to produce phenol.

7. References

(1) Yan, B.; Shi, C.; Beckham, G. T.; Chen, E. Y. -X.; Román-Leshkov, Y. Electrochemical Activation of C−C Bonds through Mediated Hydrogen Atom Transfer Reactions. *ChemSusChem* **2022**, *15*, e202102317.

(2) Nechab, M.; Einhorn, C.; Einhorn, J. New Aerobic Oxidation of Benzylic Compounds: Efficient Catalysis by N-Hydroxy-3,4,5,6-tetraphenylphthalimide (NHTPPI)/CuCl under Mild Conditions and Low Catalyst Loading. *ChemInform* **2004**, *35*, chin.200444053.

(3) (a) Clark, D. E. Peroxides and Peroxide-Forming Compounds. *J. Chem. Health Saf.* **2001**, *8*, 12–22; (b) Osterberg, P. M.; Niemeier, J. K.; Welch, C. J.; Hawkins, J. M.; Martinelli, J. R.; Johnson, T. E.; Root, T. W.; Stahl, S. S. Experimental Limiting Oxygen Concentrations for Nine Organic Solvents at Temperatures and Pressures Relevant to Aerobic Oxidations in the Pharmaceutical Industry. *Org. Process Res. Dev.* **2015**, *19*, 1537–1543.

(4) Jiao, Y.; Cao, C.; Zhou, Z. Direct Synthesis of Anti-1,3-Diols through Nonclassical Reaction of Aryl Grignard Reagents with Isopropenyl Acetate. *Org. Lett.* **2011**, *13*, 180–183.

(5) Gross, B. H.; Mebane, R. C.; Armstrong, D. L. Transfer Hydrogenolysis of Aromatic Alcohols Using Raney Catalysts and 2-Propanol. *Appl. Catal. A Gen.* **2001**, *219*, 281–289.

(6) Ghorai, S. K.; Jin, M.; Hatakeyama, T.; Nakamura, M. Cross-Coupling of Non-Activated Chloroalkanes with Aryl Grignard Reagents in the Presence of Iron/N-Heterocyclic Carbene Catalysts. *Org. Lett.* **2012**, *14*, 1066–1069.

(7) (a) Asressu, K. H.; Chan, C.-K.; Wang, C.-C. One-Pot Synthesis of 1,5-Diketones under a Transition-Metal-Free Condition: Application in the Synthesis of 2,4,6-Triaryl Pyridine Derivatives. *ACS Omega* **2021**, *6*, 7296–7311. (b) Nishimura, T.; Yasuhara, Y.; Sawano, T.; Hayashi, T. Iridium/Chiral Diene-Catalyzed Asymmetric 1,6-Addition of Arylboroxines to α,β,γ,δ-Unsaturated Carbonyl Compounds. *J. Am. Chem. Soc.* **2010**, *132*, 7872-7873. (c) Xia, X.-F.; Zhu, S.-L.; Gu, Z.; Wang, H.; Li, W.; Liu, X.; Liang, Y.-M. Catalyst-Controlled Dioxygenation of Olefins: An Approach to Peroxides, Alcohols, and Ketones. *J. Org. Chem.* **2015**, *80*, 5572–5580.

(8) Kushch, O.; Hordieieva, I.; Novikova, K.; Litvinov, Y.; Kompanets, M.; Shendrik, A.; Opeida, I. Kinetics of N-Oxyl Radicals' Decay. *J. Org. Chem.* **2020**, *85*, 7112–7124.

(9) Frisch, M. J.; Trucks, G. W.; Schlegel, H. B.; Scuseria, G. E.; Robb, M. A.; Cheeseman, J. R.; Scalmani, G.; Barone, V.; Petersson, G. A.; Nakatsuji, H.; et al. Gaussian 16, Revision C.01. **2016**.

(10) Becke, A. D. Density-functional Thermochemistry. III. The Role of Exact Exchange. *J. Chem. Phys.* **1993**, *98* (7), 5648–5652.

(11) Stephens, P. J.; Devlin, F. J.; Chabalowski, C. F.; Frisch, M. J. Ab Initio Calculation of Vibrational Absorption and Circular Dichroism Spectra Using Density Functional Force Fields. *J. Phys. Chem.* **1994**, *98* (45), 11623–11627.

(12) Vosko, S. H.; Wilk, L.; Nusair, M. Accurate Spin-Dependent Electron Liquid Correlation Energies for Local Spin Density Calculations: A Critical Analysis. *Can. J. Phys.* **1980**, *58* (8), 1200–1211.

(13) Lee, C.; Yang, W.; Parr, R. G. Development of the Colle-Salvetti Correlation-Energy Formula into a Functional of the Electron Density. *Phys. Rev. B* **1988**, *37* (2), 785.

(14) Vereecken, L.; Peeters, J. The 1,5-H-Shift in 1-Butoxy: A Case Study in the Rigorous Implementation of Transition State Theory for a Multirotamer System. *J. Chem. Phys.* **2003**, *119* (10), 5159–5170.

(15) Lym, J.; Wittreich, G. R.; Vlachos, D. G. A Python Multiscale Thermochemistry Toolbox (pMuTT) for Thermochemical and Kinetic Parameter Estimation. *Comput Phys. Commun.* **2020**, *247*, 106864.

(16) Neese, F. Software Update: The ORCA Program System—Version 5.0. *WIREs Comput. Mol. Sci.* **2022**, *12* (5), e1606.

(17) Liakos, D. G.; Guo, Y.; Neese, F. Comprehensive Benchmark Results for the Domain Based Local Pair Natural Orbital Coupled Cluster Method (DLPNO-CCSD(T)) for Closed- and Open-Shell Systems. *J. Phys. Chem. A* **2020**, *124* (1), 90–100.

(18) Bhattacharya, A. Kinetic Modeling of Liquid Phase Autoxidation of Cumene. *Chemical Engineering Journal* **2008**, *137*, 308–319.

(19) Wu, Y.; Zhao, J.; Meng, Q.; Bi, M.; Ma, C.; Yu, Z. Effects of Oxygen: Experimental and VTST/DFT Studies on Cumene Autoxidation with Air under Atmospheric Pressure. *ACS Omega* **2022**, *7*, 34547–34553.

(20) Oh, S.; Stache, E. E. Chemical Upcycling of Commercial Polystyrene via Catalyst-Controlled Photooxidation. *J. Am. Chem. Soc.* **2022**, *144*, 5745–5749.

(21) Sullivan, K. P.; Werner, A. Z.; Ramirez, K. J.; Ellis, L. D.; Bussard, J. R.; Black, B. A.; Brandner, D. G.; Bratti, F.; Buss, B. L.; Dong, X.; Haugen, S. J.; Ingraham, M. A.; Konev, M. O.; Michener, W. E.; Miscall, J.; Pardo, I.; Woodworth, S. P.; Guss, A. M.; Román-Leshkov, Y.; Stahl, S. S.; Beckham, G. T. Mixed Plastics Waste Valorization through Tandem Chemical Oxidation and Biological Funneling. *Science* **2022**, *378* (6616), 207–211.

8. NMR Spectra

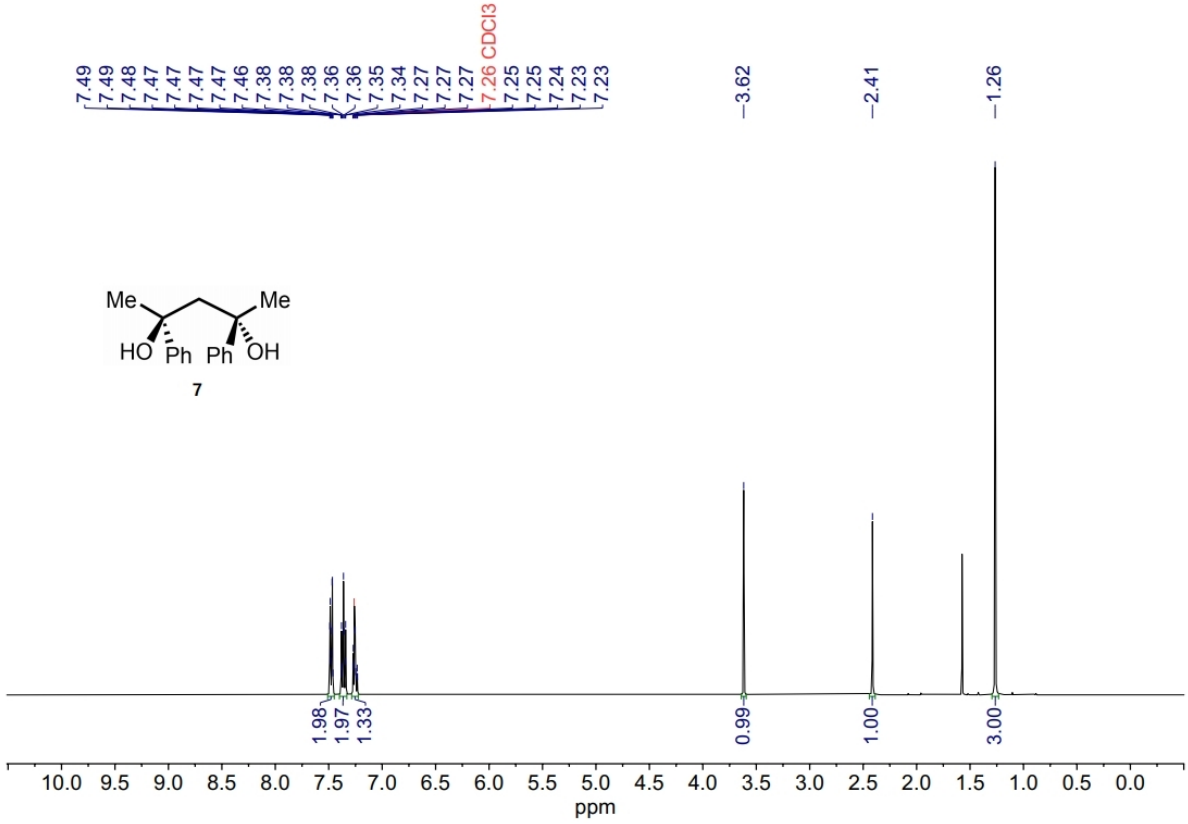

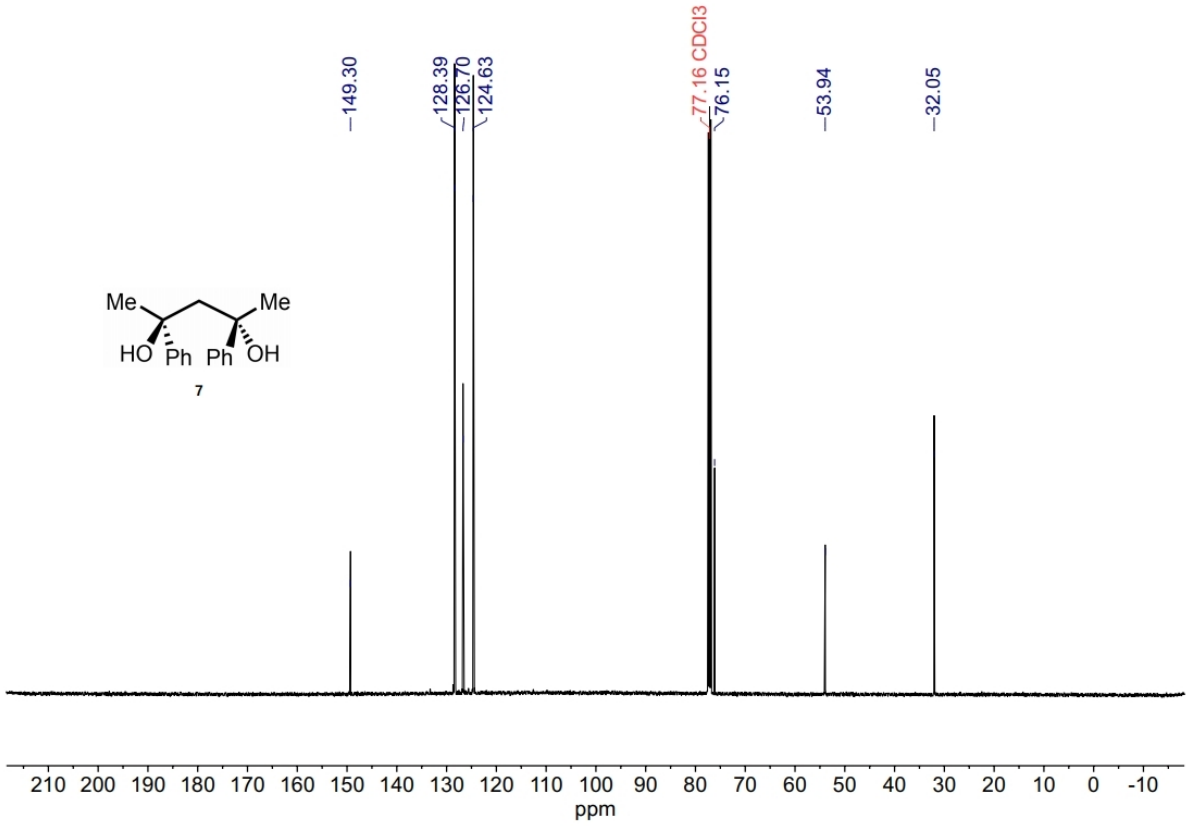

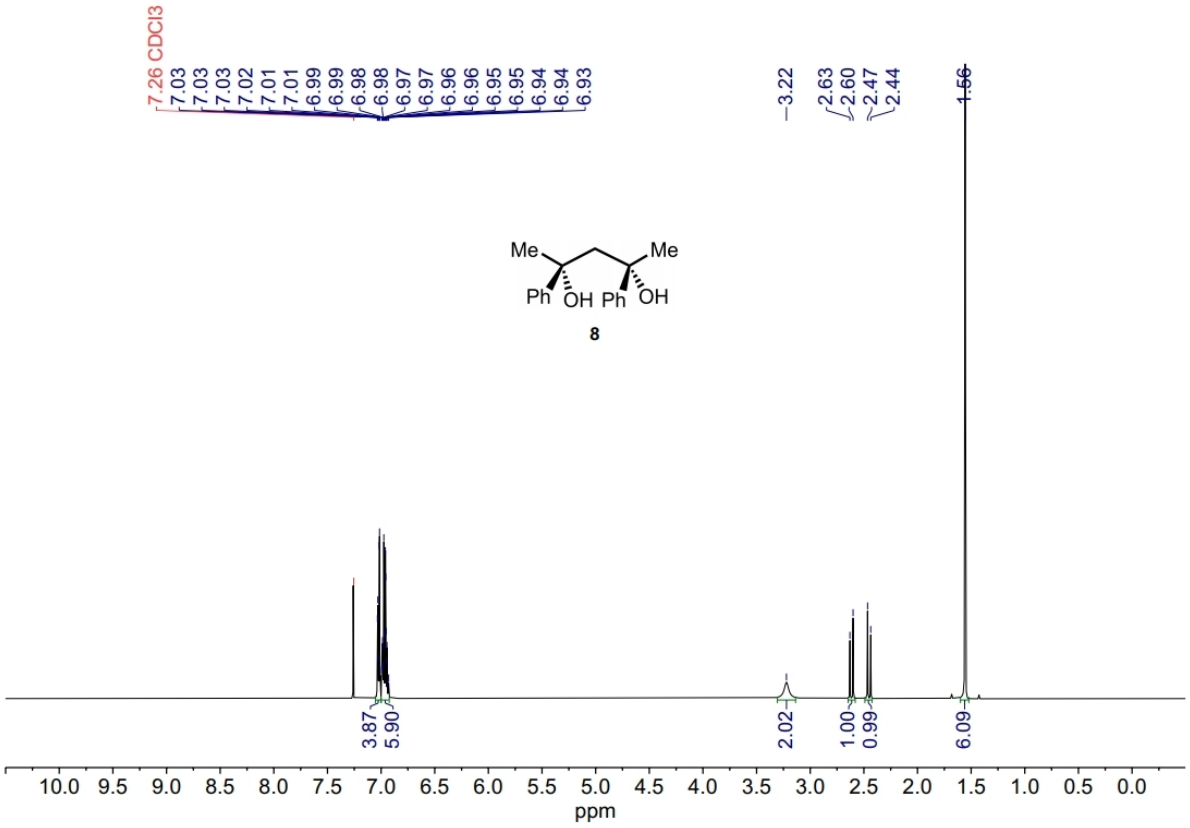
7.26 CDCl3
7.03
7.03
7.03
7.02
7.01
7.01
6.99
6.99
6.98
6.98
6.97
6.97
6.96
6.96
6.95
6.95
6.94
6.94
6.93
3.22
2.63
2.60
2.47
2.44
1.66
Me
Me
Ph
OH
Ph
OH
8
3.87
5.90
2.02
1.00
0.99
6.09
10.0 9.5 9.0 8.5 8.0 7.5 7.0 6.5 6.0 5.5 5.0 4.5 4.0 3.5 3.0 2.5 2.0 1.5 1.0 0.5 0.0
ppm

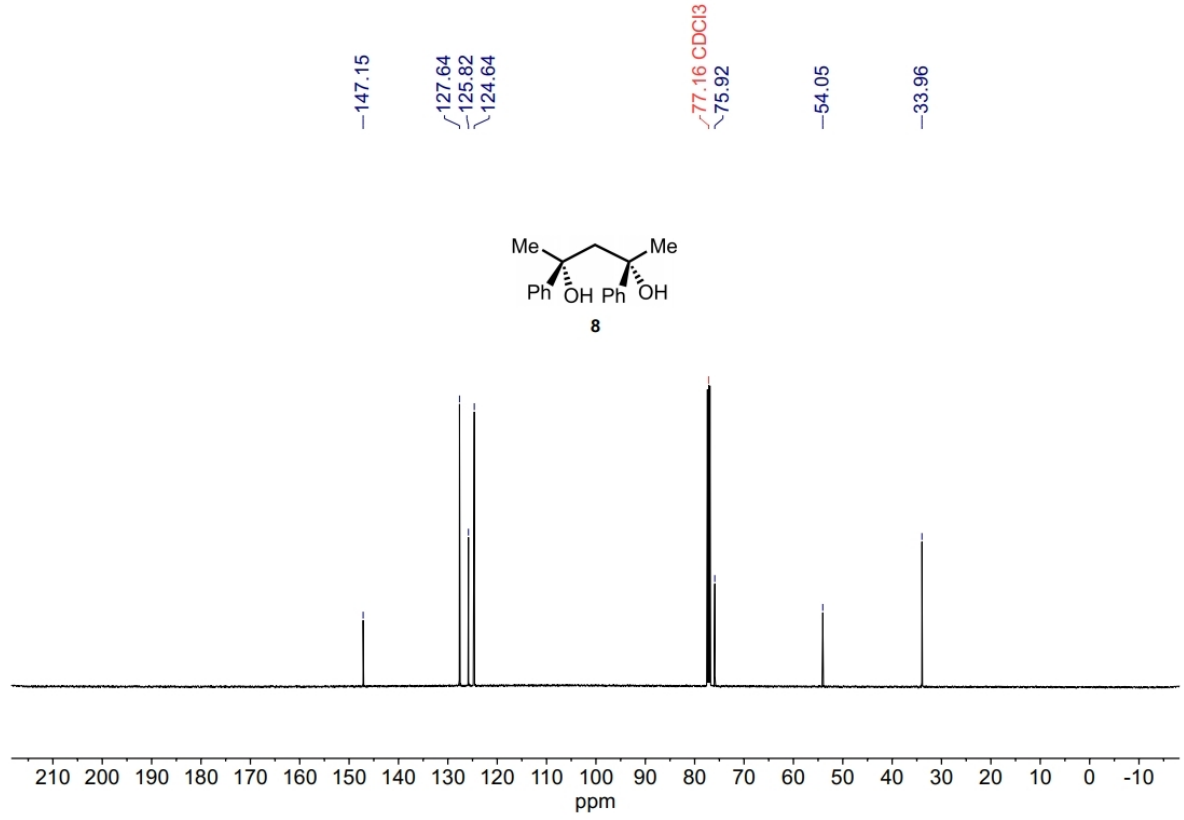
147.15
127.64
125.82
124.64
77.16 CDCl3
75.92
54.05
33.96
Me
Me
Ph
OH
Ph
OH
8
210 200 190 180 170 160 150 140 130 120 110 100 90 80 70 60 50 40 30 20 10 0 -10
ppm

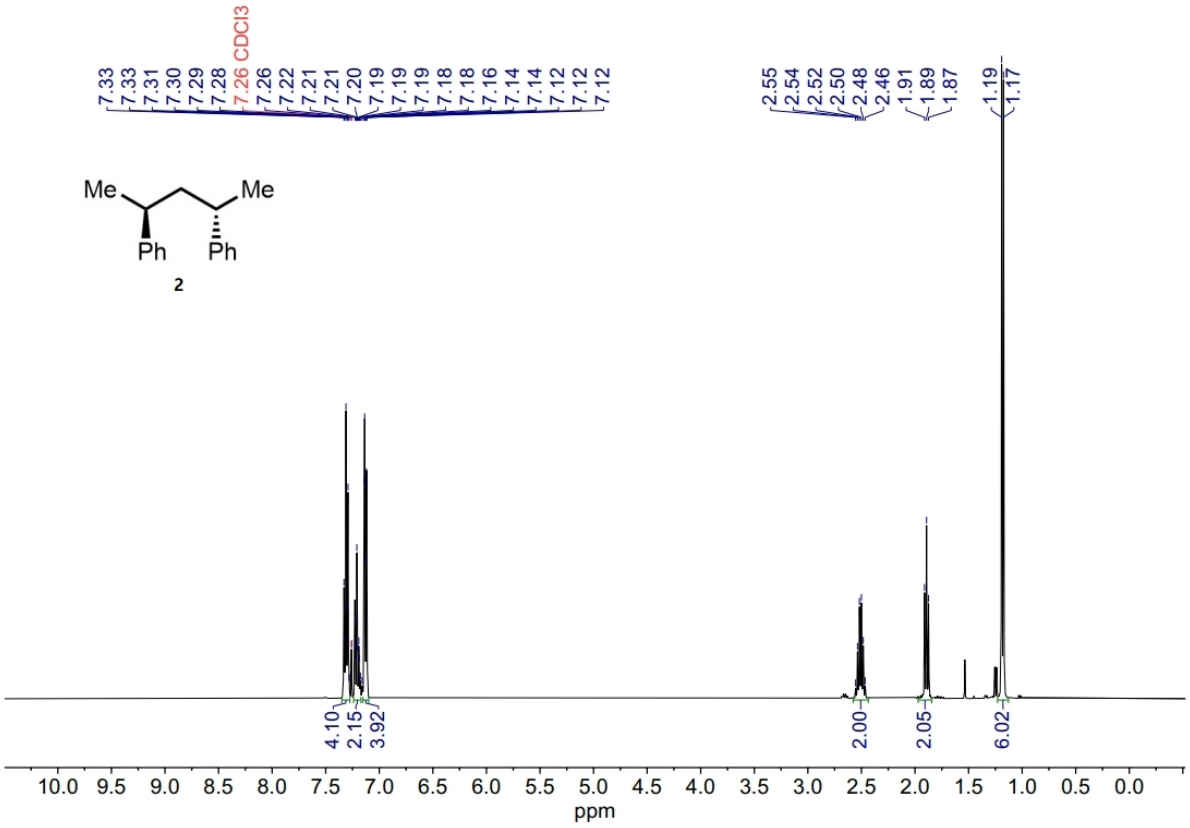
7.33
7.33
7.31
7.30
7.29
7.28
7.26 CDCl3
7.26
7.22
7.21
7.21
7.20
7.19
7.19
7.19
7.18
7.18
7.16
7.14
7.14
7.12
7.12
7.12
2.55
2.54
2.52
2.50
2.48
2.46
1.91
1.89
1.87
1.19
1.17
Me
Me
Ph
Ph
2
4.10
2.15
3.92
2.00
2.05
6.02
10.0 9.5 9.0 8.5 8.0 7.5 7.0 6.5 6.0 5.5 5.0 4.5 4.0 3.5 3.0 2.5 2.0 1.5 1.0 0.5 0.0
ppm

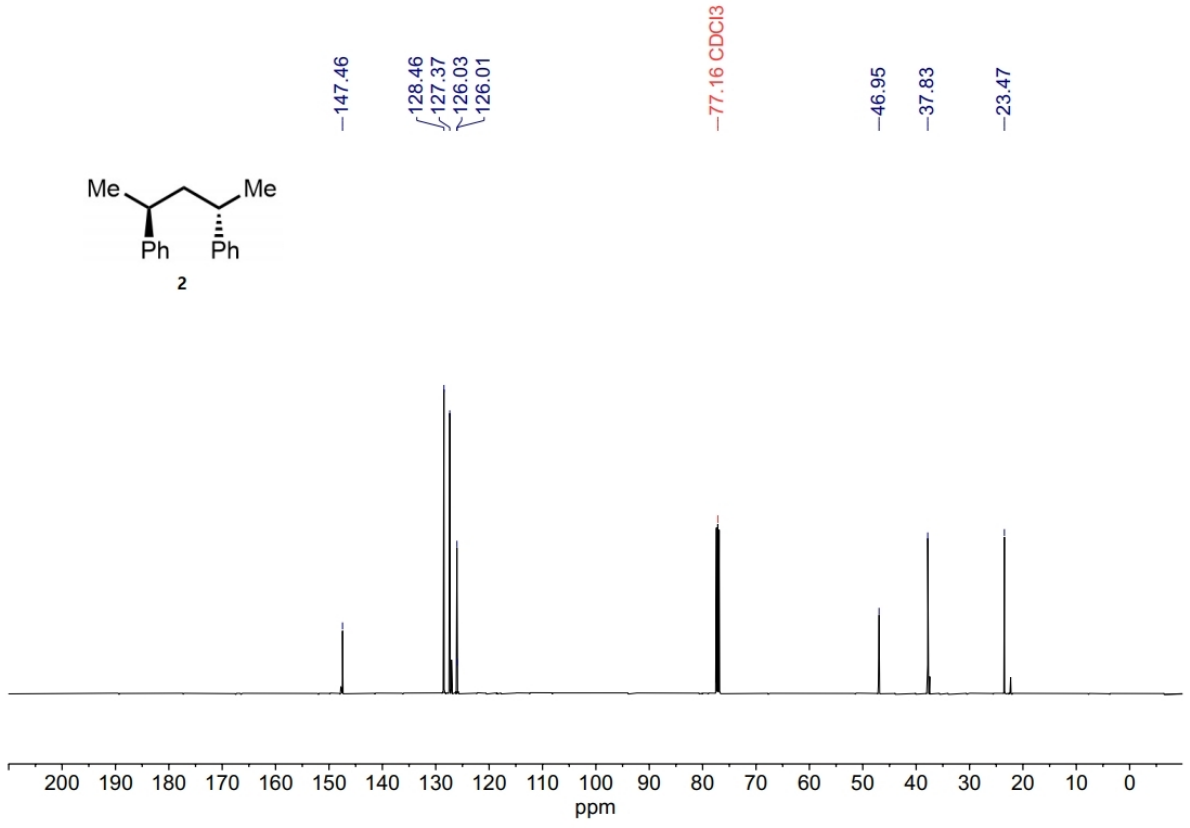
147.46
128.46
127.37
126.03
126.01
77.16 CDCl3
46.95
37.83
23.47
Me
Me
Ph
Ph
2
200 190 180 170 160 150 140 130 120 110 100 90 80 70 60 50 40 30 20 10 0
ppm

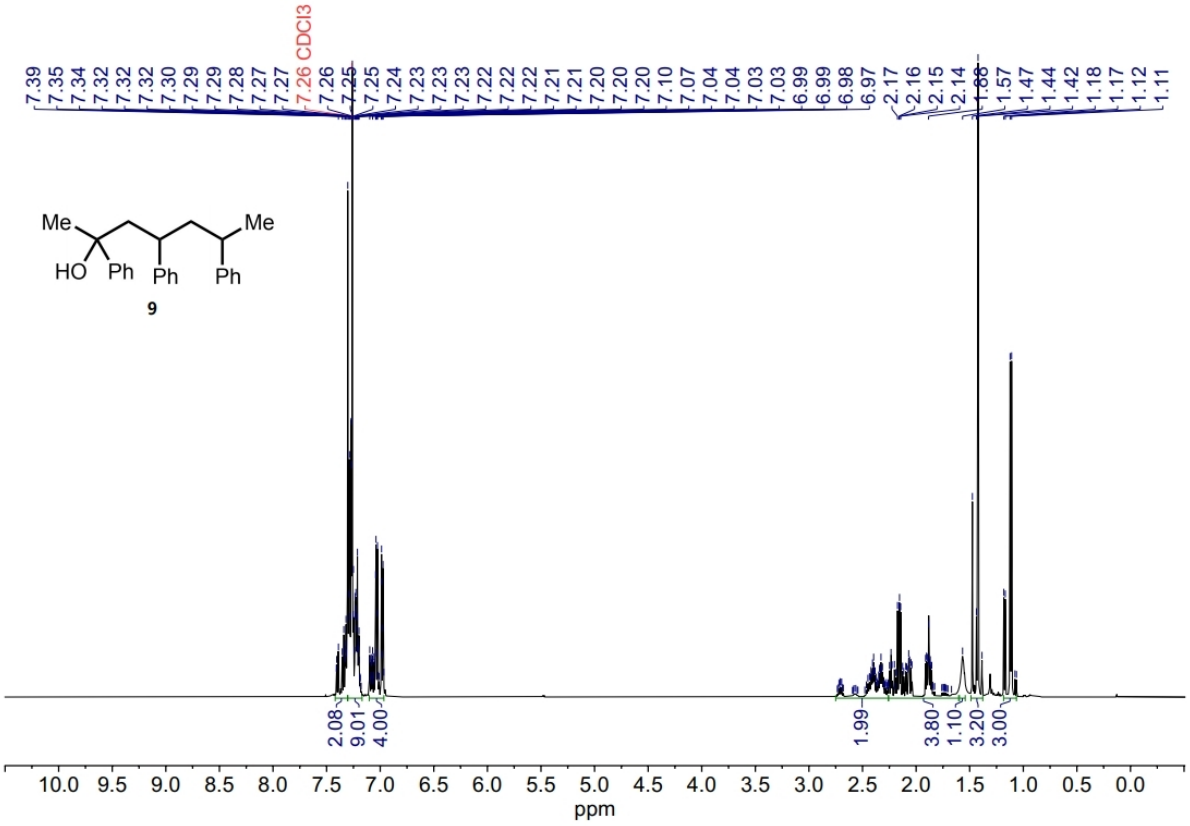
7.39 7.35 7.34 7.32 7.32 7.32 7.30 7.29 7.29 7.28 7.27 7.27 7.26 CDCl3 7.26 7.25 7.25 7.24 7.23 7.23 7.23 7.22 7.22 7.22 7.21 7.21 7.20 7.20 7.20 7.10 7.07 7.04 7.04 7.03 7.03 6.99 6.99 6.98 6.97 2.17 2.16 2.15 2.14 1.88 1.57 1.47 1.44 1.42 1.18 1.17 1.12 1.11
Me
HO
Ph
Ph
Ph
Me
9
2.08 9.01 4.00 1.99 3.80 1.10 3.20 3.00
10.0 9.5 9.0 8.5 8.0 7.5 7.0 6.5 6.0 5.5 5.0 4.5 4.0 3.5 3.0 2.5 2.0 1.5 1.0 0.5 0.0
ppm

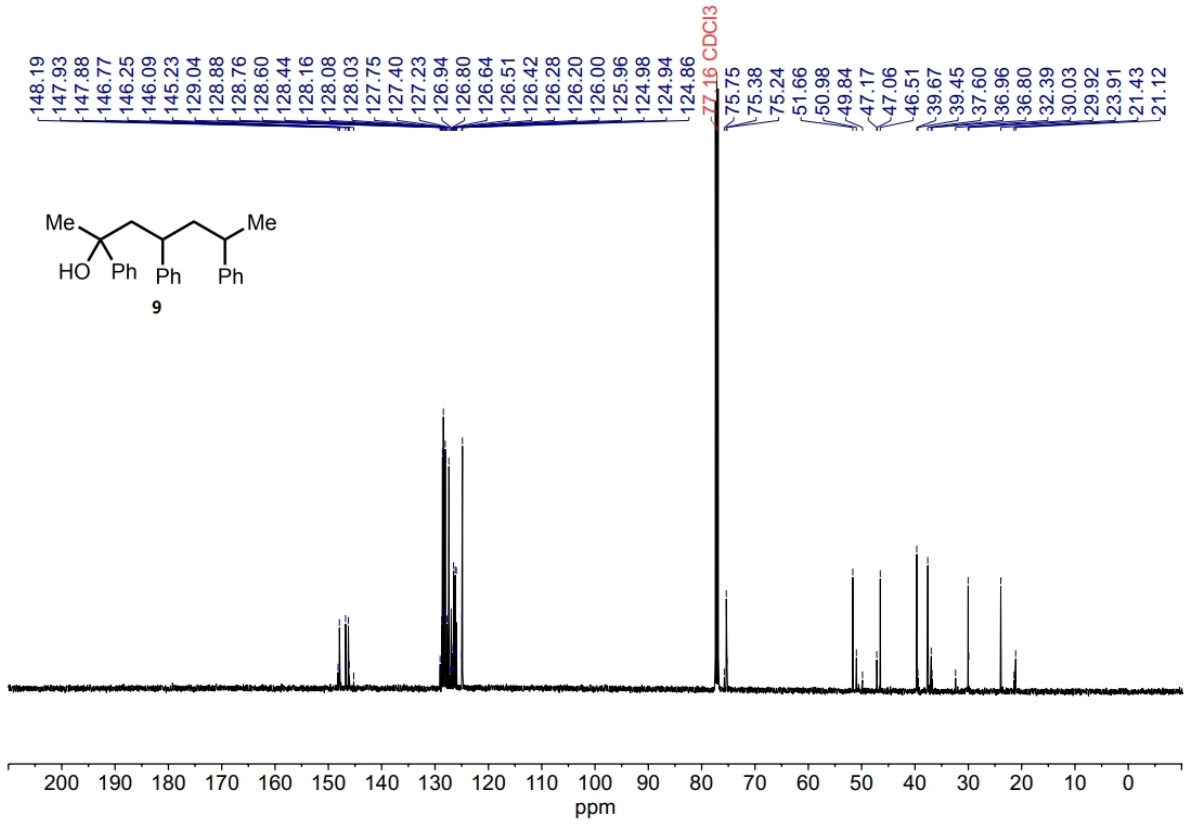
148.19 147.93 147.88 146.77 146.25 146.09 145.23 129.04 128.88 128.76 128.60 128.44 128.16 128.08 128.03 127.75 127.40 127.23 126.94 126.80 126.64 126.51 126.42 126.28 126.20 126.00 125.96 124.98 124.94 124.86 77.16 CDCl3 75.75 75.38 75.24 51.66 50.98 49.84 47.17 47.06 46.51 39.67 39.45 37.60 36.96 36.80 32.39 30.03 29.92 23.91 21.43 21.12
Me
HO
Ph
Ph
Ph
Me
9
200 190 180 170 160 150 140 130 120 110 100 90 80 70 60 50 40 30 20 10 0
ppm

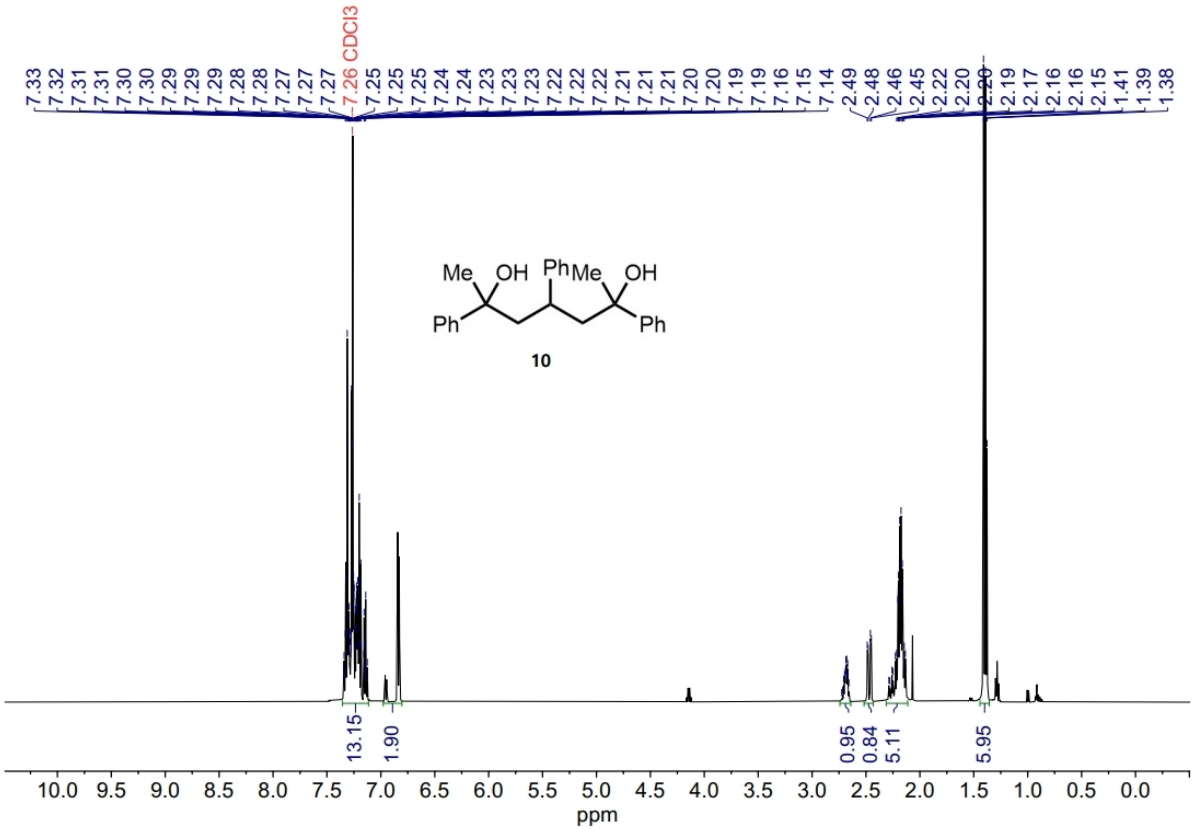
7.26 CDCl3
Me OH Ph Me OH
Ph Ph
10
13.15
1.90
0.95
0.84
5.11
5.95
ppm

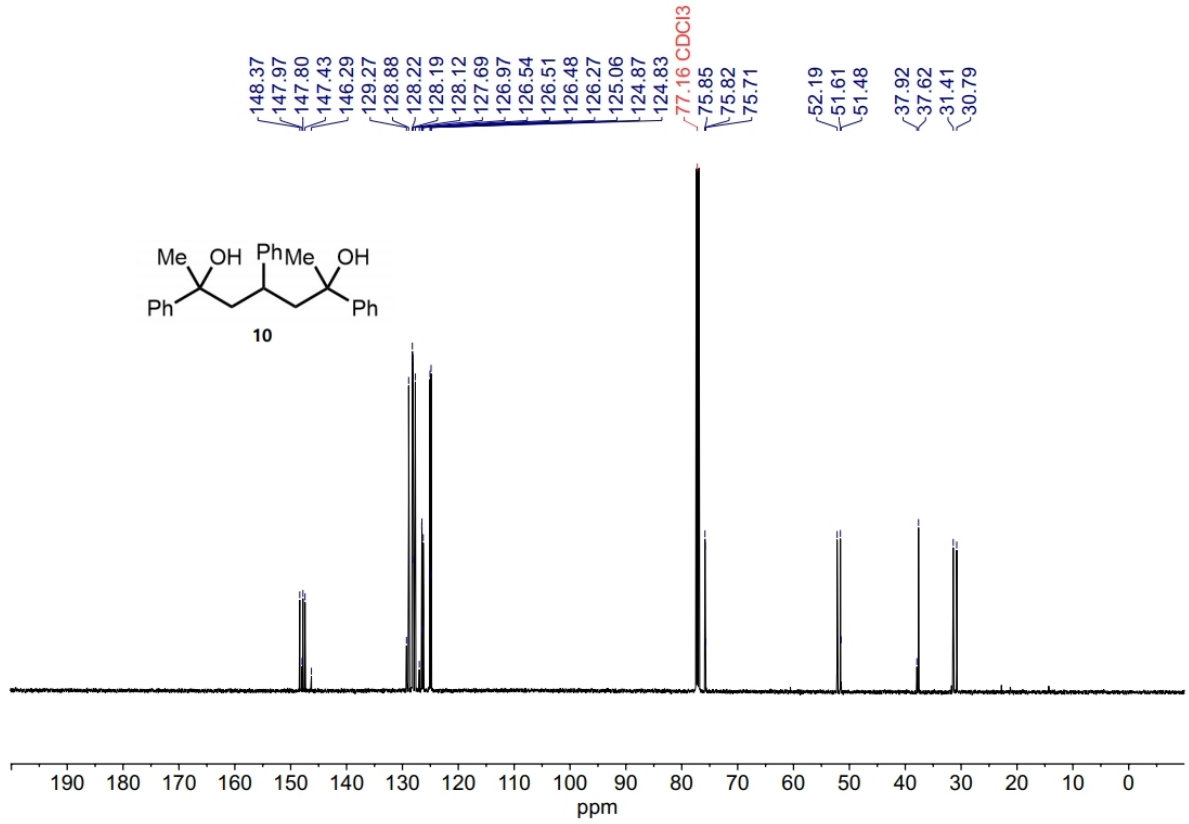
77.16 CDCl3
Me OH Ph Me OH
Ph Ph
10
ppm

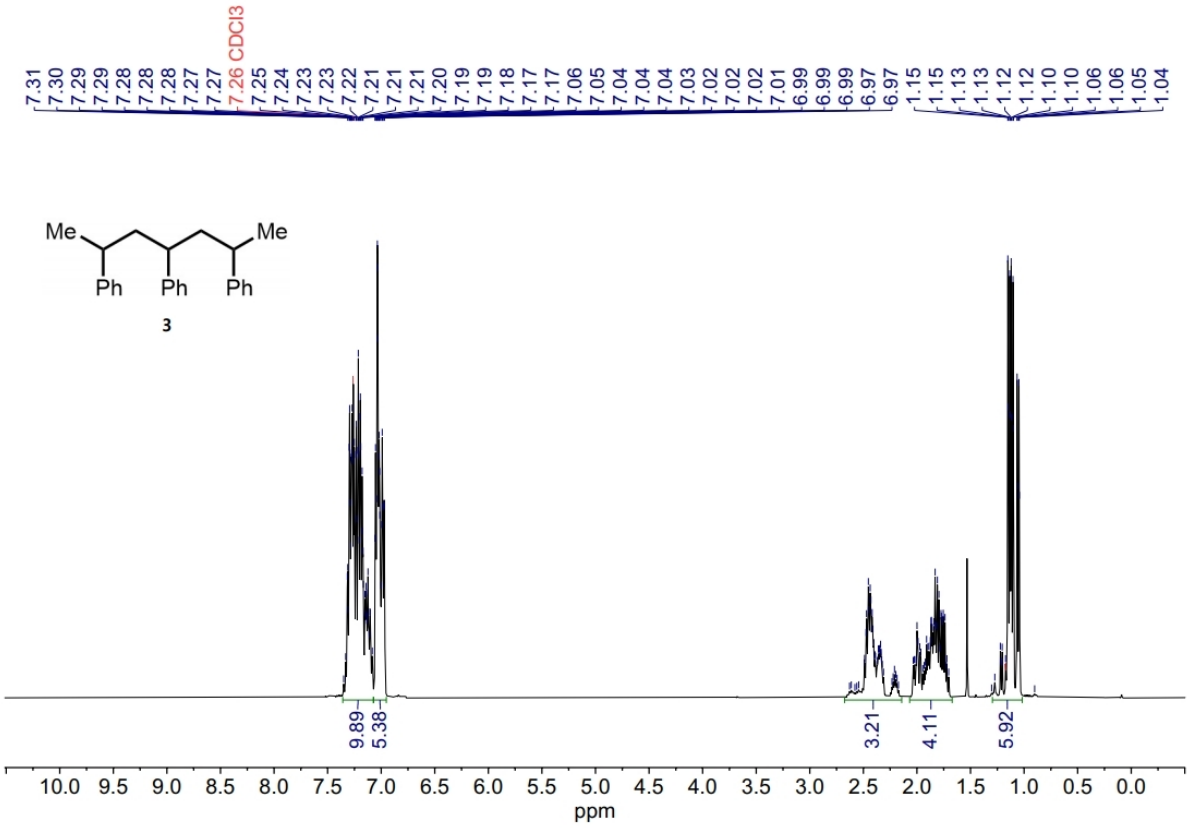
7.31 7.30 7.29 7.29 7.28 7.28 7.28 7.27 7.27 7.26 CDCl3 7.25 7.24 7.23 7.23 7.22 7.21 7.21 7.21 7.20 7.19 7.19 7.18 7.17 7.17 7.06 7.05 7.04 7.04 7.04 7.03 7.02 7.02 7.02 7.01 6.99 6.99 6.99 6.97 6.97 1.15 1.15 1.13 1.13 1.12 1.12 1.10 1.10 1.06 1.06 1.05 1.04
Me Ph Ph Ph Me
3
9.89 5.38 3.21 4.11 5.92
10.0 9.5 9.0 8.5 8.0 7.5 7.0 6.5 6.0 5.5 5.0 4.5 4.0 3.5 3.0 2.5 2.0 1.5 1.0 0.5 0.0
ppm

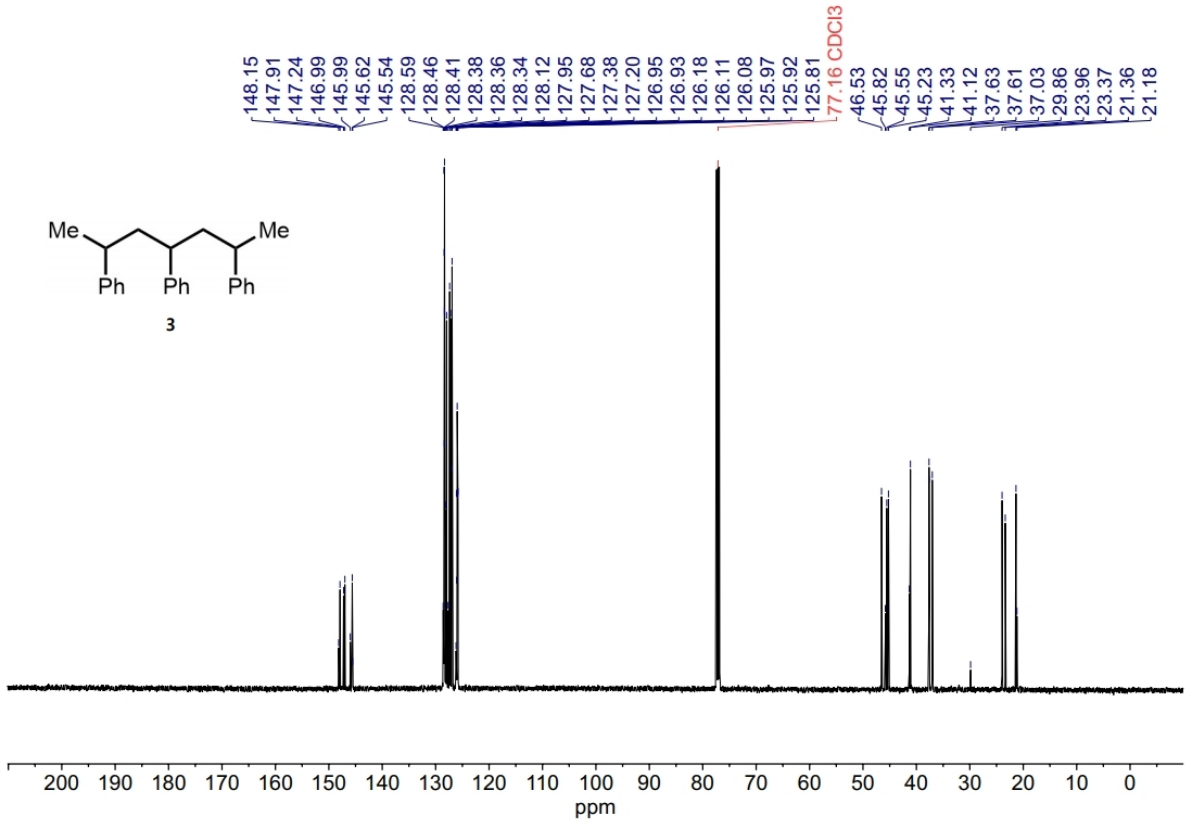
148.15 147.91 147.24 146.99 145.99 145.62 145.54 128.59 128.46 128.41 128.38 128.36 128.34 128.12 127.95 127.68 127.38 127.20 126.95 126.93 126.18 126.11 126.08 125.97 125.92 125.81 77.16 CDCl3 46.53 45.82 45.55 45.23 41.33 41.12 37.63 37.61 37.03 29.86 23.96 23.37 21.36 21.18
Me Ph Ph Ph Me
3
200 190 180 170 160 150 140 130 120 110 100 90 80 70 60 50 40 30 20 10 0
ppm